Performance Analysis and Evaluation of Advanced Designs for Radio Communication Systems for Communications-Based Train Control (CBTC)

Farooq, Jahanzeb

Publication date:
2017

Document Version
Publisher's PDF, also known as Version of record

Performance Analysis and Evaluation of Advanced Designs for Radio Communication Systems for Communications-Based Train Control (CBTC)

Jahanzeb Farooq

Ph.D. Thesis
November 2017

DTU Fotonik
Department of Photonics Engineering

PhD Thesis

Performance Analysis and Evaluation of Advanced Designs for Radio Communication Systems for Communications-Based Train Control (CBTC)

Jahanzeb Farooq

Technical University of Denmark
Kgs. Lyngby, Denmark 2017

To my father, for his unprecedented determination and dedication in educating me during my early school-age years spent in Libya, where no international schools were accessible.

Supervisors:
Lars Dittmann
José Soler
Kasper Tipsmark Therkildsen

Technical University of Denmark
DTU Fotonik
Department of Photonics Engineering
Ørsteds Plads, Building 343,
2800 Kongens Lyngby, Denmark
www.fotonik.dtu.dk

Cover photo credits:
Nils Meilvang (front)
Rasmus Thystrup Karstensen (back)

Abstract

Communications-Based Train Control (CBTC) is a modern signalling system that uses radio communication to enable the exchange of high resolution and real-time train control information between the train and the wayside infrastructure. A vast majority of CBTC systems worldwide use IEEE 802.11 Wi-Fi as the radio technology particularly due to its cost-effectiveness. The trackside networks in these systems are mostly based on conventional infrastructure Wi-Fi. It means a train has to continuously associate (i.e. perform handshake) with the trackside Wi-Fi Access Points (AP) as it moves. This is a time-consuming process associated with a certain delay. Additionally, these APs are connected to the wayside infrastructure via optical fiber cables that incurs huge costs.

To address these problems, a novel design of the CBTC trackside network was proposed at Siemens. In this design, trackside nodes function in ad-hoc Wi-Fi mode, which means no associations have to be performed with them prior to transmitting. A train simply broadcasts packets. A node upon receiving these packets forwards them to the next node and so on, forming a chain of nodes. Following this chain, packets arrive at the destination. To minimize the interference, transmissions are separated on multiple frequencies. Furthermore, redundancy is introduced in the design as a node forwards packets to not only one but two of its neighbors.

The research work presented in this thesis investigates the performance of this new design using computer-based simulations. A large number of scenarios were investigated, in particular with the objective of studying the resiliency, redundancy and scalability supported by the design. The results from the first phase of the study show that due to the frequency separation and redundancy inherent in this design, significantly large numbers of packets can be successfully transferred across large networks. Nonetheless, the results expose two shortcomings of the design as well. They show that the train node undermines the frequency separation guaranteed by the chain nodes as it is required to transmit on all frequencies, and, the design under-estimates the interference produced by distant nodes in ideal propagation conditions despite the frequency separation.

A large number of potential solutions to minimize these shortcomings were subsequently investigated, including adjusting the transmission range of the train, employing a lower number of radios on the train, employing more robust modulation and coding schemes, among others. Additionally, two extensions to the design were proposed that

involved extending the frequency separation distance by employing additional frequencies, and, introducing a separate frequency for train-to-trackside communication. The results show that substantial improvements can be achieved with these solutions.

In the last phase of the study, scenarios to investigate the impact of parameters such as the number of trains, train speed, headway distance, train's location on the track, train direction, and track layouts, were carried out. One of the objectives of this study was to investigate if high data rates can be supported by this design, to enable non-CBTC applications on top of the typical CBTC traffic. The results for these scenarios show that while the design can successfully support the data requirements of typical CBTC traffic, enabling higher data rates is challenging when the number of data traffic flows involved becomes large.

Resumé

Communications-Based Train Control (CBTC) er et moderne signaleringssystem, der anvender radiokommunikation til at muliggøre udveksling af højopløsnings- og realtids togkontrolinformation mellem toget og kommunikationsinfrastruktur på strækningen. Langt størstedelen af verdens CBTC systemer anvender IEEE 802.11 Wifi som radiokommunikationsteknologi, hovedsageligt pga. dets omkostningseffektivitet. Disse systemers trackside-netværk anvender hovedsageligt konventionel infrastruktur Wifi. Dette betyder, at et tog hele tiden skal associere (dvs. udføre handshake) med trackside-Wifi Access Points (AP) mens det kører. Dette er en tidskrævende proces som er forbundet med forsinkelse. Desuden er disse AP forbundet med Trackside-infrastrukturen med optiske fibre, hvilket giver store udgifter.

For at adressere disse problemer har Siemens lavet et nyt design af CBTC tracksidenetværket. I dette design benyttes trackside-AP i ad-hoc Wifi mode, hvilket betyder, at man ikke behøver at associere med et AP inden der kan kommunikeres. Et tog kan simpelthen bare broadcaste pakker. Når et AP modtager en pakke, kan det bare videresende den til det næste AP og så fremdeles og på den måde skabe en kæde af AP. For enden af kæden ankommer pakkerne til deres destination. For at minimere interferens, transmitteres der på flere frekvenser. Endvidere sikres redundans ved at et AP ikke kun sender til sin nærmeste nabo men til sine nærmeste to naboer.

Den forskning, der præsenteres i denne afhandling, undersøger performance af dette nye design ved hjælp af computersimulering. Et stort antal scenarier er blevet undersøgt med det specifikke formål at undersøge resiliens, redundans og skalerbarheden af designet. Resultater fra første del af studiet viser at anvendelsen af flere frekvenser og den indbyggede redundans i designet muliggør at et stort antal pakker kan sendes gennem netværket. Ikke desto mindre, viste simuleringerne også to svagheder ved designet. De viste, at transmissionerne fra toget havde en negativ effekt på den garanterede frekvensseparation, fordi det skal sende på alle frekvenser. Desuden underestimerer designet den interferens der kommer fra andre AP under ideelle transmissionsforhold, på trods af frekvensseparationen.

Et stort antal potentielle løsninger til at minimere disse to mangelfuldheder er efterfølgende blevet undersøgt, inklusive blandt andet at justere rækkevidden af togets transmissioner, brug af færre frekvenser på toget, brug af mere robust modulation og kodning. Desuden er to udvidelser til designet blevet foreslået, som involverer brug flere frekvenser og anvendelse af en separat frekvens til tog til trackside kommunikation. Resultaterne

viser, at disse to forslag forbedrer designet væsentligt.

I undersøgelsens sidste del er der undersøgt scenarier, der undersøger indflydelsen af en række parametre såsom antallet af tog, toghastighed, headway distance, togets position, retning og sporlayout. Et af målene med dette studie, var at undersøge om højhastighedsdatakommunikation var mulig med dette design, for det ville kunne understøtte ikke-CBTC applikationer oven på den sædvanlige CBTC trafik. Resultaterne viser, at selvom designet fint understøtter typisk CBTC trafik, så er højhastighedsdatakommunikation en udfordring hvis der er mange dataflows.

Preface

This dissertation is submitted to the Department of Photonics Engineering at the Technical University of Denmark (DTU) in partial fulfillment of the requirements for the degree of Doctor of Philosophy (PhD). This Industrial PhD project was financed by Siemens A/S, Denmark, and partly by the Ministry of Higher Education and Science of Denmark (Innovation Fund Denmark) within the framework of its Industrial PhD Programme. The project was carried out at the Networks Technologies and Service Platforms group at the Department of Photonics Engineering at DTU, Kgs. Lyngby, Denmark, and at Siemens A/S, Ballerup, Denmark. The project was supervised by Professor Lars Dittmann and Associate Professor José Soler from DTU and Dr. Kasper Tipsmark Therkildsen from Siemens A/S.

Jahanzeb Farooq
November 2017

Acknowledgements

"It was the Best of Times. It was the Worst of Times."
— Dickens, *A Tale of Two Cities*

After having worked a few years in the industry, my habit of challenging myself and going deeper into details brought me back to the academia for this PhD study, a decision I ended up regretting a number of times. Nonetheless, it has been a journey nothing short of exhilarating; a roller-coaster ride with its share of highs and extreme lows. And I have had a number of highly supportive companions in this journey to whom I would like to dedicate this section.

First and foremost, I would like to thank my manager at Siemens A/S, Simon Staudt, for believing in this project, for taking the initiative, and for his consistent support and understanding all the way til the end. Likewise, I would like to extend my special gratitude to my colleagues Rasmus Thystrup Karstensen and Lars Bro, for their interest and support in this work. The outcome of the numerous extended discussions we had as well as their feedback was indispensable for the success of this project. My supervisor from Siemens A/S, Kasper Tipsmark Therkildsen, deserves a special mention for his phenomenal support in this project and for his remarkable ability of empathy. I must admit I was lucky to have him as my supervisor.

I would like to thank my supervisors at DTU, José Soler, for showing interest in getting on board this Industrial PhD project and for his feedback on my work, and Lars Dittmann, for his support throughout.

Additionally, I would like to thank Carsten Vandel Nielsen, my previous supervisor from Siemens A/S, for his consistent support in the early stages of the PhD, and Glenn Ferslev, for being my backup supervisor.

This section would not be complete without mentioning my wife, Zerka. Without her consistently dependable support and understanding, this PhD would not have been possible. My kids as well deserve a mention, as it was largely their time that I was stealing from. I definitely owe them quite a few trips to BonBon-Land, Legoland and what not.

I would like to thank my colleagues at DTU, namely Aleksander Sniady, Cosmin Caba, Justas Poderys, Angelos Mimidis Kentis, Andrea Marcano, Matteo Artuso, Artur

Pilimon, Line Maria Pyndt Hansen, Jakob Thrane, and Eder Ollora Zaballa, for their fantastic companionship and support, and for playing an important role in making this time memorable. Additional thanks to Justas Poderys for a fruitful collaboration.

A number of my colleagues at Siemens A/S deserve a place here, for reviewing my work, providing feedback, and, helping me finding the required information on various occasions. A special mention goes to Hans-Henrik Munch, Jens Peter Haugaard, and Claus Winskov Jørgensen. Likewise, I would like to thank my German colleagues Mikael Voss, Frank Ohnesorge, and Joachim Schumacher for their support.

Special thanks go to Kell Quist Jensen at Siemens A/S for his outstanding support, particularly in relation to the patent applications involved in this project.

Thanks to Henrik Christiansen for translating the abstract in this thesis to Danish.

Special thanks to my parents for their love and blessings.

Last but not least, I would like to thank Siemens A/S and the Ministry of Higher Education and Science of Denmark (Innovation Fund Denmark) for providing me with this invaluable opportunity.

Contents

List of Figures

List of Tables

List of Acronyms

AP	Access Point
API	Application Programming Interface
BER	Bit Error Rate
BPSK	Binary Phase Shift Keying
CBTC	Communications-Based Train Control
CCK	Complementary Code Keying
COTS	Commercial-off-the-Shelf
CSMA/CA	Carrier Sense Multiple Access/Collision Avoidance
CSV	Comma-Separated Values
D2D	Device-to-Device
DCS	Data Communication System
DSRC	Dedicated Short Range Communications
DSSS	Direct Sequence Spread Spectrum
DTO	Driverless Train Operation
EMA	External Model Access
ESP	Encapsulating Security Payload
ERTMS	European Rail Traffic Management System
FER	Frame Error Rate
FSM	Finite State-Machine
FSPL	Free-Space Path Loss
GSM-R	Global System for Mobile Communications - Railway
GUI	Graphical User Interface
HKT	HastighedsKontrol og Togstop
IEC	International Electrotechnical Commission
IAPP	Inter-Access Point Protocol
ISM	Industrial, Scientific and Medical
IPSec	IP Security
KPI	Key performance indicators
LOS	Line Of Sight
LTE	Long-Term Evolution

MAC	Medium Access Control
MRP	Media Redundancy Protocol
OFDM	Orthogonal Frequency-Division Multiplexing
PBCC	Packet Binary Convolutional Code
PER	Packet Error Rate
PLCP	Physical Layer Convergence Procedure
QAM	Quadrature Amplitude Modulation
QoS	Quality of Service
QPSK	Quadrature Phase Shift Keying
RAMS	Reliability, Availability, Maintainability and Safety
RCS	Radio Communication System
RF	Radio Frequency
RSSI	Received Signal Strength Indicator
RTS/CTS	Request to Send/Clear to Send
SNR	Signal-to-Noise Ratio
STO	Semi-Automated Train Operation
SSID	Service Set Identifier
TCC	Traffic Control Center
TGMT	Trainguard Mass-Transit
UTO	Unattended Train Operation
V2I	Vehicle-to-Infrastructure
V2V	Vehicle-to-Vehicle
WAVE	Wireless Access in Vehicular Environments
WMN	Wireless Mesh Network
ZC	Zone Controller

PhD Publications

Papers

[Farooq2017a] **J. Farooq** and J. Soler. "Radio communication for Communications-Based Train Control (CBTC): A tutorial and survey". In: *IEEE Communications Surveys & Tutorials* 19.3 (2017), pp. 1377–1402. ISSN: 1553-877X, DOI: 10.1109/COMST.2017.2661384.

[Farooq2017b] **J. Farooq**, L. Bro, R. T. Karstensen, and J. Soler. "A multi-radio, multi-hop ad-hoc radio communication network for Communications-Based Train Control (CBTC)". In: *Proc. IEEE 86th Vehicular Technology Conference (VTC 2017-Fall)*. Sept. 2017.

[Farooq2017c] J. Poderys, **J. Farooq**, and J. Soler. "A novel multimedia streaming system for urban rail environments using Wi-Fi peer-to-peer technology". In: Proc. *12th International Workshop on Communication Technologies for Vehicles, Nets4Cars / Nets4Trains / Nets4TrainsAircraft*. Vol. 10222. Lecture Notes in Computer Science. Toulouse, France: Springer, May 2017, pp. 41–53.

[Farooq2017d] **J. Farooq**, L. Bro, R. T. Karstensen, and J. Soler. "Performance evaluation of a multi-radio, multi-hop ad-hoc radio communication network for Communications-Based Train Control (CBTC)". In: *IEEE Transactions on Vehicular Technology* PP.99 (Nov. 2017). pp. 1–1. ISSN: 1939-9359, DOI: 10.1109/TVT.2017.2777874.

[Farooq2017e] **J. Farooq**, L. Bro, R. T. Karstensen, and J. Soler. "A multi-radio, multi-hop ad-hoc radio communication network for Communications-Based Train Control (CBTC): Introducing frequency separation for train-to-trackside communication". In: *Proc. IEEE Consumer Communications & Networking Conference (CCNC)*. Jan. 2018.

[Farooq2018a] J. Poderys, **J. Farooq**, and J. Soler. "A novel multimedia streaming system for urban rail environments using Wi-Fi peer-to-peer technology". In: *Proc. IEEE 87th Vehicular Technology Conference (VTC 2018-Spring)*. June 2018. Accepted for publication.

[Farooq2018b] **J. Farooq**, L. Bro, R. T. Karstensen, and J. Soler. "A multi-radio, multi-hop ad-hoc radio communication network for Communications-Based Train Control (CBTC) with optimized frequency separation". In: *Proc. IEEE 87th Vehicular Technology Conference (VTC 2018-Spring)*. June 2018. Accepted for publication.

[Farooq2018c] **J. Farooq**, R. T. Karstensen, L. Bro, and J. Soler. "Experimental evaluation of a multi-radio, multi-hop ad-hoc radio communication network for Communications-Based Train Control (CBTC)". To be submitted.

Patents

[Farooq2017f] Siemens AG, **J. Farooq**, L. Bro, and R. T. Karstensen. "Kommunikationsnetzwerk und verfahren zum betrieb eines kommunikationsnetzwerkes, English translation: Communication network and methods for operation of a communication network". Patent application 10 2017 210 668.9 (German Trademark and Patent Office). June 2017.

CHAPTER 1

Introduction

1.1 Background

Over the last decade, there has been a huge focus on rail transport due to environmental awareness, increased urbanization, population growth, and it being a more energy-efficient, safer, higher capacity, and higher speed transport alternative. Recent studies [1]–[3] show that the European rail market grew from 122 billion euro per year to approximately 150 billion euro in the period 2008-2013, and is expected to grow to approximately 176 billion euro by 2017. Furthermore, it is estimated that a total of 1,077.8 km of rail tracks for the modern, communication-based signalling system Communications-Based Train Control (CBTC) will be installed in the period 2011-2021, compared to only 188.9 km in 2001-2010 [4].

Rail traffic is characterized by poor braking capabilities because of low friction on rails, fixed path, and the inability to avoid obstacles. Therefore, at its most basic, the objective of a railway signalling system (or train control system) is to prevent trains from colliding and derailing [5]. Conventional railway signalling is based on trackside equipment including color light signals, and track circuits and axle counters to determine the train location. However this technology is nearly half a century old. It is nearing its expiry in most of the installations worldwide and is responsible for most of the delays experienced every day. This is one reason why the conventional signalling systems are rapidly being replaced by modern signalling systems [2], [4], [6], [7].

In modern, communication-based railway signalling, different means of telecommunication are used to transfer train control information between the train and the wayside infrastructure—note that trackside generally includes components located on or close to the tracks and is considered a part of the the wayside infrastructure, as shown later in Figure 2.3. However, today the term is used almost exclusively for radio-communication-based signalling. CBTC is a modern, radio-communication-based signalling system that enables the exchange of high resolution and real-time train control information using radio communication. This increases the line capacity by safely reducing the distance (headway) between trains travelling on the same line, and minimizes the number of trackside equipment needed [8]–[11]. CBTC is the first choice of railway operators for mass-transit operations today, with currently over one hundred CBTC systems installed worldwide [8]. Note that although communication-based train control is a generic term, today the term CBTC is used specifically to imply systems used for mass-transit, mostly employing IEEE 802.11 Wireless LAN (WLAN) [12], popularly known as Wi-Fi, for

radio communication. Thus, CBTC systems are considered distinct from the European Rail Traffic Management System (ERTMS)—another modern, communication-based signalling system, targeted towards mainline railway operations.

1.1.1 The Danish Signalling Programme

Denmark is currently one of the front-runners in Europe as it is carrying out a total renewal of its entire railway signalling before 2021, with an investment of 3.2 billion euros. In 2011, Denmark's state-owned railway infrastructure company Banedanmark (Rail Net Denmark) awarded Siemens, Denmark, with the 252 million euros worth of project of replacing the signalling system of the Copenhagen mass-transit network S-train (S-bane in Danish) with CBTC [13].

The S-train network is composed of approximately 170 kilometers of total track length, 7 lines, and 84 train stations. The current signalling system used by S-train—since 1975—is an inductive loop-based system called HKT (HastighedsKontrol og Togstop, *English translation: SpeedControl and Trainstop*). In HKT, the train control information is transferred to the train via the rails, using low-bandwidth audio frequency signals. For further details on these conventional signalling systems, see Section 2.2.

The new signalling system is expected to enable greater capacity and a 80% reduction in signalling related train delays [14]. The goal is to initially enable a Semi-Automated Train Operation (STO), and subsequently to more automated operations with either minimum or no driver involvement—called Driverless Train Operation (DTO)—, and optionally to a fully automated operation without any onboard staff—called Unattended Train Operation (UTO). The first line segment—Jægersborg-Hillerød—equipped with CBTC went into operation in February 2016 and the second roll-out is planned for 2018, as illustrated in Figure 1.1.

1.2 Problem statement

CBTC systems have historically used Wi-Fi as the radio technology, mainly due to its cost-effectiveness, as discussed further in Chapter 2. To ensure a continuous wireless connectivity, hundreds of Wi-Fi Access Points (APs) are installed at the trackside, as illustrated in Figure 1.2. Each AP is next connected to the wayside (normally a Traffic Control Center (TCC)) using a wired connection. This is referred to as a CBTC trackside network. The train must associate (i.e. perform handshake) to an AP first to be able to transmit, just like in an ordinary infrastructure Wi-Fi network. Likewise, the train must roam (handover) from one AP to the other as the train moves. These operations are performed by the *radio communication system*—a component of the CBTC system running on the train onboard equipment.

However, there lie a number of challenges with this approach:

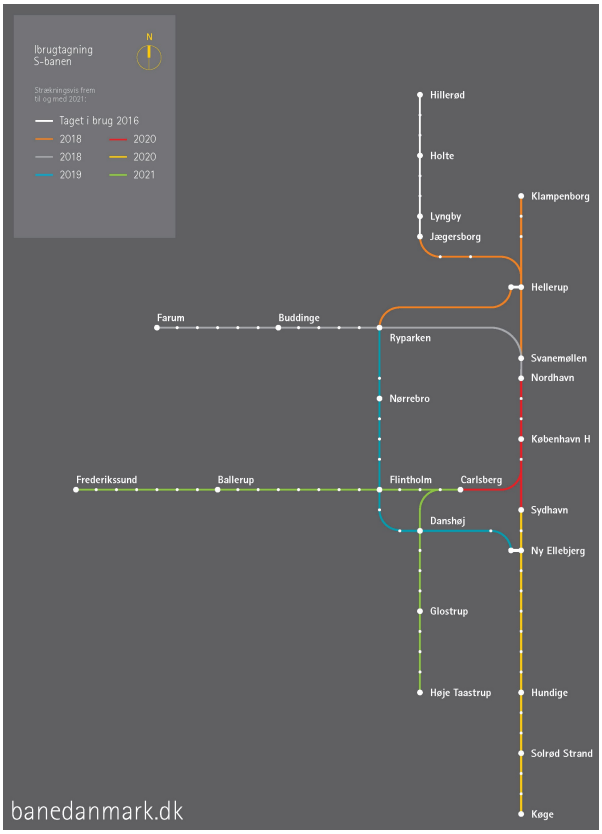

Figure 1.1: Copenhagen S-train CBTC roll-out plan (Source: Banedanmark)

- Firstly, installing cables to connect each AP to the wayside is expensive and time-consuming. The cost of installing optical fiber cables and their maintenance can be as high as around 30,000 EUR per kilometer [15].

- Secondly, roaming results in delays in communication and limits the supported train speed as well. The IEEE 802.11 technology was originally designed for users in stationary office environments and thus inherently lacks support for mobility. Therefore, complex algorithms are employed by the CBTC radio communication system to enable support for roaming. Often different roaming algorithms are employed for train's front and rear antennas due to different alignments with respect to the antennas on the trackside APs, as discussed in detail in Chapter 2. As an example, a train travelling at 300 kilometers per hour with APs deployed at

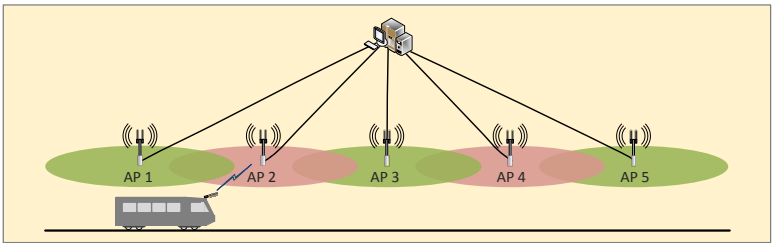

Figure 1.2: CBTC trackside network: Conventional design

every 300 meters must perform roaming every 3.6 seconds.

Additionally, the roaming decision is often made based solely on the signal quality received from the AP. This might lead to a situation where train connects to an AP which, despite having an acceptable signal quality, is not fully functional. Specifically, it might not be capable of communicating to the wayside for example due to a software bug, a broken Ethernet cable, an incorrectly configured firewall, etc. To avoid this situation, additional mechanisms have to be introduced to verify that the train can actually communicate to the wayside over this connection. However this adds to the complexity of the radio communication system as well as the delay involved.

It is noted that while some of the more recent standards of the IEEE 802.11 technology, for example 802.11r [16], enable support for minimizing the roaming delay, the delay is still not entirely eliminated. Furthermore, as discussed in Chapter 2, a vast majority of the Wi-Fi equipment currently in use is based on the IEEE 802.11a, 802.11b, or 802.11g standards. Upgrading the Wi-Fi equipment on hundreds of trackside APs is therefore an expensive and time-consuming undertaking.

1.2.1 Proposal for a new design of the CBTC trackside network

Siemens' current CBTC solution is called Trainguard Mass-Transit (TGMT). The radio communication system used by TGMT is called Airlink and has been developed at Siemens, Denmark. Airlink is composed of the train onboard radio equipment and the trackside radio network. Fundamentally, Airlink enables a radio connection between the train and the trackside. Nonetheless, since Airlink is likewise based on the infrastructure Wi-Fi, it is prone to the same above mentioned challenges. Therefore, Siemens proposed a novel design for an ad-hoc based radio communication system. In this design, there are no "APs". Nodes function as plain Wi-Fi nodes, in an ad-hoc manner. A node broadcasts packets to the nodes within its range. A nearby node, upon receiving a packet, re-transmits (forwards) the packet, which is then picked up by the next nearby node. As a result of this multi-hop communication, a chain of nodes is thus formed, following which the packets reach at the last node in the chain and are then forwarded to the wayside infrastructure

over a wired connection. Thus, a train does not have to worry about first associating with an AP, as well as roaming. Figure 1.3 presents a simplified view of the proposed design to illustrate the fundamental idea behind the design. An overview of the complete design is presented in Chapter 3. As seen in Figure 1.3, wired connections between the nodes and wayside infrastructure are no longer needed, except for the two nodes at each end of the chain. Furthermore, to make the chain resilient against failures and interference, in the proposed design, transmissions are separated on multiple frequencies and a node forwards packets to two of its neighbors rather than one.

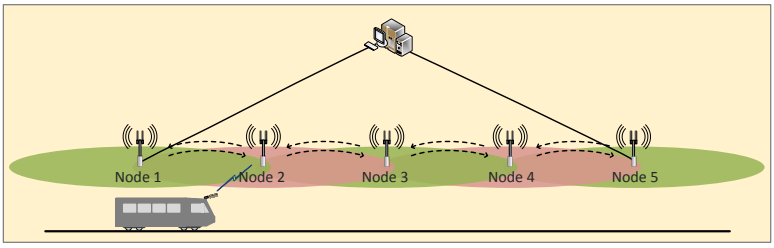

Figure 1.3: CBTC trackside network: A simplified view of the proposed design

An additional advantage of the proposed design is that a node can be placed anywhere at the trackside and not only at designated points where connections to the pre-installed Ethernet cables are accessible. Likewise, this design is more resilient to the problem where a train can block another train's radio signals to the AP as the number of trains increases at busy train stations, as has been witnessed in the London Crossrail railway network. In the proposed design, in the event of this problem, a train can in principal just act like a trackside node in that it can forward the packets to the train whose radio signals to the trackside nodes have been blocked.

It is worth noting that the proposed design is not limited to using Wi-Fi. For example, LTE (Long-Term Evolution), with the Device-to-Device (D2D) support in its upcoming releases, can be used as an alternative radio technology. Likewise, it is noted that despite originally intended for a CBTC trackside network, the application of the proposed design is not limited to it, e.g. it can serve as a superior alternative to the conventional "Wi-Fi over Long Distance" (WiLD) method used to provide low-cost, long-distance wireless access to rural areas.

Note that when this PhD study started, the process of the development of a product based on the proposed design was in its particularly initial stages, i.e. development and testing of the prototype, examining the feasibility, and the process of securing funding for the development. In the course of this study, the full-fledged development of the product has commenced.

1.3 Motivation and scope

During the initial stages of this PhD study, an independent field experiment [17] was carried out in order to provide a proof-of-concept of the proposed design. A brief overview of this experiment is provided in Chapter 4. Nonetheless, while the field experiment successfully demonstrated the prototype of the design, it suffered from a number of limitations. In particular, the limited availability of hardware equipment, time constraints, and the tedious work involved in carrying out such an experiment effected the usability and scalability of the experiment. As a consequence, only a small network of seven nodes could be experimented.

The objective of this Industrial PhD study was to extend the scope of the study to a larger scale with various additional scenarios, beyond the limits imposed in the field experiment, by taking an advantage of computer-based simulations. The objective is to study the performance of the design primarily in terms of number of packets transferred across the chain, the resiliency and redundancy enabled by the design, and its scalability. This study uses a number of Key Performance Indicators (KPIs) to evaluate the performance of the design. These KPIs are discussed in detail in Chapter 5.

The major objectives of this study are as follows.

- **Resilience and redundancy**: One of the fundamental KPIs for the new design to work is how well it supports redundancy. In the event of failure of one or more nodes in the network, it shall still be able to transfer packets across, to the last node in the chain. One objective, therefore, is to study how the performance is impacted if for example, every second node or a random number of nodes, in the network are deliberately failed.

- **Data transfer rate/throughput**: Note that while CBTC traffic itself does not require high data rates as discussed further in Chapter 2, one objective of this study is to investigate how much data rate the proposed design can support, as any excessive bandwidth can be utilized for providing modern, non-CBTC applications such as remote diagnostics and maintenance, remote software upgrade, CCTV, passenger infotainment, onboard Internet etc., which are likely to become more widespread in near future. Thus, the objective is to study how much data could actually be transferred over this network without negatively impacting the network performance.

- **Scalability**: It is not unusual for CBTC trackside networks to be composed of hundreds of APs, depending on the inter-AP distance, which normally varies between 200 and 600 meters. As discussed further in Section 1.5, conventional multi-hop wireless communication results in severe throughput degradation as the number of hopes increases, because of the shared nature of wireless medium. One objective, therefore, is to demonstrate that due to the use of multiple frequencies, the proposed design is not prone to the same problems. Furthermore, the objective is to

study how varying network sizes, e.g. of up to 100 nodes, impact the performance, and, optionally, to study what the optimal network size of such a network is.

Siemens' current CBTC solution supports a train speed of up to 180 kilometers per hour. However, whether the new design is compatible with it or not was unclear. An additional objective, therefore, is to study the performance of the network with varying train speeds, i.e. the impact of train movement on the packet transfer rate. Additional interesting questions include the maximum number of trains such a network could support within a given distance. Likewise interesting are the scenarios involving multiple trains and tracks, e.g. trains following each other or running in the opposite direction, and the direction of the train movement relevant to the shorter and longer ends of the chain.

Note that the focus of this study is open lines (or tracks) in contrast to train stations. At stations, the capacity of the system can be improved by deploying additional chain nodes if for example the number of trains stopping or passing through a station is expected to increase. However, this is not easily achievable outside the stations. This study involves a maximum of three trains, as a number greater than this within a certain distance is less likely.

It is noteworthy that the focus of this study evolved significantly in the course of the PhD. The initial plan was to validate the fundamentals of the proposed design with stationary scenarios—i.e. where the train node is stationary—before following with scenarios with moving trains. Nevertheless, after a number of shortcomings in the design were identified in the course of the first set of simulations, the focus was gradually altered. Namely, the simulations that were focused on identifying solutions to the shortcomings were prioritized first, to support the actual product development which by that time had already started. As a consequence, a number of new simulation scenarios were designed and a number of previously designed scenarios were either discarded or updated to focus the shortcomings. Note that due to a large number of parameters and their values involved, the number of simulation experiments grew exponentially with each new parameter. As an example, the results presented in this thesis were finalized out of a set of 366 simulation experiments. Notably, this number does not include the simulation scenarios that were discarded or redesigned, as well as multiple runs of the same scenario. That said, while an innumerable number of additional scenarios could have been carried out, at the end, the scenarios that supported the development of the product had to be prioritized first.

1.4 Patent and publications

The public dissemination of this work was initially not permitted by Siemens due to their interest in filing a patent application outlining the fundamentals of the proposed design. Unfortunately, the patent filing process took an exceptionally long time. The patent application ([18]) was finally filed on February 24, 2017. Note that as discussed in Chapter 3, the author was not involved in the initial phases of the development of this design and therefore is not included in this patent application as an author. Subsequently,

as an outcome of this PhD study, a number of improvements to the design were proposed, as outlined in Chapter 7 and Chapter 8. Based on one of these improvements discussed in Chapter 8, a second patent application ([Farooq2017f]) was subsequently filed on June 23, 2017. The filing process of these two patent applications resulted in a significant delay in publishing the results from this PhD study. A list of the publications made in this PhD study is included in the beginning of this thesis.

1.5 Related Work

A multi-hop ad-hoc network formed as a chain of nodes presents a suitable candidate for a long-distance network. Most of the related work, however, focuses on networks where all nodes operate on a single frequency. Since nodes must forward packets for other nodes, the capacity degrades sharply with the growing size of the network as a node must contend with additional nodes than its two immediate neighbors. Thus, these networks offer only a fraction of the capacity achieved by a single-hop network, as the capacity drops to one-half with each hop and to 1/7 as the number of nodes increases beyond 10 [19]–[22]. Additional reasons include the *hidden node problem* in which two nodes are in the transmission range of a common node but not in each other's range. The hidden node problem is well-known in the context of the conventional infrastructure Wi-Fi networks. In a multi-hop scenario where two nodes communicating to another node are not necessarily in each other's range, the hidden node problem is inevitable.

Additionally, IEEE 802.11's Carrier Sense Multiple Access/Collision Avoidance (CSMA/CA) mechanism—which is based on carrier sensing—does not work ideally in wireless networks where the interference range is often larger than the transmission range, as the power sufficient to introduce noise in a transmission is much lower than that required for a successful transmission [23]–[27].

Unfortunately, there exist very limited research work on multi-hop ad-hoc networks in the context of vehicular communication, in particular CBTC, and with the objectives of the proposed design. The IEEE 802.11p [28] standard—also known as Wireless Access in Vehicular Environments (WAVE)—is targeted towards vehicular communication, in particular roadway safety, and is based on the Dedicated Short Range Communications (DSRC) standard. The works in [29]–[31] discuss the multi-radio/multi-channel feature of this technology, although the focus is single-hop communication. The works in [32]–[35] discuss multi-hop communication, although for vehicle-to-vehicle (V2V) communication rather than vehicle-to-infrastructure (V2I) communication, where roadway vehicles relay messages to each other.

An advanced version of an ad-hoc based network is a Wireless Mesh Network (WMN) which employs a multi-radio design, and despite it merits, has not been considered for CBTC except for a limited application in [36]. The work in [37] discusses an IEEE 802.11-based WMN with the focus of studying handover delay, although not in the context of rail transport.

1.6 Thesis organization

A comprehensive overview of CBTC is presented in Chapter 2, including the functions and components of a CBTC system and the role of radio communication in it. Besides the overall architecture of CBTC presented in Section 2.1, the reader is encouraged to read Section 2.4 and Section 2.5 that provides an overview of the challenges involved in enabling a continuous radio connection for the train in a CBTC system. Chapter 3 presents a detailed overview of the proposed network design. Chapter 4 includes an overview of the field experiment that was carried out simultaneously and involved the development of a real-life hardware prototype, due to its relevance to this PhD study. Chapter 5 presents an overview of the simulation setup, including the details of the simulation model used and the key KPIs implemented for the simulation study. The simulations study and the results are then presented in four chapters, namely Chapter 6, Chapter 7, Chapter 8, and Chapter 9, which loosely reflects the four phases of the simulation study. Finally, Chapter 10 presents the conclusions of this PhD study.

CHAPTER 2

Overview of CBTC

Unlike many other research and development areas, the state-of-the-art in CBTC is driven by the industry rather than the academia. In addition, due to the highly competitive nature of the industry, the amount of publicly available literature on this topic that openly discusses implementation details is highly insufficient. This chapter aims to present a comprehensive overview of CBTC, and in particular, the use of radio communication in CBTC. The available industrial and scientific literature on this topic was consulted for this purpose, besides the knowledge acquired from the author's own experience of working on the development of a CBTC system. Notably, this overview is based on [Farooq2017a] that presents a comprehensive survey and tutorial on the topic. It is mainly the tutorial part of the paper that has been reproduced here.

Section 2.1 presents an overview of CBTC, its function and components, and the role of radio communication in it. The reader is recommended to read this section at a minimum in order to be able to follow the rest of the work presented in this thesis.

Section 2.2 discusses the evolution of communication technologies for communication-based railway signalling.

CBTC systems have historically used IEEE 802.11 Wi-Fi as the radio technology, mainly due to its cost-effectiveness. In contrast to radio communication for non-safety related rail applications such as CCTV and onboard Internet, radio communication for safety-related application such as train control imposes stringer reliability and availability requirements. Section 2.3 discusses the historical reasons behind the success of Wi-Fi as the de-facto technology for CBTC despite its lack of support for mobility and susceptibility to interference. Roaming, being an inevitable reality in the CBTC systems, is discussed in Section 2.4.

Section 2.5 presents the best practices in the design and architecture of a CBTC radio communication network, and the measures to ensuring high system performance.

There has been a general lack of standardization efforts for CBTC, the result of which is that nearly all existing CBTC installations are incompatible, proprietary systems [9]. Although there exists an IEEE standard for CBTC [38], [39], it has not gained much attention from CBTC suppliers due to its limited scope. Section 2.6 presents an overview of the CBTC standardization efforts, alongwith a summary of the IEEE CBTC standard.

Finally, Section 2.7 presents a brief overview of the leading CBTC solutions and suppliers.

For the complete survey, a discussion of the relevant IEEE 802.11 parameters to optimize the radio communication performance in CBTC, as well as a summary of the

future research directions, refer to [Farooq2017a].

2.1 CBTC operation

In CBTC, continuous, high capacity radio communication is used to exchange train control information between the train and the wayside, enabling automatic train control (ATC) functions, namely automatic train protection (ATP) and automatic train operation (ATO).

The train continuously sends its current speed, direction, and location to the wayside over the radio connection. Based on this information received from all trains currently on the track, as well as a train's braking capability, the traffic control center at the wayside calculates the maximum speed and distance the train is permitted to travel, collectively known as "limit of movement authority" (LMA), and sends it to the train. Based on this information, the train onboard ATC equipment continuously adjusts the train speed and maintains the safety distance to any preceding trains. Thanks to this real-time information exchange, the trackside equipment used in conventional systems, such as color light signals and track circuits, is not needed, and can be removed.

The speed and location of a train is determined using a combination of devices such as speedometers, tachometers, transponders ("balises"), Doppler radar, odometers, and geolocation systems such as Global Positioning System (GPS) [40]. Location accuracy, in particular, is highly critical. Transponders or balises are fixed reference points mounted between rails. As a train passes over a balise, the location information is transmitted from the balise to the train using an antenna mounted under the train. Between the balises, location is continuously estimated using onboard odometry measurements. Any inaccuracies accumulated over distance are corrected when train passes the next balise [40]. The IEEE CBTC standard discussed in subsequent sections recommends a location accuracy of 5 to 10 meters [38]. There are a number of problems associated with using a geolocation system such as GPS as the primary means for localization. The location accuracy of geolocation systems might not be high enough, e.g. to differentiate trains traveling closely to each other. Satellite signals cannot be reliably received inside tunnels. Furthermore, CBTC suppliers are generally reluctant to depend on a system that is controlled by an external authority. Therefore, the use of a geolocation system in CBTC is normally supplementary.

2.1.1 Fixed block vs. moving block

In conventional railway signalling, tracks are divided into blocks (or "track sections"), and track circuits are installed to determine if a train is inside a block. Each block is protected by a signal. Various factors dictate the length of the block, including how busy the line is, the maximum allowed speed on that line, the maximum speed and braking capabilities of different trains, sighting, etc. When a train is inside a block, since there is no real-time method to determine its exact location inside the block, the entire block is declared as

occupied, and other trains are not permitted to enter it. As the boundaries of these blocks are fixed, regardless of a particular train's speed and braking capability, and are further reinforced by track circuits, this type of operation is called "fixed block operation" [40], [41].

In contrast, in the "moving block operation" employed in CBTC, thanks to the real-time communication between the train and the wayside, the train location is continuously updated. As a result, the occupancy zone—or block—"moves" with the train and reflects its actual location. There are no fixed blocks boundaries. As shown in Figure 2.1, this allows trains to run closer to each other.

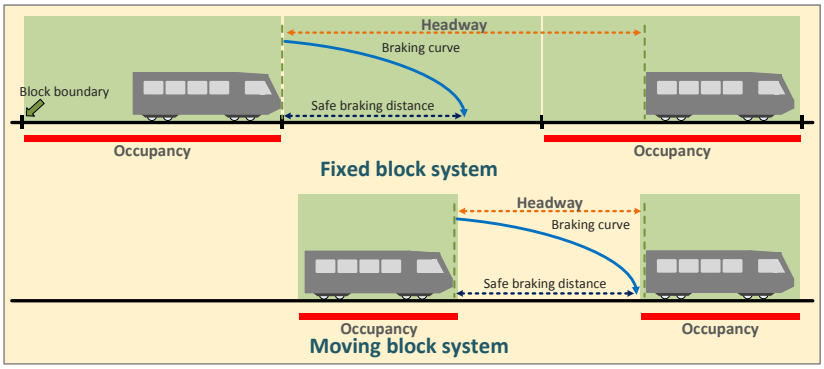

Figure 2.1: Fixed vs. moving block

2.1.2 The role of radio communication

Radio communication is generally unreliable. Designing a reliable train control system over an unreliable radio link is a challenging task. In conventional signalling systems, the distance between trains following each other is large, as seen in Figure 2.1. Thus a certain number of communication errors can be tolerated. However, in CBTC, headways are very short, which means in the event of a communication failure, a train may not receive the location of the train in front of it in time. In this situation, a typical approach in CBTC systems is to apply emergency brakes and then drive it in manual mode. In the worst case, this could trigger a chain-reaction with the following trains, all stopping [42], [43].

The timeout interval before emergency brakes are applied varies from project to project, depending on multiple factors, including the frequency of CBTC control messages. A typical value is between 5 to 10 seconds.

Compared to the conventional train control systems, in CBTC, the responsibility of determining a train's location has been moved from the track circuit to the train itself [41]. This train-centric location determination results in lower certainty. Previously, the train location was determined by the wayside (with the help of a track circuit), independent

of the train. On top of that, the fail-safe design of track circuits meant a failure was interpreted as a train presence. However, in CBTC, the wayside depends on the train to get the location information, which in turn depends on the radio communication [44]. The failure of the radio communication link, therefore, is highly critical for a functional CBTC system.

For these reasons, CBTC systems normally allocate a fixed "protection margin" in the calculation of their safe braking distance [38]. Additionally, CBTC systems normally employ a conventional train detection method as a fallback, for location determination in the event of a radio communication failure, as well as for non-CBTC trains operating concurrently with CBTC trains [41]. This is also a requirement of the IEEE CBTC standard discussed later. An example is the Copenhagen S-train CBTC system, which uses axle counters as fallback.

Radio communication failures lead to transmission errors and a large handover latency, resulting in packet delays and losses [43], [45]–[48], as further discussed in subsequent sections.

2.1.3 Data traffic requirements

The typical size of a CBTC control message is 400-500 bytes. A message transmission time of shorter than 100 milliseconds is normally supported. Given that the typical frequency of these messages is about 100-600 milliseconds, data requirement for a CBTC system is typically in the range of 20-40 kbps, and not more than 100 kbps [42], [49]–[55].

2.1.4 Components and networks

This section discusses the major components of a typical CBTC system, as well as the two-way communication network that connects the train and the wayside. This network further consists of the following three integrated networks: [43], [56], [57]

1. Train onboard network
2. Train-to-trackside radio network
3. Trackside backbone network

The train onboard network and the trackside backbone network use Ethernet, while the train-to-trackside radio network generally uses Wi-Fi.

2.1.4.1 Onboard components

This section discusses the major onboard components of a CBTC system, as shown in Figure 2.2. Together, these components comprise the train onboard network.

The onboard equipment includes Vehicle On-Board Controller/Computer (VOBC), sometimes also called Carborne Controller or Onboard Control Unit (OBCU). This system

is responsible for sending train control information to the wayside on periodic basis. It either includes, or works together with, the onboard ATP and ATO subsystems [38].

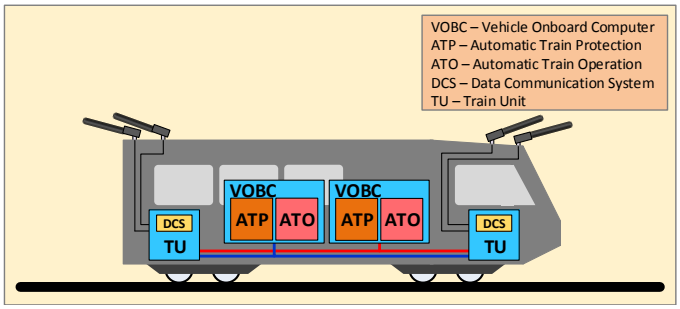

Figure 2.2: CBTC onboard components

The ATP and ATO subsystems are part of the onboard ATC functionality. ATP controls safety-related functions and ATO controls the actual train driving functions. Each of these has both onboard and wayside components.

As probably the most critical subsystem, the ATP subsystem helps prevent collisions as a result of the driver's failure to observe a signal or speed restriction. It monitors and controls the train speed and applies brakes if necessary. The ATO subsystem is responsible for automating the train operation, including basic operations normally performed by a driver, such as starting and stopping the train, energy-efficient braking and acceleration, and stopping accuracy.

Another critical onboard component is the Data Communication System (DCS), also referred to as Radio Communication System (RCS). DCS is typically a combination of software and hardware, including radios and antennas, and is responsible for the radio communication between the train and the wayside. DCS can either be a completely independent system or integrated into VOBC. If independent, the computer system running DCS is also frequently referred to as a Train Unit (TU).

2.1.4.2 Wayside components

Figure 2.3 illustrates typical wayside components of a CBTC system. The terms wayside and trackside are often used interchangeably. However, trackside generally contains the components located either on or close to the tracks, and is considered a part of the wayside.

A Zone Controller (ZC), or Wayside Controller, is responsible for controlling a particular zone in the railway network. Dividing the wayside network into multiple, independent zones, such that each zone comprises its own wayside infrastructure, improves availability even if one or more zones experience failures. The fundamental function of

a ZC is to maintain safe train separation in its zone. A ZC also typically includes the wayside ATP and ATO subsystems [8], [38].

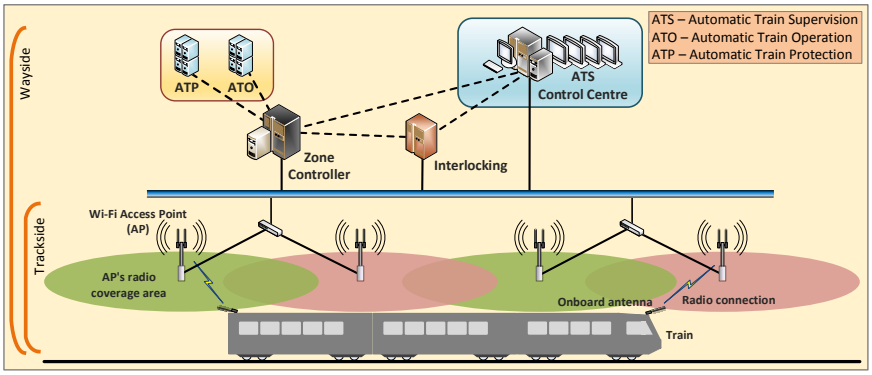

Figure 2.3: CBTC wayside components

The ATP subsystem of a ZC manages all the communication with the trains in its zone. It is also this subsystem that calculates the movement authority for every train in its zone. A Computer-based Interlocking (CI) system is either included as an independent system or as a part of the ATP subsystem. CI controls the trackside equipment such as point/switch machines and signals, and is responsible for setting routes for trains. The ATO subsystem provides all the trains in its zone with their destination as well as dwell times [8].

Independent from the ZC is the automatic train supervision (ATS) system, which is responsible for monitoring and scheduling the traffic.

Trackside is divided into multiple Wi-Fi cells, each served by one Access Point (AP). Figure 2.3 uses the green and red colors to differentiate the APs' radio coverage areas. In the later sections of this paper, they will be used to represent two different radio frequencies as well. APs are either deployed on one side of the track or both, in alternating fashion. Trains communicate to the APs through a radio connection. This constitutes a typical CBTC train-to-trackside radio network, and is considered the trackside part of the DCS system discussed above. APs are in turn connected to the wayside components through the trackside backbone network.

A typical configuration of the trackside backbone network is star-topology, as shown in Figure 2.4 (a), where each AP is connected directly to the wayside infrastructure using fiber optic cables [56], [58]–[63].

An advanced alternative is ring-topology, shown in Figure 2.4 (b) [64], [65]. This configuration minimizes cabling, as the distance between an AP and the backbone network is usually much larger than the distance between two adjacent APs. An inherent limitation of a ring-based network is that a single failed node can disrupt the whole network.

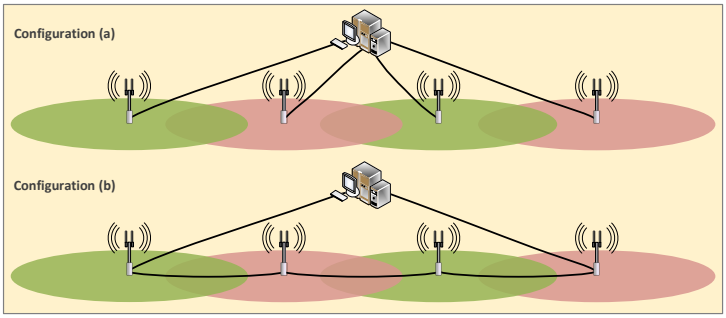

Figure 2.4: Star vs. Ring based trackside network

However, a number of Ethernet ring redundancy protocols, such as Media Redundancy Protocol (MRP), exist to mitigate this problem [66], [67]. Additionally, multiple rings can be employed to enable excessive redundancy, or to keep the number of nodes in a ring network under the limit.

2.2 The evolution of communication technologies for railway signalling

2.2.1 Conventional signalling systems

In a slightly evolved form of the conventional signalling, known as "track-based train control" (TBTC), rails are used for communication between train and wayside infrastructure. These systems use coded alternating current (AC) track circuits, also called audio frequency (AF) track circuits because of the range of the frequencies used, to modulate data [40], [68]. The train control data sent via rails is then used for cab-signalling—the feature of displaying signal aspect information to the driver inside the train—, and to enforce the permitted speed [41]. Since in these systems, track circuits are used to determine train location, this sort of signalling is also referred to as "track-circuit signalling". This technology can be considered an early form of communication-based train control. An immediate example is the driverless Copenhagen Metro.

However, the low resolution of train location determined by track circuits and the low capacity of rail communication leads to less accurate train location information. This results in larger headways to ensure safety and thus low line capacity. Typical headway in conventional train control systems is several minutes [5], [43].

2.2.2 Modern signalling systems

2.2.2.1 Inductive loop-based CBTC

Early CBTC systems in the 1980s used inductive loop as the communication technology [5], [69]. This type of signalling was also called "transmission-based train control" (TBTC) [8]. The first CBTC system was based on this technology, and was installed in Toronto, Canada, in 1985, on the Toronto Transit Commission Scarborough RT Line [5], [70]–[72]. Two other such early inductive loop-based systems were called VAL, deployed on Lille light metro in 1983, and Meteor, in service on Paris Line 14 since 1998 [73]–[75].

In these systems, inductive loop cables were mounted on tracks, and were coded with certain frequencies at regular intervals. The train verified its location by reading these signals via a detector mounted beneath it [40], [76]–[78]. As seen, this method could be considered an advanced alternative to the track-circuit signalling discussed above. For this reason, track-circuit signalling is occasionally argued to be a form of communication-based train control.

In contrast to today's CBTC systems that work in the GHz frequency range with Wi-Fi, inductive loop systems worked in the kHz range. However, despite its demerits, inductive loop is a proven technology that has been used for railways for three decades. It is cost-effective, as it uses unshielded standard wire, which is easy to repair. However, the downside is that it is not easy to install, and is vulnerable to vandalism and theft [71].

2.2.2.2 Radio-based CBTC

As discussed above, the modern CBTC systems use continuous and high capacity radio communication between the train and the wayside infrastructure to transmit train control information. The high resolution and highly accurate train location enables the "moving block" operation. The result is short headways and increased line capacity. A typical headway in CBTC systems is 90 seconds or less [5], [38], [43], [44]. Furthermore, it enables advanced features such as driverless and unattended train operations [41], [79].

The first radio-based CBTC system was supplied by Bombardier and was installed at San Francisco airport in 2003 [8].

Radio-based CBTC systems can roughly be divided into two categories: those based on the modern, high capacity radio communication—which can be further divided into custom and commercial-off-the-shelf (COTS) technologies—and those based on the older leaky waveguide technology.

Custom and Commercial-off-the-shelf (COTS) radio: Most of the earlier CBTC radio systems were custom solutions, built specifically to fit a project's requirements, and used a proprietary radio technology. An example is Andrew Corporation's Model 2400 radio solution, based on the leaky waveguide technology, used by Bombardier in its initial CBTC installations. Its cost was $22,000 (per radio), roughly 100 times the cost of a Wi-Fi based solution [71]. The downside of custom solutions is their lack of compatibility with systems developed by other suppliers. Later, Bombardier opted for a

spread-spectrum based COTS solution developed by Safetran Systems Corporation (now Siemens) [75], which cost only $1600, though still roughly 10 times the cost of a Wi-Fi based solution [71].

Similarly, to keep the radio system independent of a particular supplier, New York City Transit (NYCT) opted for a COTS solution for its Culver and Canarsie Line projects. The chosen solution was called RailPath, and was developed by Springboard Wireless Networks Inc. It was based on the spread-spectrum technology and operated in 2.4 GHz band [75], [80], [81].

The radio system used in the Copenhagen S-train CBTC system, called Airlink [64], is based on Wi-Fi. However, previous generations of Airlink still use proprietary custom-built radio technology, based on spread-spectrum and operating in the 2.4 and 5.9 GHz bands. The latest project using this spread-spectrum based system is the recently contracted NYCT's Queens Boulevard Line [82].

Leaky waveguide: A leaky waveguide is a coaxial cable with periodic openings in its shielding to allow radio signals leak out or in, thus acting as a continuous antenna. Leaky waveguide is also known as leaky feeder, leaky cable, or radiating cable. For decades, it has been successfully used to provide voice radio service in metros [71], [83].

Leaky waveguide offers certain advantages. Radio communication in open-air locations is unpredictable in general, as the propagation loss a signal experiences depends heavily on the obstructions it encounters in its way. Leaky waveguide involves very limited open-air communication, which takes place over a very short distance—normally in the range of 0.3 to 0.6 meters—between the leaky cable and the receiver antenna on the train. Thus, leaky waveguide guarantees a more predictable propagation loss and is less susceptible to interference [69], [84]–[86].

Given these advantages, certain railway operators have used a combination of radio communication and leaky waveguide. While radio communication is used in tunnels, leaky waveguide is used in open-air locations where interference is significantly higher, or in the critical locations where radio communication is exceedingly problematic [84]–[86]. An example is stations in tunnels, where several standing trains could obstruct the line-of-sight (LOS) path to the nearest AP. However, one challenge in these solutions is the seamless switching between the two technologies at the transit areas. A separate set of antennas must be used for each technology [85].

The downside with leaky waveguides is that they are not cost-effective and installation and maintenance requires lots of effort, especially in the congested tunnel environments [42], [85]. Furthermore, when installed in open-air locations, they are prone to signal degradation due to environmental effects such as rain and snow. For these reasons, leaky waveguide has not been proven very popular for CBTC systems [83].

2.3 Why radio/Wi-Fi for CBTC?

This section presents the major reasons radio, particularly Wi-Fi, has been chosen as the communication technology for CBTC, starting by summarizing its benefits and drawbacks first.

2.3.1 Benefits

The major benefits of radio-based CBTC systems include [5], [72]:

- High capacity — i.e. data throughput
- Low costs and easy upgradability — cost-effective radio equipment, easy software upgrade
- Less trackside equipment — e.g. as a result of removal of track circuits and axle counters
- Easy scalability — e.g. by adding more radio equipment
- Easy installation and maintenance — as a result of fewer cables
- Fault-tolerance/redundancy — e.g. through multiple radios, and overlapping radio coverage
- Low susceptibility to vandalism — as a result of fewer cables

In addition, the major reasons for choosing Wi-Fi as the radio technology include [61], [71], [72], [87]:

- Freely available Industrial, Scientific and Medical (ISM) frequency band
- A large vendor market and industry support
- Low costs — cost-effective and readily available COTS radio equipment
- Interoperability among multiple vendors, thanks to the Wi-Fi Alliance
- Open standard protocols

Contrary to mainline railway (i.e. long-distance, suburban trains), the number of trains in mass-transit is larger, also as a result of shorter headways. Therefore, mass-transit requires a higher capacity radio technology compared to GSM-R (Global System for Mobile Communications - Railway), adopted by the European mainline standard ERTMS [69].

While actual CBTC traffic itself does not demand high data rates, as discussed above in Section 2.1.3, it is still the key to enabling modern CBTC applications such as remote

diagnostics and maintenance, remote software upgrade, CCTV, transmission redundancy, as well as passenger infotainment applications such as onboard Internet. Data rate for supporting these applications can easily reach a few megabits per second per train. Wi-Fi, supporting data rates of up to 300 Mbps, not only fulfills this requirement but also has the capability to do so in the near future.

The underground nature of the mass-transit railway means it is not feasible to install antennas on high masts like in open-air locations. It is therefore inevitable to install numerous APs along the track to cover a large area. The availability of low cost COTS Wi-Fi equipment therefore has played a decisive role in the success of Wi-Fi for CBTC [9].

While the more advanced cellular technologies such as LTE may fulfill the data rate requirement, they are comparatively less cost-effective as it either requires the CBTC supplier to deploy their own network infrastructure or obtain the radio connection form a telecommunication company and pay on usage basis. Furthermore, providing radio coverage in the underground locations is problematic as the high frequency radio waves these technologies operate on cannot penetrate solid objects well.

It is worth pointing out that although significantly less compared to a conventional technology such as inductive loop, Wi-Fi equipment is still vulnerable to vandalism, nonetheless. In particular, the trackside APs, while enclosed in protective metal enclosures and mounted on masts, are still visible and in reach. Common examples are causing damage to the AP enclosure, and cutting the cables to the enclosure or to the AP antennas.

2.3.2 Drawbacks

A few of the drawbacks of choosing Wi-Fi include:

- Susceptibility to interference
- Requires stringent security measures
- Lack of support for mobility
- Short range
- Network congestion

Susceptibility to interference from other Wi-Fi and non-Wi-Fi users is a known issue (see next section). However, again, it proves to be less of a problem due to the underground nature of the mass-transit transport. In underground environments, the probability of interference from other users is comparatively lower and can be controlled more effectively [9].

Although the security concerns outlined here apply to any broadcast-based radio technology, the use of ISM band (see next section) makes them even more relevant to Wi-Fi. Appropriate security measures are required to be in place to prevent unauthorized

users from connecting to a CBTC AP with their Wi-Fi devices, sniffing the traffic, or stealing bandwidth resources. Of relevant concern are the jamming attacks that can disrupt the entire radio network, or the man-in-the-middle attacks where an intruder may pose as a legitimate CBTC AP, causing trains to connect to it. Authentication and end-to-end data encryption methods thus are highly critical. Therefore, relevant standards specifying appropriate security measures, such as EN 50159 discussed in Section 2.6, are normally implemented by CBTC systems.

The IEEE 802.11 standard was primarily developed to replace cables in local area networks such as office environments, and therefore inherently does not support mobility and large ranges [43]. Handover was therefore not considered. For this reason, the CBTC radio communication systems generally implement their own handover algorithms [50]. The generally low speeds of mass-transit trains further minimize this inherent lack of support for mobility in IEEE 802.11 [9].

In cellular networks such as GSM (Global System for Mobile communication) or LTE, the distance between a mobile node and a base station is normally large. Comparatively, in mass-transit, the distance between a train and a trackside AP is short, mostly due to the congested tunnel environments. This makes the short range of Wi-Fi less an issue [9]. The problem is further minimized by having large number of APs deployed on the trackside.

Poor Quality of Service (QoS) due to congestion in contention-based medium access networks such as IEEE 802.11 is a well-known issue, especially when the number of users is large. However, it is not as serious an issue in the CBTC scenario. It is unlikely that there is more than one train in a Wi-Fi cell at a time, because trains on rails cannot get too close to each other for safety reasons. This is due to the larger length of train compared to the size of a cell. Furthermore, in a typical configuration, only two radios transmit, one at each end of the train. The probability of both ends being in the same cell are therefore further decreased [50], [62], [63].

2.3.3 Frequency band and interference

Nearly all CBTC installation today work in one of the three, license-free ISM bands: 900 MHz, 2.4 GHz, and 5 GHz. Of these, 2.4 GHz is the most popular among CBTC suppliers, followed by 5 GHz [83]. Table 2.1 lists the ISM band frequency ranges together with their user applications [88]–[93].

2.3.3.1 Interference

Interference, both co-channel and adjacent-channel, is a well-known issue in Wi-Fi networks.

As discussed above, one major reason for choosing Wi-Fi is its use of the ISM band. This means railway operators don't have to worry about acquiring a license from a regulatory body.

Table 2.1: ISM frequency bands and users

Frequency range	Users
902 - 928 MHz	Microwave ovens, cordless phones, industrial heaters, military radar, RFID, IEEE 802.11ah
2.4 - 2.4835 GHz	IEEE 802.11b/g, microwave ovens, cordless phones, Bluetooth, garage doors openers, baby monitors, car alarms, printers, keyboards/mice
5.725 - 5.825 GHz	IEEE 802.11a/h
61 - 61.5 GHz	IEEE 802.11ad

In the US, these band has been designated by the Federal Communications Commission (FCC) as license-free, which means it can be used by anyone, without the need for acquiring a license. Some restrictions on the transmission power do apply though [94]. In Europe, similar regulations are applied by European Telecommunications Standards Institute (ETSI), Body of European Regulators for Electronic Communications (BEREC), and European Commission (EC).

However, since the number of users using a license-free band is significantly larger, there is a higher probability of interference from other users in the band. As an example, in a recent study [95] on Chongqing Rail Transit Line 1 in China, up to 1,300 unique SSIDs were observed over a period of one second—SSID (Service Set Identifier) is a sequence of characters that uniquely identify a Wi-Fi network (or AP). The increasing use of the 2.4 GHz band for CBTC systems by railway operators has therefore raised concerns. As an example, CBTC failures at Shenzhen Metro have been attributed to interference caused by the non-CBTC Wi-Fi users in the surrounding locations [96], [97]. Given these reasons, an RF (radio frequency) site survey is normally first conducted to determine the amount of interference before planning AP placement. However, the rapid and widespread proliferation of smartphones and other handheld devices means it is not trivial for such surveys to accurately predict the interference even in the near future.

To minimize adjacent-channel interference, adjacent APs in CBTC systems are deployed on alternating frequency channels. This is discussed in greater details in subsequent sections.

2.3.3.2 Licensing

Acquiring a licensed band is the optimal solution to prevent the risk of interference in CBTC systems. However, it is a lengthy administrative process with limited chances of success due to the scarcity of spectrum. The spectrum that is available exists in bands for which there is little or no radio equipment available. Allocation in these bands therefore would require a significant investment in research and development by radio vendors prior to deploying a fully functional CBTC system [83], [94].

There are a few exceptions though, notably the Copenhagen S-train CBTC system, for which the 5.925-5.975 GHz band has been licensed.

2.3.3.3 Factors for choosing a frequency band

In CBTC, choosing between 2.4 GHz and 5 GHz frequency bands is generally driven by the following factors:

- Availability of cost-effective radio equipment: Such equipment is more likely to be available at 2.4 GHz because of the large vendor market as discussed above. CBTC vendors will rather provide a communication system based on readily available COTS equipment than developing their own proprietary solution [83] .
- User density and interference: As discussed above, due to a significantly large number of Wi-Fi and non-Wi-Fi users, the 2.4 GHz band is much more prone to interference compared to the 5 GHz band, as seen in Table 2.1.
- Signal range: In general, the higher the frequency of a radio wave, the shorter the distance it can travel. Thus, the 2.4 GHz radio waves cover a substantially larger distance than the 5 GHz waves, with the same transmission power. This is due to the characteristics of high frequency radio waves that not only attenuate faster but also do not penetrate solid objects nearly as well as the low frequency waves. However, an advantage of high frequency signals is that since they do not travel as far, they also interfere less with the neighboring signals.
- Ease of installation: Operating frequency also drives the number of APs installed. The shorter signal range of 5 GHz radio waves means shorter distances between APs, resulting in a greater number of AP installations. Furthermore, frequency also drives the location and height of AP installation, due to the propagation characteristics discussed in Section 2.5.1.
- Number of available channels: When configuring frequency channels for adjacent APs, as a rule of thumb, non-overlapping channels are preferred to further limit the interference. However, only 3 and 4 non-overlapping channels are available in IEEE 802.11b (DSSS modulation) and IEEE 802.11g (OFDM modulation), respectively [98], [99]. Comparatively, IEEE 802.11a, which operates in the 5 GHz band, enables 23 non-overlapping channels [90].

2.4 Roaming in CBTC systems

In contrast to cellular communication, roaming in railway environments is not a mere possibility but is an inevitable reality. Even worse, unlike the cellular networks, Wi-Fi are short range networks, where larger networks are built by deploying more APs closely together. This means APs are placed at regular intervals on the trackside network, such

that their coverage areas overlap, and a train has to continuously find a new suitable AP and re-connect as it moves along.

A critical aspect of roaming in CBTC thus is how a radio communication system smoothly switches from one AP to another (i.e. handover), without causing interruptions and delays in the communication. As discussed above, a large handover latency might result in a delayed reception of the movement authority information, and the train might have to apply emergency brakes [38], [43].

Furthermore, since in CBTC it is very common to deploy adjacent APs on different frequencies, the radio communication system must switch between them when switching from one AP to another. This, combined with the high speeds of modern trains, results in rapidly changing channels, and renders the handover algorithms successfully used in the stationary Wi-Fi environments, inefficient for CBTC [50], [99].

2.4.1 Handover frequency and latency

The frequency of handover is determined by the distance between the two APs (or the AP coverage areas, see Section 2.5.1) and train speed. The handover in IEEE 802.11 is the so-called "hard handover", in which the mobile node breaks the current connection before establishing the next connection, resulting in delays and packet loss [43], [100]. High speed and short inter-AP distance result in more frequent handovers, further worsening the situation [63], [101].

Studies show that the number of packets lost due to handover is much larger than that due to radio propagation [50]. The authors in [43] propose a method for determining packet loss rate based on the handover time, the AP coverage range, and the overlapping coverage area between APs. They show that with a train speed of 200 km/h, the maximum handover time of 180 milliseconds, and the overlap area of 20 meters, the calculated packet loss rate is approximated to be 10%.

Handover time in CBTC is typically in the range of 70-120 milliseconds, with 1 second as an upper limit [43]. As long as this time is shorter than the CBTC control message interval discussed above, it does not impose a serious threat, as it only means one lost message in the worst case.

2.4.2 Roaming algorithm

Normally a smooth transition is achieved by equipping a train with at least two radios, one at each end, such that at least one of these radios is always connected to an AP.

In its simplest form, it works as follows. As the train moves, the front radio continues to search for a new AP. When it finds a new AP, it breaks the current connection and establishes a new one with the new AP (connection 1 in Figure 2.5), while the rear radio stays connected. Next, the rear radio switches the connection to the new AP (connection 2), while the front radio stays connected. Sophisticated roaming algorithms might develop some sort of a distributed algorithm to prevent both radios from roaming at the same time. Next, the first step is repeated and the front radio connects to a new AP (connection 3).

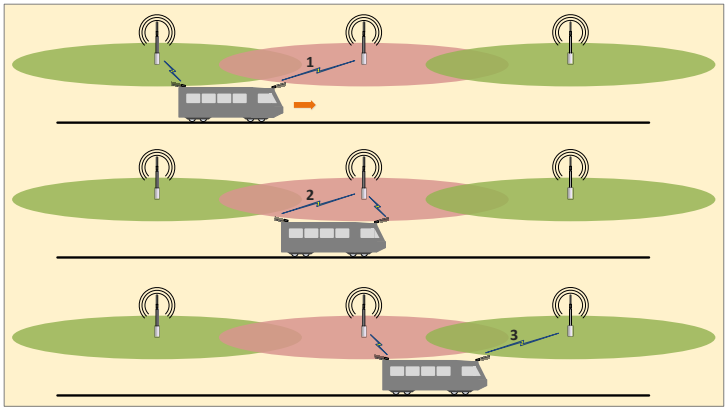

Figure 2.5: Roaming/handover in CBTC

An analogy is that of climbing a rope—or more accurately—a Tarzan-style swing from rope to rope.

However, before the execution of a handover, it must be detected, i.e. when to execute the handover. How this is achieved is not specified by the IEEE 802.11 standard, and therefore, CBTC systems typically develop their own roaming algorithm. Typical approaches are to monitor the quality of the link e.g. by monitoring the number of un-acknowledged packets (i.e. packet loss), or by monitoring when signal quality falls below a certain threshold [102]. A couple of approaches for the latter are to measure signal quality (e.g. by means of Received Signal Strength Indicator (RSSI)) from the beacon frames received from an AP, and to measure how consist the signal quality is, by monitoring the frame reception rate [51]. If more than one potential APs are found for the new connection, the same criteria is used to select the best AP among them. The highly dynamic environments of rail transport makes the detection of handover further challenging.

2.4.2.1 Roaming threshold

A typical approach in CBTC systems is to perform the handover as soon as the train receives a signal from a new AP, with the power above a certain threshold, even if the signal power of the current AP is greater and still increasing. This is illustrated in Figure 2.6, where, for example, a handover from AP-1 to AP-2 is performed at a time when the current signal power of AP-1 (red) is greater than that of AP-2 (green).

The objective mainly is to avoid the acute drop in the signal power as the train moves past the current AP. This is in part due to the misconception that uni-directional antennas don't have coverage at their backside, as implied in Figure 2.6 as well. However, this is far from reality. The "front-to-back ratio" antenna parameter specifies the ratio of radiations

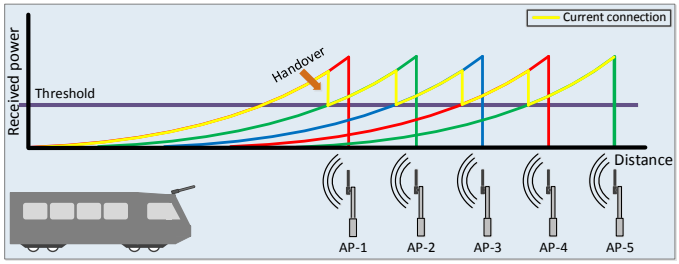

Figure 2.6: A typical roaming algorithm

transmitted in the forward direction to that transmitted in the backward direction [103]. For example, the HUBER+SUHNER Sencity SPOT-S antenna used in Copenhagen S-train CBTC has a front-to-back ratio of 20 dB [57]. This means, its coverage in backward direction is -20 dB worse than that in forward direction, but there is still coverage, except in the rare cases when it is entirely blocked by the mast on which the antenna is installed. This misconception leads to incorrect implementations of roaming algorithms, which connect to a new AP prematurely, anticipating an acute signal drop as the train moves past the AP.

Yet another approach is to use two different thresholds: a "leaving threshold" and a "joining threshold". The roaming is performed if the current AP's signal power falls below the leaving threshold and/or the new AP's signal power is above the joining threshold.

Nonetheless, these thresholds must be set carefully. A too low leaving threshold may result in a prolonged connection to the current AP. The result is a delayed roaming, which may lead to the train losing the signal altogether as it moves past the AP. A too low joining threshold can result in the train connecting to an AP with poor signal quality [72].

Note that if APs employ uni-directional antennas—see Section 2.5 for a detailed overview of different antenna configurations—the roaming performance also depends on the roaming direction. In Figure 2.7 (a), the direction of the train movement is the same as the antenna pointing direction on the APs. Thus, it allows sufficient time for the train to see the gradual decrease in signal strength and connect to a new AP based on the leaving threshold. In contrast, when roaming in the opposite—face-to-face—direction, as shown in Figure 2.7 (b), the train sees a gradual increase in signal strength. Nevertheless, it still needs to connect to the next AP based on the joining threshold, before it moves past the current AP. Otherwise, it might hold the connection to the current AP for too long and then disconnect abruptly [49], [72].

2.4.3 IEEE 802.11 handover

This section presents a brief discussion on the IEEE 802.11 handover mechanism, with the intention of highlighting potential improvements.

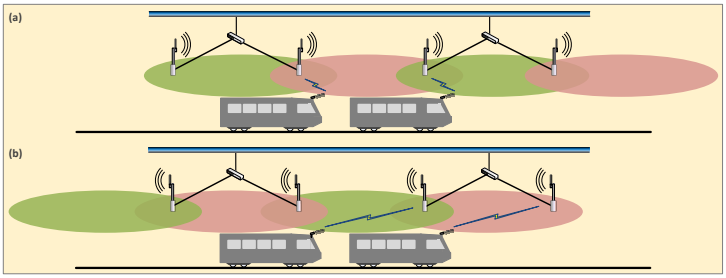

Figure 2.7: Roaming direction vs. antenna direction

Handover in IEEE 802.11 has 3 phases: (1) scanning, (2) authentication, and (3) re-association.

2.4.3.1 Scanning

Scanning is the process of finding a suitable AP to connect to. Of the three handover phases, scanning takes the longest time. As per studies, the latency of the scanning phase accounts for approximately 90% of the total handover latency [43], [104].

In passive scanning, a wireless node waits for the beacon messages sent by the APs to announce their presence. Passive scanning is slow as most hardware vendors set the beacon interval to 100 milliseconds, by default. In active scanning, the node sends probe request messages, to which nearby APs reply with probe response messages. Generally, in CBTC systems, active scanning is adopted to minimize the latency [43], [50]. However, since normally the node needs to probe all frequency channels (11 in 802.11b, for example), it still takes significant time [50].

The choice of frequency channels to use when deploying a trackside radio network is often independent of the development of the CBTC radio communication system. As a consequence, even if only two channels are used, it is not uncommon that a CBTC radio communication system is developed in a way to still scan all channels by default, to be on the safe side. One reason is that often these CBTC systems are either not customized for a particular customer's needs, or, are unaware of the actual channels used. In an adaptive approach, once having learned the channels, only these channels are used afterwards, only to fall back to all channels in case of failure to find an AP.

Different approaches are taken to reduce the time spent on scanning. Often a sort of background passive scanning is employed where the node learns about the next available APs while still connected to the current AP [105].

Due to the linear nature of a trackside radio network, the next AP to connect to can be pre-determined, provided that the train maintains an up-to-date database of AP information, and, all APs are in a healthy state.

2.4.3.2 Authentication

In the authentication phase, a node establishes its identity with the AP it found in the scanning phase, by exchanging special authentication messages. However, depending on the vendor implementation, this phase could take significant time, e.g. up to one second if an IEEE 802.1X [106] based centralized security architecture is used that involves communicating with an authentication server, such as RADIUS [107].

A few Wi-Fi products support the IEEE 802.11f [108] extension, also known as Inter-Access Point Protocol (IAPP). IAPP offers a pre-authentication method in which an AP, upon successful authentication with a node, shares the node's authentication information with the nearby APs [50]. The authentication process can thus be skipped when connecting to those APs subsequently.

In CBTC scenarios, where seamless handover is critical, one approach is to skip the authentication phase altogether. However, the drawback is that authentication then must be performed at packet level using a higher layer security protocol, such as IP Security (IPSec).

2.4.3.3 Association

In the association phase, the node registers itself to the AP by exchanging special messages, so that the AP could forward data to/from it. There is no room for improvement in this phase's latency as it is dictated only by the message transfer delay [50].

2.5 Radio network configuration

This section presents the best practices and some of the key parameters considered while designing a CBTC train-to-trackside radio network.

2.5.1 Inter-AP distance

Redundancy is critical to providing reliable radio communication in CBTC and is a deciding factor when planning the number and placement of the trackside APs, as well as the onboard radios. Redundancy is further discussed in Section 2.5.3.1. As the train's movement is fixed, the configuration of the train-to-trackside radio network is linear, which is helpful in reducing installation efforts. The APs are placed as close to the track as possible to get the best possible signal quality on the train and to avoid any obstructions in the line-of-sight (LOS) path. To provide continuous connectivity, the inter-AP distance, which is the distance between two adjacent APs, is chosen in a way that APs' coverage areas overlap. RF (radio frequency) link budget calculations are typically made to determine the inter-AP distance, and AP signal range plays a key role in these calculations [53]. As stated above, an RF site survey is normally subsequently performed to determine the number and placement of APs.

A common approach is to use a short inter-AP distance, as well as a high transmission power, to overcome interference from other devices/users.

To aid a smooth handover, the inter-AP distance is designed in a way that the train is always inside the coverage of at least two APs. Another advantage of a short inter-AP distance is that the front radio can hear not just the AP ahead of it, but also the next one. It increases the availability as the front radio has twice as many APs as it needs [83]. Note that the adjacent APs must be deployed on different frequencies to avoid interference in this case.

The following subsections discuss parameters affecting the inter-AP distance.

2.5.1.1 AP SIGNAL RANGE

Table 2.2 lists the "rule-of-thumb" ranges for the indoor and outdoor environments for IEEE 802.11b, which offers the largest ranges compared to the other most commonly used IEEE 802.11 standards, 802.11a and 802.11g [109].

Table 2.2: Rule-of-thumb IEEE 802.11b signal ranges

Mode	Modulation	Outdoor range (m)	Indoor range (m)
1 Mbps	DSSS	550	50
2 Mbps	DSSS	388	40
5.5 Mbps	CCK	235	30
11 Mbps	CCK	166	24
5.5 Mbps	PBCC	351	38
11 Mbps	PBCC	248	31
6 Mbps	OFDM	300	35
12 Mbps	OFDM	211	28
18 Mbps	OFDM	155	23
24 Mbps	OFDM	103	18
36 Mbps	OFDM	72	15
48 Mbps	OFDM	45	11
54 Mbps	OFDM	36	10

However, the range of IEEE 802.11 radio signal depends on various factors and can be enhanced.

The parameters such as the antenna height, transmission power, gain, and receiver sensitivity can be adjusted to enhance the signal range. Additionally, the signal range depends on the operating frequency, discussed in Section 2.3.3.3, and the propagation loss.

As a signal travels from a transmitter to a receiver, it incurs loss in signal power due to various propagation phenomena such as reflection, refraction, diffraction, absorption, and multipath effect, due to the environment and the obstructions in the way. Besides the height and location of the antennas, propagation loss is further dependent on the distance between the transmitter and the receiver [110].

When planning a CBTC radio network, all these parameters are used in the link budget calculations to determine the AP coverage. Note that, the aim with these calculations is often to provide a guaranteed, minimum number. To be on the safe side, often the worst-case propagation loss, as well as various "margins", e.g. "link margin" and "fade margin", are used in these calculations. As a result, a mere +6 dBm difference in the actual received power doubles the achievable distance. As an example, a study [111] found that the APs deployed for the Copenhagen S-train CBTC could be heard as long as 4 kilometers away, despite the link budget calculation of approximately 600 meters.

Nonetheless, mostly COTS radio equipment is used in CBTC systems which offers limited flexibility to adjust the above mentioned parameter values. Thus, to take into consideration that radio signals attenuate greatly due to various propagation phenomena, an effective range of only 200-300 meters is assumed in CBTC. The studies in [43] and [49] show that in poor propagation conditions, the probability that the received power falls below the receiver sensitivity increases when an inter-AP distance greater than 200 meters is used. Furthermore, the probability of receiving a signal of acceptable power level is greater than 95% when an inter-AP distance of smaller than 200 meters is used. Choosing a distance shorter than 200 meters, on the other hand, means higher costs as well as more frequent handovers.

For these reasons, typical inter-AP distances range from 100 to 600 meters, depending on the track and terrain topology, e.g. curves, elevations, slopes, obstructions, etc., and the transmission power used [61]. A study of CBTC installations show that an inter-AP distance of 200-300 meters is more common, however greater distances of more than 350 meters have also been seen [36], [43], [49]–[51], [56], [59], [85]. One example is the Copenhagen S-train CBTC where an inter-AP distance of approximately 600 meters has been used.

Additionally, significantly larger distances of up to 100 kilometers in point-to-point links can be achieved by adjusting the IEEE 802.11 MAC (Medium Access Control) layer parameters such as ACK (acknowledgement packet) timeout, slot time, and Contention Window (CW) size [112], [113]. See [Farooq2017a] for further details.

The above stated methods have widely been used to enable deployment of low-cost, long-distance Wi-Fi based wireless networks in rural areas. These kind of networks are formally known as "Wi-Fi over Long Distance" (WiLD) [112].

2.5.1.2 Receiver sensitivity

Receiver sensitivity is the minimum signal power required at the receiver antenna to demodulate the signal. The more advance the modulation scheme used is, the greater the signal power (or Signal-to-Noise Ratio (SNR)) required to correctly demodulate the signal [103].

Table 2.3 lists the receiver sensitivity requirements specified by the IEEE 802.11a standard, which is based on OFDM and operates at 5 GHz [12]. When making link

budget calculations, it is recommended that the receiver sensitivity values specified by the hardware manufacturer are followed.

Table 2.3: Receiver sensitivity requirements by the IEEE 802.11a standard

Data rate	Modulation	Coding rate	Minimum sensitivity (dBm)
6 Mbps	BPSK	1/2	-82 dBm
9 Mbps	BPSK	3/4	-81 dBm
12 Mbps	QPSK	1/2	-79 dBm
18 Mbps	QPSK	3/4	-77 dBm
24 Mbps	16-QAM	1/2	-74 dBm
36 Mbps	16-QAM	3/4	-70 dBm
48 Mbps	64-QAM	2/3	-66 dBm
54 Mbps	64-QAM	3/4	-65 dBm

Receiver sensitivity is directly related to a particular Bit Error Rate (BER), Packet Error Rate (PER), or Frame Error Rate (FER) [103]. As an example, the IEEE 802.11a standard states that the minimum required receiver performance at the 54 Mbps data rate is -65 dBm with a PER of 10% or less, as seen in Table 2.3.

2.5.2 Antenna configuration

An omni-directional antenna provides equal coverage in all directions, resulting in a wider coverage area, though the covered distance is short. In contrast, a uni-directional antenna provides coverage in a specific direction, resulting in a larger distance but a narrow coverage area. The type of antenna used varies across CBTC solutions.

2.5.2.1 Trackside antenna

In general, uni-directional antennas provide better coverage in the line-of-sight (LOS) environments and omni-directional antennas perform better in the non-line-of-sight (NLOS) environments, for example in tunnels with curves [114].

The use of omni-directional antennas on linear environments such as a trackside network provides a more "wide" coverage. Due to their short range, the train should only "see" one AP ahead of it, if the APs are appropriately spaced. This means faster and less complex roaming as the "AP selection" part of the algorithm can be avoided [72]. The obvious disadvantages are a large number of APs required to cover a given area, and higher susceptibility to interference from nearby users, e.g. Wi-Fi hotspots at train stations.

Often two uni-directional antennas are used instead, facing in opposite directions, as discussed subsequently in Section 2.5.3.1. It reduces the number of APs and makes for a more predictable, linear pattern, which suits well to a trackside network. It does offer

some challenges, however. The width of the coverage area of a uni-directional antenna depends on the size of the antenna's beamwidth. An AP antenna with a very narrow beamwidth means the train cannot see the AP before it is properly "aligned" to the AP's coverage area [72].

Both with uni-directional and omni-directional antennas, the train sees a gradual increase in the signal strength as it approaches the AP, followed by a slight drop while it is adjacent to the AP. However, where it differs is when the train subsequently moves away from the AP. In the case of an omni-directional antenna, the train sees a gradual decrease in the signal strength. In contrast, in the case of a uni-directional antenna, it sees a rapid drop in the signal strength immediately after moving past the AP [72] .

Depending on the track and terrain topology, APs are mounted on masts to provide optimal coverage as well as ease of maintenance [61]. The height of these masts ranges from 50 centimeters to the more typical 4 meters for underground installations, and 4-6 meters for open-air installation [42], [43], [49], [85], [115]. Often the antenna height is chosen to be reasonably above the level of the train roof, e.g. between 0.5 and 1 meter, to ensure that radio waves are not shielded by the train. Ray-tracing models can be employed to determine the desired height.

2.5.2.2 Onboard antenna

Antennas are generally installed at a sufficient height on the train roof so that the line-of-sight (LOS) path to the AP does not get obstructed by other trains. Generally uni-directional antennas are preferred onboard, for the reason discussed above. However, using uni-directional antennas on both AP and train might make roaming harder, as it means that their coverage areas have to be aligned perfectly to be able to see each other. For this reason, some CBTC systems use a combination of uni-directional and omni-directional antennas, e.g. uni-directional antennas on trains and omni-directional antennas on APs, or vice-versa [36], [52].

2.5.3 System availability

Since it is about railway operations and the safety of passengers, system availability is highly critical. It is no surprise that CBTC suppliers boast of 99.999% (6.05 seconds of downtime per week) or better system availability of their solutions, particularly of the radio communication systems [86], [116], [117].

2.5.3.1 Redundancy

In CBTC, redundancy is the key to high availability. The general rule is that at any given location on the track, minimum two APs shall be available to connect to. A train is typically equipped with two TUs (Train Unit), one at each end, to provide sufficient redundancy. Each TU is typically equipped with one radio, though solutions with two radios are also seen. Each radio is then equipped with one or two antennas.

As discussed in detail subsequently, redundancy is realized by the following various means:

- Two TUs per train
- Two radios per TU
- Two antennas per radio
- Two or more frequencies
- Redundant AP coverage areas
- Redundant APs per location
- Redundant AP/trackside backbone networks

Redundancy is additionally ensured by diversity. Having two antennas per radio, separated by a certain distance, provides spatial diversity, as two independent signals can be received at a given time, of which the stronger signal can be used. Antenna diversity helps overcome multipath fading [72], [110]. Additional spatial diversity is automatically provided by having two TUs per train, separated by the length of the train [69]. Employing two or more frequencies, as presented later in this section, is itself a form of diversity—called frequency diversity—as it decreases the probability that all signals in a particular area are corrupted in the same way. Likewise, a typical practice in CBTC of repeating the transmission of the same information, e.g. over different radios/antennas, is a form of temporal diversity [72], [110]. Yet another form of redundancy is the power redundancy. When using the multi-ring topology discussed in Section 2.1.4.2, to make the AP rings (or backbone networks) completely independent of each other, they are deployed with independent power supplies.

The following discussion presents an overview of some of the typical configurations employed in CBTC. In Figure 2.8 and Figure 2.9, presented for this purpose, the green and red colors of the AP coverage areas represent two different frequencies. Furthermore, the onboard antennas do not represent a specific antenna type, i.e. uni-directional or omni-directional, unless specifically stated.

Figure 2.8 (a) shows a configuration with no onboard redundancy. In this configuration, there is only one TU on the train, with one (uni-directional or omni-directional) antenna. The trackside AP also has one radio with one uni-directional antenna. Radio frequencies have been used in an alternating fashion. For example, an inter-AP distance of 300 meters implies that the distance between the two consecutive APs operating on the same frequency is 600 meters, which helps in minimizing the interference.

Note that on APs, the use of uni-directional antennas only in one direction as in Figure 2.8 (a) might lead to the famous "hidden node problem", where two nodes are in the range of a common node but not in each other's range. This makes the "carrier

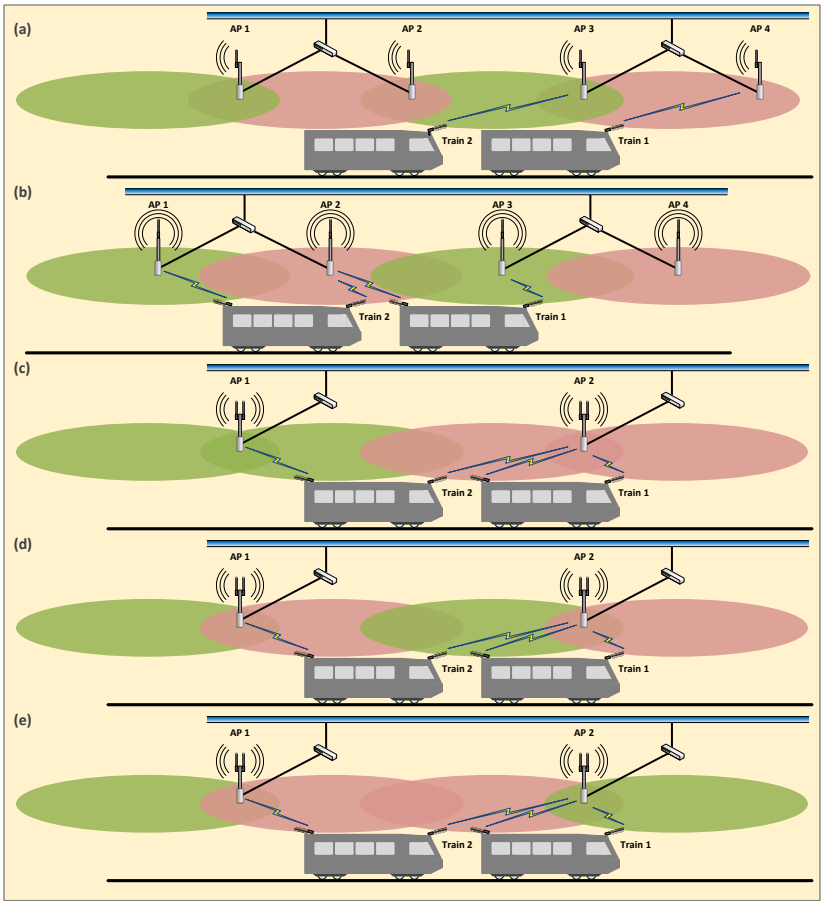

Figure 2.8: Configurations with no or only onboard redundancy

sensing" protocol CSMA/CA (Carrier Sense Multiple Access/Collision Avoidance) used to avoid collisions in IEEE 802.11 MAC ineffective, as the two nodes cannot hear each other. As discussed above in Section 2.5.1.1, it is not uncommon that the actual AP signal range is much larger than the "guaranteed" range. Let's suppose that in Figure 2.8 (a), AP 3's signal can be heard by a train currently in AP 1's coverage area. AP 1 and AP 3 cannot hear each other, because (1) AP 1's antenna is pointed in the opposite direction, and (2) it has a very low front-to-back ratio. This may lead to a situation where AP 1 starts transmitting, while AP 3 is already transmitting, resulting in a collision. This problem is solved in configuration Figure 2.8 (c) where AP 1 has an additional antenna in the opposite direction, allowing it to hear AP 3's transmission, and thus suspend its

transmission.

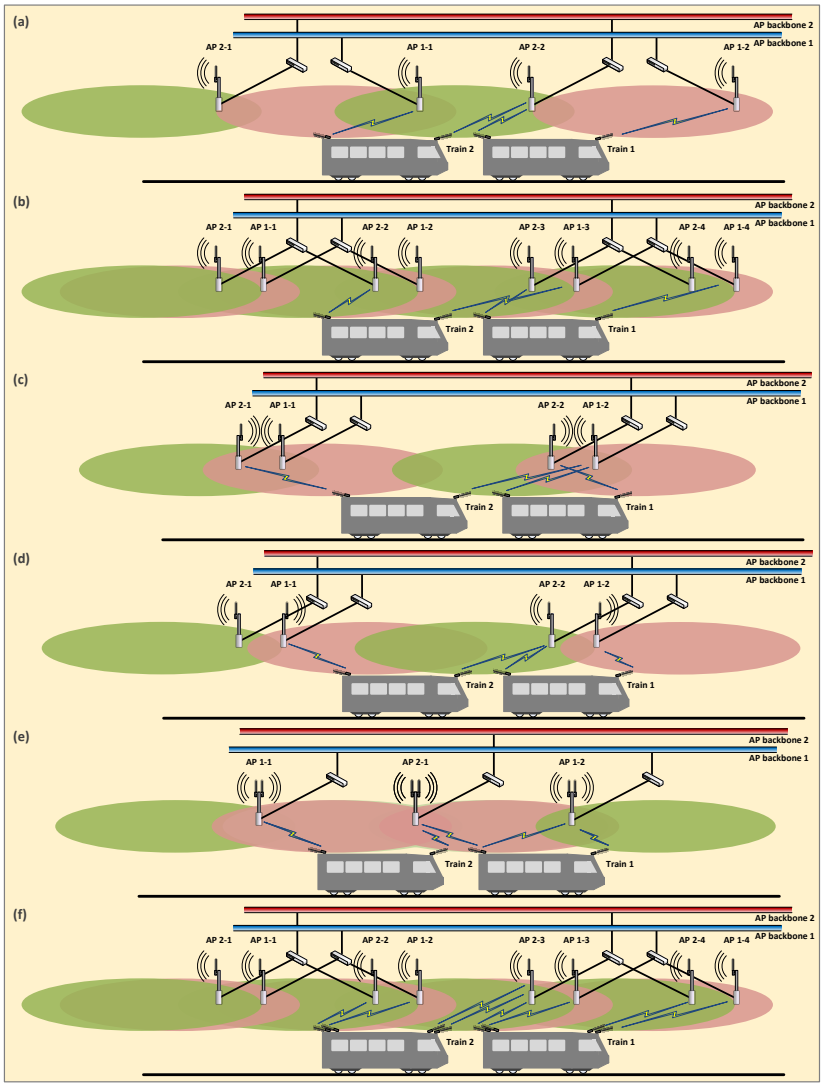

Figure 2.9: Configurations with both onboard and wayside redundancy

Figure 2.8 (b-e) presents configurations with onboard redundancy. Onboard redundancy is provided by having two independent TUs on the train, such that these TUs are connected to two different onboard networks, as seen earlier in Figure 2.2. The specific

configuration varies across solutions. In most configurations, both TUs are connected to APs all the time, where the second TU is either used to transmit simultaneously, as a fallback, or to connect to the next AP in advance. In certain solutions, TUs are purposely configured with different SSIDs so that they do not connect to the same AP.

A typical configuration, presented in Figure 2.8 (b), is to equip each AP with one radio and one omni-directional antenna. In contrast, the configuration shown in Figure 2.8 (c) uses two uni-directional antennas pointing in each direction, which extends the radio coverage. Compared to Figure 2.8 (b), there are half as many APs in this configuration to provide the same coverage area. The antenna configuration in Figure 2.8 (c) closely resembles that of the Copenhagen S-train CBTC system, which, with a radio coverage area of approximately 600 meters at each side, allows a distance of approximately 1200 meters between the two consecutive APs operating on the same frequency.

Figure 2.8 (d) shows a configuration in which each AP is equipped with two radios, enabling it to operate on two frequencies/SSIDs simultaneously. If TUs are configured with different SSIDs, this configuration is more suitable compared to the one in Figure 2.8 (c), in which the coverage area of a single AP might be large enough to cover the whole train, thus making it less likely for the two TUs to connect to different APs.

The hidden node problem discussed above appears here again. Since an AP's radios/antennas are on two different frequencies, AP 1 is still not able to hear what AP 2 transmits on the "green" frequency. Figure 2.8 (e) shows an alternative configuration that solves this problem by employing frequencies in the "ABBA" fashion, rather than the normal "ABAB" fashion. The placement of the same frequency antennas face-to-face improves the effectiveness of the CSMA/CA protocol. Additionally, the increased distance between the new potential hidden nodes, e.g. AP 1 and AP 3 (not visible in the figure), minimizes the probability of AP 3's signals reaching AP 1.

Figure 2.9 presents configurations with additional wayside redundancy. As shown in Figure 2.9 (a), besides the basic wayside redundancy in the form of overlapping coverage areas, additional redundancy is provided by deploying two separate AP backbone networks, and placing APs in the two networks in alternating fashion [63], [100]. The failure of one network thus does not affect the other. Note that this very much resembles the multi-ring topology discussed in Section 2.1.4.2.

The configuration in Figure 2.9 (b) adds two additional levels of redundancy: (1) improved coverage redundancy, as there is a greater overlap between the coverage areas of the neighboring APs, and, (2) AP redundancy, as there are two APs at each location. Even a complete failure of one of the backbone networks won't affect the coverage. Nonetheless, this additional level of redundancy comes at the expense of an increased—twice as many—number of APs.

If the two TUs are configured to connect to APs in different backbone networks, as shown in Figure 2.9 (b), the result is less frequent handovers, as handover is required only when both TUs lose connections. Note that when two APs are placed next to each other in this fashion, their antennas can point to the same direction, as in Figure 2.9 (b), or in opposite directions, outward or inward, as in Figure 2.9 (c) and Figure 2.9 (d) [63], [100].

As discussed before, normally uni-directional antennas are believed to be highly directional, with no coverage at their backsides. The objective behind installing antennas pointing inward seen in some configurations [100], as in Figure 2.9 (c), is to avoid this blind spot. However, as discussed in Section 2.4.2, uni-directional antennas are not that directional in real life. Thus, instead, the coverage behind antenna looks more like as shown in Figure 2.9 (d).

Figure 2.9 (e) shows a configuration with a complete coverage redundancy. A close examination of the figure shows that there is a near 100% overlap of the coverage areas of the neighboring APs—half of the coverage areas of AP 1-1 and AP 1-2 (green) are completely hidden by the coverage area of AP 2-1 (red). Note that this is fundamentally the same configuration presented earlier in Figure 2.8 (c), except that the inter-AP distance has been reduced greatly to enable this near complete overlap. The Copenhagen S-train CBTC system uses a similar coverage area overlap.

Finally, Figure 2.9 (f) presents the same configuration as in Figure 2.9 (b), except that it enables additional onboard redundancy by using two radios/antennas per TU instead of one, allowing four simultaneous connections at a time.

2.6 Standardization

The IEEE 1474.1 standard [38], [39], originally published in 1999, defines performance and functional requirements for CBTC. An additional standard 1474.3 [118], published in 2008, defines recommended practice for CBTC system design and functional allocations. However, unlike European Union's standard for mainline railway operations, ERTMS, the IEEE CBTC standard serves as mere guidelines, and is not strictly followed by the suppliers. As a result, nearly all existing CBTC installations are incompatible, proprietary systems [9]. As an example, of all the CBTC supplier advertisement material consulted for this study [64], [65], [74], [116], [119]–[133], only Ansaldo STS's [126] claims to be compliant to the standard.

Additionally, International Electrotechnical Commission (IEC), and its counterpart in Europe, European Committee for Electrotechnical Standardization (CENELEC), are responsible for the development of standards for the rail industry [134]. These standards address both general, safety related, and software related requirements [5], [135]–[142]. Table 2.4 lists the relevant standards, with equivalent standards listed next to each other [143], [144].

In the US, American Railway Engineering and Maintenance-of-Way Association (AREMA) is responsible for the development of a manual for recommended practices in railway. Sections 21-23 of this manual address communication-based signalling [145].

European Union's research project MODURBAN [146] has similar objectives to develop core system architecture and key interfaces for urban guided rail systems.

Table 2.4: IEC and CENELEC standards

Description		IEC	CENELEC
Urban guided transport management and command/control systems	System principles and fundamental concepts	62290-1	
	Functional requirements specification	62290-2	
	System requirements specifications	62290-3	
Communication, signalling and processing systems - Safety-related communication in transmission systems			50129, 50159
Specification and demonstration of reliability, availability, maintainability and safety (RAMS)		62278	50126
Communication, signalling and processing systems - Software for railway control and protection systems		62279	50128

2.6.1 IEEE CBTC standard

This section outlines a few key and relevant requirements from the IEEE CBTC standard 1474.1.

Table 2.5: IEEE CBTC guideline parameters

Category	Parameter		Typical value
Performance limitations	Maximum number of trains that can be handled by a Zone Controller		10 to 40 trains
Location	Onboard train location measurement	Resolution	$\pm$ 0.25 m to $\pm$ 6.25 m
		Accuracy	$\pm$ 5 m to $\pm$ 10 m
	Resolution of wayside calculated movement authority limits		$\pm$ 0.25 m to $\pm$ 6.25 m
Speed	Onboard speed measurement	Resolution	$\pm$ 0.5 km/h to $\pm$ 2 km/h
		Accuracy	$\pm$ 3 km/h
	Resolution of wayside calculated speed limits		$\pm$ 0.5 km/h to $\pm$ 5 km/h
Communication delay	Delay in train control messages, in both directions		0.5 s to 2 s
Equipment reaction time	Wayside		0.07 s to 1 s
	Onboard		0.07 s to 0.75 s

2.6.1.1 Definition

The IEEE standard defines a CBTC system as a continuous, automatic train control system with the following primary characteristics:

- High-resolution train location determination, independent of track circuits
- Continuous, high capacity, bi-directional train-to-wayside data communications

- Train-borne and wayside equipment capable of implementing ATP functions, as well as *optional* ATO and ATS functions

2.6.1.2 Performance and functional requirements

The standard states that in the event of equipment or data communication failure, trains shall continue to move safely, in degraded mode, e.g. at reduced speeds, with the help of a supplementary wayside system (i.e. for train detection).

Additionally, the standard specifies a number of parameters to achieve high level of performance, along with their typical values. Table 2.5 lists some of the most relevant parameters.

Equipment reaction times include the time required to calculate new movement authority limit at the wayside after receiving a location update from the train, and the time to determine a new ATP profile on the train after receiving a new movement authority limit.

The standard states that the CBTC equipment shall have a design life of 30 years. Additionally, a CBTC system shall enable, among others, the following to provide for ease of maintenance.

- Maintenance and diagnostic capabilities, including remote diagnostic capabilities
- Built-in test capabilities
- Timely identification of failed components and functions
- Data logging, enabling recreation of the events leading to an error
- Periodic verification of ATP hardware/software/data

The standard specifies parameters for developing a safe braking model, and provides with an example of a typical model as well. The safe braking model must take into account any location inaccuracies, e.g. due to interruptions in the radio communication.

2.6.1.3 Radio communication requirements

The standard states that the quality of the radio communication link between the train and the wayside shall be verified periodically.

The following functional requirements are specified. The communication link shall be able to:

- Support all required ATP, ATO, and ATS functions
- Provide continuous coverage, including in tunnels, cuts, elevated structures, and slopes
- Support bi-directional data transfer with sufficiently low latency
- Support safe, timely, and secure delivery of train control messages

2.7 CBTC projects and solutions

Currently over 150 radio-based CBTC projects exist worldwide, including both operational and ongoing projects. Figure 2.10 shows a breakdown of these projects according to the regions and suppliers [8], [64], [116], [147]–[151].

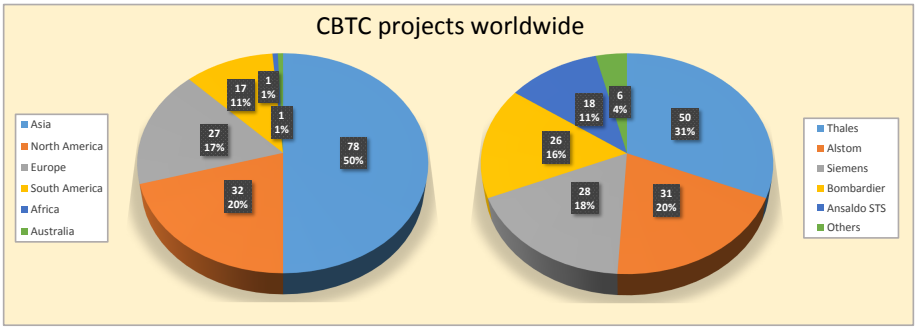

Figure 2.10: CBTC projects worldwide

Table 2.6 lists the names of the major CBTC solutions as well as their individual components, including the radio communication systems and the frequency bands used (for a complete version, see [Farooq2017a]) [44], [64], [65], [74], [83], [116], [119]–[133], [152].

Table 2.6: CBTC suppliers and solutions

Supplier	CBTC solution	DCS	Frequency band
Siemens	Trainguard MT	Airlink	2.4, 5.8 & 5.9 GHz
Bombardier	CITYFLO 450, CITYFLO 650	–	2.4 GHz
Alstom	Urbalis 400, Urbalis Fluence	–	2.4 & 5.8 GHz
Thales	SelTrac	ComTrac	2.4 GHz
Invensys (now Siemens)	Sirius	–	900 MHz & 2.4 GHz
GE (now Alstom)	Tempo	–	–
Hitachi	–	–	2.4 GHz
Ansaldo STS	–	–	–

GE Transportation and Hitachi are two comparatively young players in the CBTC market. GE Transportation has recently become a part of Alstom [153]. On the other hand, Hitachi now partly owns Ansaldo STS [154].

2.8 Summary

Radio communication plays a key role in the modern communication-based signalling systems as it connects train to wayside to transfer high resolution and real-time train control information. With the help of this information, CBTC offers a number of major benefits over a conventional signalling system, namely, shorter headways resulting in greater capacity, fewer trackside equipment, greater punctuality, improved safety, and support for automated train operations. This chapter presented a comprehensive tutorial of CBTC and the state-of-the-art of the use of radio communication in it. An overview of the evolution of communication technologies for railway signalling compared the radio-based communication to the early inductive loop-based and leaky waveguide-based communication. While these early technologies incur high installation and maintenance costs, the greatest challenge with the radio-based communication is interference. A thorough examination of the benefits and drawbacks of using a radio communication technology, in particular IEEE 802.11 Wi-Fi, for CBTC, showed that the success of Wi-Fi can mainly be attributed to its high data rates, ease of installation and maintenance, and its cost-effectiveness as a result of readily available COTS radio equipment and license-free operation. On the other hand, the susceptibility to interference, lack of support for mobility, and short signal range are some of its disadvantages. The chapter included an overview of the fundamental components of a CBTC system, both onboard and wayside, as well as the three types of networks involved. A comparison of the Wi-Fi based radio equipment to the early COTS and custom-built equipment proved the former to be of orders of magnitude cheaper. An in-depth overview of the CBTC radio network configuration showed that although a typical inter-AP distance in CBTC is only 200-300 meters because of the short range of Wi-Fi signals, significantly longer range of up to various kilometers could be achieved by adjusting various parameters. An evaluation of the alternative designs and topologies for the train-to-trackside radio network showed that redundancy is the key to providing high availability in CBTC, and the availability can be increased dramatically by ensuring redundancy at multiple levels. Roaming in a CBTC environment is an inevitable reality due to the short range of Wi-Fi networks and the high speeds of trains. Thus, a smooth handover from one Wi-Fi AP to another is a critical requirement. The IEEE 802.11 standard was primarily developed for stationary users within a limited area, and therefore inherently does not support mobility. The chapter presented an overview of the roaming algorithm designs for CBTC that showed that a complex and intelligent roaming algorithm is thus a critical component of a CBTC radio communication system. A summary of different standardization efforts for CBTC has been included. With the intention to bring more attention to the IEEE CBTC standard, a brief summary of the standard has been presented, including the guideline parameter values for optimal performance.

CHAPTER 3

Proposed Network Design

This chapter provides a detailed overview of the proposed design for a CBTC trackside network. It is noted that the design was developed at Siemens and proposed before the commencement of the PhD studies. The author was not formally involved in the development of the design until then. However, later on, once the PhD studies had started and the author got involved, the design was documented in a greater detail and a number of the aspects of the design were elaborated and refined.

Figure 1.2 and Figure 1.3 from Chapter 1 have been reproduced here as Figure 3.1. Figure 3.1 (a) illustrates the conventional design for a CBTC trackside network and Figure 3.1 (b) presents a simplified view of the proposed design to illustrate the fundamental idea behind the design.

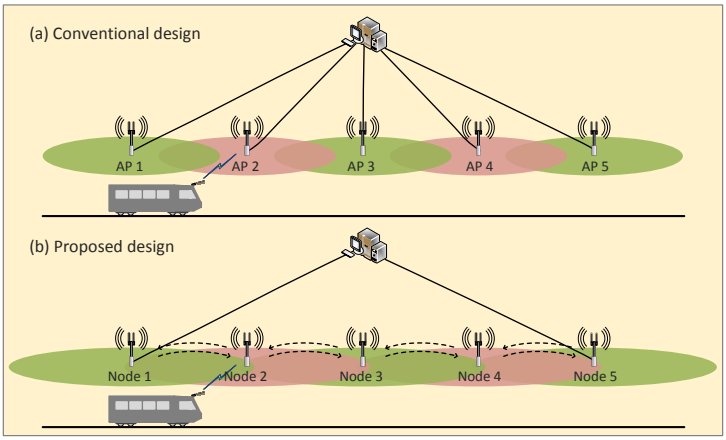

Figure 3.1: CBTC trackside network: Conventional vs. proposed design

The fundamental idea behind the proposed design is to take advantage of the broadcast nature of radio communication to present a replacement for the conventional design which involves excessive wired connections to connect each trackside AP to the wayside infrastructure. Thus, at its basic, a train broadcasts packets which are then picked up by a node in the chain and forwarded to its neighboring node, and so on, as illustrated in Figure 3.1 (b). No AP scanning and association are thereby required. This saves the

train 70-120 milliseconds—the typical handover latency in CBTC as noted in Chapter 2—every time it transmits to a new node in the chain.

Essentially, Figure 3.1 (b) illustrates the conventional multi-hop ad-hoc network where all nodes operate on the same frequency, as discussed in Chapter 1.5. There lie two major challenges with this approach.

1. If all nodes transmit on the same frequency, the probability of interference rises sharply. Additionally relevant is the well-known *hidden node problem*.

2. A single failed node results in a practically broken chain (i.e. a single point of failure).

In a hidden node problem, two nodes are in the transmission range of a common node but not in each other's range. Since they cannot hear each other, it effectively renders the Carrier Sense Multiple Access/Collision Avoidance (CSMA/CA) mechanism used in IEEE 802.11 MAC to avoid collisions ineffective. For example, in Figure 3.1 (b), Node 1 and Node 3 are within Node 2's transmission range but not in each other's range. The consequence of this is that Node 1 and Node 3 might start transmitting to Node 2 simultaneously, without being able to hear the other node's transmissions, and thus resulting in collisions at Node 2.

In the conventional infrastructure Wi-Fi networks, this problem is solved by employing the Request to Send/Clear to Send (RTS/CTS) mechanism. There are two reasons why the RTS/CTS mechanism is not applicable in the context of the proposed solution. Firstly, for this mechanism to work optimally, all the nodes that might interfere must be in the transmission range of the node that sends the CTS message, such as an AP. However, as previously discussed in Section 1.5, this is not the case in an ad-hoc and multi-hop scenario where nodes are not necessarily in each other's range, such as the one shown in Figure 3.1 (b). Secondly, the idea behind the proposed design is to use broadcast transmissions, in which case the RTS/CTS mechanism is irrelevant.

To address the above mentioned challenges, a novel design is proposed, as outlined in the following sections.

3.1 The proposed network design

This section provides a detailed overview of the proposed design. In the context of this PhD study and while disseminating the results, the proposed design has been referred to as *a multi-radio, multi-hop ad-hoc radio communication network for Communications-Based Train Control (CBTC)*.

3.1.1 Frequency separation and redundancy

To solve the interference problem, the proposed design uses three frequencies to ensure a certain separation between nodes transmitting on the same frequency just like the

frequency-reuse in cellular networks. Each node is equipped with three radios, all operating on different frequencies. The two side radios use uni-directional antennas one in each direction. These radios are used both for transmitting and receiving. The third top radio is equipped with an omni-directional antenna and is used only for receiving. Figure 3.2 illustrates this configuration where the colors red, blue and green represent three frequencies.

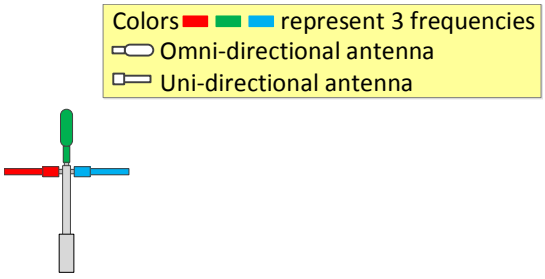

Figure 3.2: Node with three radios each operating on a different frequency

Essentially, an omni-directional antenna is used on the top radio—instead of a uni-directional antenna—to be able to receive from the nodes on both sides.

Transmissions are made not only to the immediate neighbor node but also the following node. The three frequencies are then used in an alternating fashion on subsequent nodes. Figure 3.3 illustrates the mechanism. The arrows on the lines indicate the direction of the transmission. Note that the two transmission lines coming out of, for example, Node 1's right radio (blue), are shown only to emphasize that the transmissions are received on both Node 2 and Node 3. Nonetheless, in reality, it will be one broadcast transmission received at both nodes. As seen in Figure 3.3, the function of the top radio is to receive transmissions from the immediate neighbor and that of a side radio is to receive from the second neighbor.

A predefined address included in each packet indicates the direction of the traffic flow. The three radios on a node work cooperatively. As a radio receives a packet, depending on the direction of the traffic, it delivers the packet to the correct side radio (i.e. left or right) which transmits it further. This forms a "rope-like" interleaving.

As seen in Figure 3.3, the radios transmitting on the same frequency on two adjacent nodes face opposite—e.g. red radios on Nodes 1 and 2—thus ensuring frequency separation with the help of uni-directional antennas. The 2-node transmission range solves the single point of failure problem and introduces redundancy to the design as the same packet is received by two nodes rather than one. It further solves the hidden node problem by ensuring that two nodes transmitting to a third common node are always in each other's range. Specifically, if Node 1 right radio and Node 3 left radio intend to transmit to Node 2 top radio, the CSMA/CS mechanism will prevent them from transmitting simultaneously

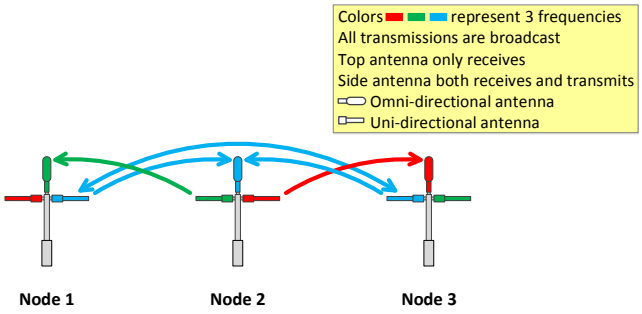

Figure 3.3: A network of three nodes

as they are in each other's range and therefore can hear each other. Furthermore, due to the frequency separation, now at any given location, there are at most only two radios to compete for the medium, e.g. Node 1 right radio and Node 3 left radio, Node 2 right radio and Node 4 left radio, etc, as shown in Figure 3.4 presented in the following section.

3.1.2 Node types: Chain node and terminal node

The node type discussed above is referred to as a *chain node*, as these nodes are what make the chain. A second type of node is the *terminal node*, which is either a train or a TCC (Traffic Control Center). Basically, it is the node that uses the chain network to get its packets transferred to another terminal node at the other end of the chain. A train intends to send packets to the TCC, and a TCC intends to send packets to one or more trains. A train travels along the chain and broadcasts packets, which are then picked up by a chain node, and following the chain, arrive at TCC. Likewise, packets sent by TCC follow the chain in the opposite direction and are picked up by a passing train. Note that a TCC is a stationary server machine connected to a node at the end of the chain using a wired connection, typically through the wayside backbone network. Therefore, it does not use radio communication.

While a chain node transmits only on two frequencies (in one direction each), a train transmits on all three frequencies, as illustrated in Figure 3.4 that shows a scenario in which a train transfers packets to a TCC node over a chain of five nodes. Note how the three-frequency design ensures a frequency separation distance of 3 nodes, e.g. the blue frequency is used by Node 1 and Node 4.

The reason why a train transmits on three frequencies in contrast to a chain node is that the train shall be able to communicate to the chain regardless of what direction or position the train is travelling relative to the chain. For example, let's suppose that the train transmitted on only one frequency. It might lead to a situation where the train meets a node whose respective antenna is a side antenna that faces opposite and—since it is a uni-directional antenna—cannot hear the train's transmission. This is shown in Figure 3.5

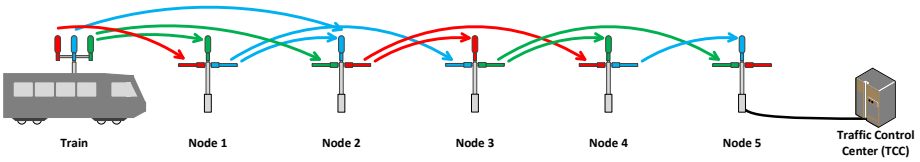

Figure 3.4: A train node transfers packets to a TCC node over a chain of five nodes (a uni-directional traffic flow)

where Node 1 is not able to receive transmissions from the train. For packets flowing from train to the chain, it is not a problem as Node 2 is still able to receive from the train. However, note that the top radio is not used for transmitting but only receiving. Thus, for traffic flowing in the opposite direction, train will not be able to receive from either of the two nodes, as they will transmit on the red and green frequencies but the radio on the train is operating on the blue frequency.

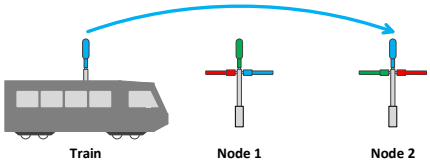

Figure 3.5: Node 1 is not able to receive train's transmissions in a possible scenario if train transmitted on only one radio

Thus, the design requires that the train must transmit on minimum two frequencies, as in this way, a chain node with any of the three possible frequency combinations will be able to receive from train on minimum one frequency. Nonetheless, to maximize the availability further, the design dictates that the train transmits on all three frequencies. The consequences of using fewer than three radios on the train are discussed later in Chapter 7 together with the results from simulation experiments. For the same reason, in contrast to a chain node, all three antennas on a train are omni-directional, as shown in Figure 3.4. It shall be noted that the same affect can be achieved by using uni-directional antennas as well, such that instead of using one omni-directional antenna per frequency, two uni-directional antennas will be used to cover each direction (i.e. left and right). However, the consequence will be that the train must then be quipped with six antennas instead of three.

As shown in Figure 3.4, note that for simplicity, it is assumed that the train is located at the end of the chain. Nonetheless, in real-life, the train will travel along the chain.

3.1.3 Addressing and forwarding

The terminal nodes are assigned predefined addresses different than those assigned to the chain nodes. In this way, a node upon receiving a packet is able to distinguish if the packet was transmitted by a terminal node or a chain node.

There are two types of destination addresses involved in the design: the actual destination address—which will always be of a terminal node—and an address that indicates the direction of the packet flow. This so-called *direction address* is added to each packet and is one of *left*, *right* and *both*.

When a train transmits, it uses *both* as the direction address. A chain node, upon receiving a packet from a train, creates a copy of the packet, replaces the direction in the packets with *left* and *right*, and forwards the packets one in each direction. Thus, one of these packets is transmitted in the backward direction, a mechanism referred to as *backward forwarding* subsequently in this study. Note that to ease the installation and maintenance efforts, a chain node must be deployed in a way that it is unaware of its location in the chain. Thus, forwarding the packet in both directions ensures that it takes the shortest path to TCC. The following chain node (in each direction) upon receiving this packet continues to forward it in one direction.

3.1.4 Duplicate packets

An inherent result of the redundancy in the design is the duplicate packets, which are both a requirement and a problem. Specifically, if each node forwards the duplicate packets, they quickly grow exponentially along the chain and congest the network. For example in Figure 3.4, Node 1 will receive two copies of the same packet from the train. Next, Node 2 will receive four copies of the same packet, two forwarded by Node 1 and two received directly from the train. Likewise, Node 3 will receive six copies of the same packet, and so on. Specifically, three types of duplicate packets exist:

1. Type 1: A node receives multiple copies of the same packet from two different nodes.

2. Type 2: A node receives multiple copies of the same packet from the same node.

3. Type 3: Packets sent by a node in the forward direction are received on a previous node in backward direction, due to antenna issues.

In Figure 3.4, example of duplicate type 1 is when Node 3 receives one copy of a packet from Node 1 (blue) and another from Node 2 (red). Example of duplicate type 2 is when Node 1 receives two copies from the train on its left (red) and top (green) radios. However, note that for type 2, the sending node is always a train, because only a train could be heard by the same chain node on more than one frequency. Node 2 in Figure 3.4 receives duplicates of both types 1 and 2. It receives two copies from the train directly and one copy from Node 1.

Duplicate type 3 is a special case which is defined as when on two neighboring nodes, the side antennas that are facing opposite are able to hear from each other. An example is when a packet sent by Node 2 right (red) is received on Node 1 left (red). However, since uni-directional antennas are used on the side radios, the probability of duplicate type 3 is negligible, as it will only happen if the antenna is faulty, e.g. have directivity issues due to a really low gain, or due to an error while installing a node in a way that the antennas point in the wrong (opposite) direction.

Thus, to avoid the above situations, in the proposed design, duplicate packets are eliminated at each node with the help of a unique sequence number included in each packet.

Note that even though Figure 3.4 shows TCC placed directly next to the chain, in reality, as described in Section 3.1.2, a TCC will be connected to the chain typically through the wayside backbone network, which will resemble more the illustration in Figure 2.3. Likewise, note that in Figure 3.1 (b), the TCC is illustrated as connected to both chain ends for the sake of simplicity. In real-life, the TCC might as well be connected to only one end of the chain, especially if the chain size is within the reasonable limits. Nonetheless, in the case that the two ends of the chain are connected to the same TCC, an additional intermediary component must be deployed which will perform duplicate handling—if two copies of the same packet are received following the two paths—before delivering the packet to the TCC.

3.1.5 Reliability and security

Note that although the proposed design omits association prior to transmitting, this does not necessarily reduce the reliability of the communication. Namely, the broadcast nature of the design and the inherent redundancy (i.e. each packet is received by two nodes) compensates for this lack of reliability.

Note that no IEEE 802.11 MAC layer retransmissions are made in this design. Further note that the design is based on broadcast transmissions and that each packet is received by two nodes. Thus, as the sender node will receive two ACKs packets—instead of one—in reply to one data packet, the IEEE 802.11 MAC will behave unexpectedly as there is no way of knowing which node sent which ACK and exactly which packet was acknowledged. Nonetheless, this lack of retransmissions is compensated by the the inherent redundancy in the design that already ensures that a packet is received by two nodes. Furthermore, retransmissions will have a negative impact on the bandwidth anyway.

Note that due to this broadcast nature and the lack of retransmissions, the proposed design is not truly an ad-hoc wireless network in the conventional sense because the conventional ad-hoc networks involve unicast transmissions as well as retransmissions.

Additionally, note that since the association phase is skipped, the proposed design uses the higher layer protocol IPSec for authentication and end-to-end encryption to secure the communication.

3.2 Summary

This chapter presented an overview of the proposed design for a CBTC trackside network. A node in this design functions in ad-hoc mode, receiving broadcast packets and forwarding to its neighbors, thus forming a chain of nodes. As a result, the train does not have to associate with the nodes as it moves and the costly optical fiber cables connecting the nodes are no more needed. To minimize the interference and to solve the well-known hidden node problem, the design enables frequency separation by using three frequencies. Each node is equipped with three radios (and antennas), one per each frequency, and only one frequency is used for transmissions in one direction. The three frequencies are then used in an alternating fashion on subsequent nodes. To offer redundancy and to avoid a single point of failure, transmissions are made not only to the immediate neighbor node but also the following node. Thus, each transmission is received by two nodes in each direction. Duplicate packets—which are a result of the inherent redundancy in the design—are eliminated using a unique sequence number included in each packet. A special type of node is a terminal node, which is either a train node or a TCC node. In contrast to a regular chain node, a terminal node transmits on all three frequencies in all directions, to maximize the probability of successful train-to-trackside transmissions.

CHAPTER 4

Overview of the Field Experiment

This chapter presents an overview of the independent field experiment [17] that was carried out simultaneously to provide a proof-of-concept of the proposed design. In this experiment, a hardware prototype of the three-radio node was developed and a test involving seven nodes was subsequently performed.

Note that this experiment was a part of a master thesis project. The involvement and the contribution of the author in it was more on an informal and voluntary basis due to its relevance to the PhD study. For the same reason, an overview of the experiment is presented here. This overview reproduces certain key results from the experiment after some adaptations. An additional objective is to highlight a number of limitations that this experiment suffered from as well as to provide an insight on how such a system will be developed in real-life in contrast to a simulation environment. For further information as well as detailed hardware specifications, see [17].

4.1 Setup

The hardware node used in the field experiment was mainly based on ALIX 2D2 mainboards, with 500 MHz AMD Geode CPU and two mini PCI slots each. Each mainboard was equipped with an Atheros AR5414A WLAN radio card, which used IEEE 802.11a and operated at 54 Mbps data transmission rate. Three of these mainboards were mounted on a custom-made wooden mast and were connected together via Ethernet. Each board ran Linux (Debian Wheezy). As described in Chapter 3, the two side boards were equipped with uni-directional antennas and the top board was equipped with an omni-directional antenna. HUBER-SUHNER Sencity SPOT-S antenna, operating in frequency band 5.150-5.875 GHz was used. The node mast is shown in Figure 4.1 with the three ALIX 2D2 mainboards visible.

Notably, the figure shows the node to be equipped with four antennas rather than three. It is because due to the unavailability of a suitable omni-directional antenna, two uni-directional antennas were used for the top radio instead to achieve the coverage at both sides. Figure 4.2 illustrates the full mast.

The software component for the node model were written using Click Modular Router [155]—a framework for building configurable software-based routers—which facilitated in receiving, manipulating and forwarding packets.

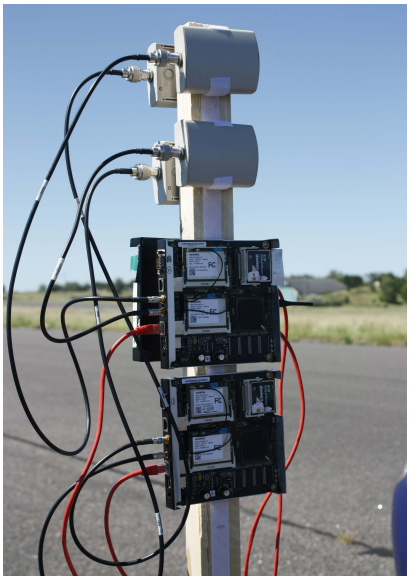

Figure 4.1: Hardware node prototype, with three mainboards and four uni-directional antennas (Photo courtesy of Lars Bro)

The sequence number contained in the Encapsulating Security Payload (ESP) header of IPSec was used for identifying duplicates and lost packets. Pre-defined MAC addresses—e.g. 00:00:00:00:00:01, 00:00:00:00:00:02 and 00:00:00:00:00:03—were used to designate the directions *left*, *right* and *both*, as discussed in Section 3.1.3, and the address field in the IEEE 802.11 MAC header was used to hold this address. Note that since only broadcast transmissions are used in this design, the MAC addresses were only used for determining the direction and not the destination. The address field in the IP header was used to specify the actual destination address, i.e. of a terminal node. By using these existing fields, the intention was to avoid a need for implementing a new protocol.

The test setup consisted of seven nodes. The nodes were placed 400 meters apart. Of these seven nodes, the nodes at the two ends of the chain—i.e. the first and the seventh nodes—were terminal nodes. In the test, the train node transmitted packets which were then transferred to the TCC node over the chain. Figure 4.3 presents a simplified illustration of the setup.

The practice of using these simplified illustrations to help in visualizing the experiment scenarios is followed in the rest of the thesis. Note that these illustrations do not show the frequencies with different colors, antennas, etc. Nonetheless, the chain nodes as well as the terminal nodes still function on three frequencies as described in Chapter 3.

The experiment was carried out at an abandoned military airfield Flyvestation Værløse,

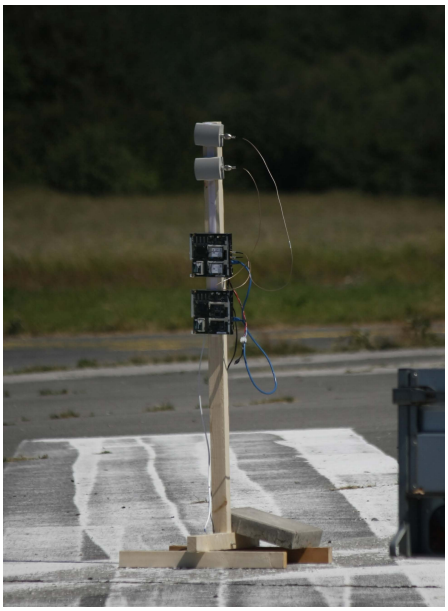

Figure 4.2: Hardware node prototype mast (Photo courtesy of Lars Bro)

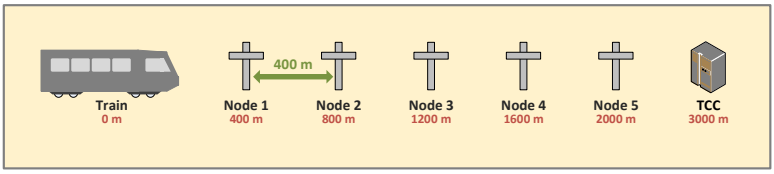

Figure 4.3: Illustration of the scenario shown in Figure 4.4, with 1 stationary train, 5 chain nodes, and 1 TCC

formerly used by the Danish air force. The reasons for choosing an inter-node distance of 400 meters were that the radio hardware was not powerful enough to transmit signals at larger distances, and, it was the largest feasible distance to fit the whole chain on the airfield runway. The actual setup is shown in Figure 4.4.

Various iterations of the test were conducted. The final test run was conducted over a period of 12 hours.

Table 4.1 lists parameters and their values used in the experiment.

Figure 4.4: Field experiment with a network of seven nodes (Photo courtesy of Lars Bro)

Table 4.1: Field experiment parameters

Parameters	**Value**
WLAN technology	IEEE 802.11a OFDM at 54 Mbps
Frequency channels (MHz)	5735, 5800, 5865
Transmission power (dBm)	11.5
Receiver sensitivity (dBm)	-74
Antenna gain (dBi)	14
Packet size (bytes)	1000
Inter-node distance (m)	400
Nodes	7
Packet rate (per second)	1000
Run time (s)	40

4.2 Results and limitations

As discussed in Chapter 2, typical CBTC traffic only uses 20-100 kbps of data rate. Nonetheless, higher rates ranging up to 8 Mbps were used in this experiment to study how much bandwidth such a network can support, as any excessive bandwidth can be utilized for providing non-CBTC services, e.g. passenger infotainment.

As shown in Figure 4.5, the results showed that for the packet rates of 100 to 400 packets per second (800 kbps to 3.2 Mbps), 97.4 to 99.2 percent of the packets were

successfully delivered to TCC. However, the packet loss increased sharply at higher packet rates. As seen, at the rate of 1000 packets per second (8 Mbps), it increased to 36.69%.

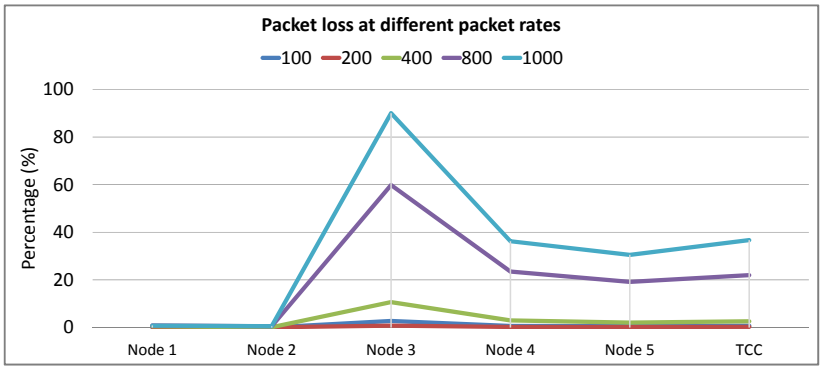

Figure 4.5: Packets lost at each node

The unusually high number for Node 3 seen in Figure 4.5 was partly due to a faulty radio on Node 2. This is visible in Figure 4.6 that shows the number of duplicate packets received at each node. The 100% on the y-axis means a duplicate copy of each packet was received. The large drop for Node 3 is because it only received the first copy of a packet (i.e. from Node 1) and not the redundant copy it was supposed to receive from Node 2. This faulty radio contributed significantly to the high packet loss seen at TCC.

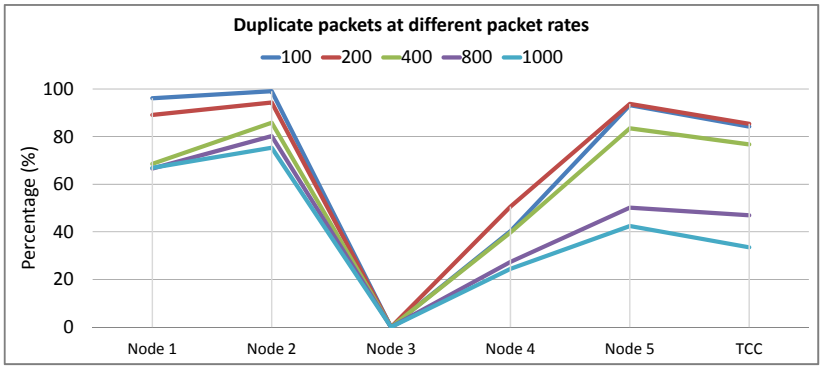

Figure 4.6: Duplicate packets received at each node

The field experiment successfully demonstrated the prototype of the design. The results showed that the chain network successfully transferred packets from one end to the other for a packet rate of up to 400 packets per second. For the higher packet rates of

800 and 1000 packets per second, the packet loss increased. Nonetheless, it shall be noted that the field experiment suffered from a number of limitations as follows.

- Due to the limited availability of hardware, mostly old and leftover hardware was used. In particular, as discussed above, the involvement of a number of faulty radio equipment negatively impacted the reliability of the results.

- Likewise, due to the unavailability of mainboard equipment with three built-in mini PCI slots for radio cards, three mainboards—equipped with one radio card each—had to be connected together with Ethernet for the node prototype. Due to this fact, the three radio cards operated in isolation from each other. This was not consistent with the design which dictated that the three radio cards worked cooperatively, controlled by a central entity. A consequence of this lack of a central entity was that the process of duplicate handling had to be performed on the outgoing radio before the packet was about to be transmitted, rather than upon receiving the packet.

- An additional limitation was that a number of design aspects were not investigated, for example, how many frequencies the train node will use for transmissions, and the type of antennas it will have. The identical prototype developed for the chain node was used for the train node as well. Later on, when the work on the simulation study started, it was concluded that a train must transmit on all three frequencies and must be equipped with omni-directional antennas to maximize the probability of successful transmissions to the chain nodes, as discussed previously in Chapter 3. This turned out to be of a particular significance later on when the simulation results revealed the interference that a train node would cause due to its use of three omni-directional antennas, as discussed subsequently in Chapter 6. Likewise, the aspect whether a train node must transmit with a 2-node range like a chain node or with a shorter range was not investigated, and was studied with simulations later, as discussed in Chapter 7.

- Additionally, time constraints imposed further challenges as one test run took several hours. Likewise, it was a tedious job to work with the node masts, due to the large distance between them, and, to collect data from all 7x3 mainboards which involved accessing them physically with a serial interface.

At a later point, an indoor demonstration was performed with six nodes and live video traffic was successfully transferred from one end to the other at a data rate of 5 Mbps. The objective mainly was to demonstrate that the development of the prototype was completed and that the prototype, particularly its software component, performed as intended. An additional objective was to secure company funding for a full-scaled development of the product. To reduce the signal loss and insulate the transmissions from any radio propagation effects, in this test, the antennas on the radios operating on the same frequency on the respective nodes were connected together with coaxial cables. Note that

for a uni-directional flow scenario illustrated in Figure 3.4, four cables are required to connect each node to its two immediate neighbor nodes.

4.3 Summary

This chapter presented an overview of the independent field experiment study that was carried out simultaneously in the initial stages of this PhD study. In this experiment, a hardware prototype of the three-radio node was developed and a test involving seven nodes was performed at an abandoned military airfield. The experiment successfully demonstrated the prototype of the design and that the chain network successfully transferred packets from one end to the other. On the other hand, the experiment also suffered from a number of limitations, in particular, due to the limited and faulty hardware equipment available and time constraints. Partly due to these limitations, a number of design aspects were not investigated. Specifically, how many frequencies the train node will use for transmissions and the type of antennas it will have. As a consequence, the prototype node developed for a chain node was used for the train node as well. Likewise, the transmission range of the train node was not investigated.

CHAPTER 5

Simulation Setup

This chapter presents an overview of the simulation setup used for this study, including an overview of the development of the simulation model, the simulation tool, and the various KPIs used to evaluate and discuss the simulation results.

Computer-based simulations is an indispensable tool to imitate a real-life system. A *conceptual model* of the real-life system is first developed based on the characteristics of the real-life system, as well as a number of assumptions if necessary. Based on this conceptual model, a simulation model of the real-life system is subsequently built in the simulation tool. The performance of the real-life system can then be predicted by performing experiments with this simulation model. The validation and verification process of the simulation model plays a crucial role. Verification is the process of confirming that the model is correctly developed as per the conceptual model. Validation is the process of confirming the accuracy of the model with respect to the real-life system. Figure 5.1 illustrates the process of developing a simulation model [156]–[158].

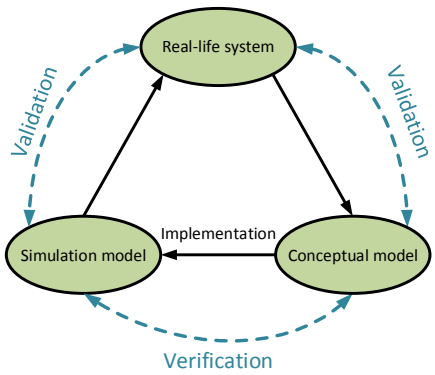

Figure 5.1: The process of simulation model development

Simulations enable a large number of benefits. Using simulations, systems that cannot be tested in real-life due to reasons for example limited resources—such as the case in the field experiment discussed in Chapter 4—or due to the complexity of the real-life system involved, can be studied in isolation to the actual system. Simulations are cost-effective

and less time-consuming. For example, the same test that required several hours to complete in the field experiment could be performed in a few minutes with simulations. This additionally enables easy repetition of experiments. Furthermore, the simulation tool provides a more controlled environment for experimentation compared to a field experiment by enabling adjustment of various related parameters in a more effortless way. The results produced by a simulation tool are significantly more reliable than those acquired in a field experiment, for example, because there is no faulty hardware equipment involved. Likewise, the results are easily reproducible as long as no changes are made to the simulation model and the parameters involved. Nonetheless, one notable drawback of using simulations is when the model is based on overly-simplified assumptions [156]–[158].

5.1 Simulation tool

The simulation experiments in this study were carried out using the discrete-event simulator OPNET Modeler 17.1 [159]. OPNET is commercially available simulation tool that enables a highly rich set of features. OPNET proved to be a natural choice for this study as it is made available for the students at the university department (DTU Fotonik) free of cost and due to the expertise that the department has acquired in its use. OPNET enables a user-friendly Graphical User Interface (GUI), and a hierarchical modeling process which enables the development of highly detailed models of real-life systems in a computer. The model can be developed at different levels, namely the *Network level*, the *Node level*, the *Process level*, and the *Code level*. An additional advantage of using OPNET is that it enables a large number of vendor provided models for their equipment. These models have been built, verified, and validated by the vendors themselves. The Network level enables the user to define the components of the network and the topology. At the Node level, the user is able to develop the node model using the various built-in components or module, such as processors, transmitters, receivers, queues, packet stream, and antennas. At the Process level, the behavior of the protocol behind the model can be defined. The process model consists of a number of Finite State-Machines (FSM). An FSM defines the various states a model can be in at a given instance and the events that lead to a transition between these states. Finally, at the lowest level in the hierarchy is the Code level. This level enables the user to define the functionality of the model, by programming it for each individual state and transition. OPNET supports the C and C++ programming languages.

Additionally, OPNET enables defining attributes at each level. For example, at the Node level, a few of the supported attributes are *node position*, *host name*, and *altitude*. A node model is composed of a number of modules. For example, a typical WLAN node is composed of a WLAN MAC (Medium Access Control) module—which models the MAC layer of the WLAN protocol—, a transmitter module, a receiver module, and an antenna module. Each of these modules is configurable with the help of the module-level attributes. Example attributes for the WLAN MAC module include *MAC address*, *data*

rate, *operating frequency*, *transmission power*, and *receive sensitivity*.

Besides that, OPNET provides support for collecting simulation results as *statistics*. It provides a number of predefined statistics and enables users to specify their own statistics. The most commonly used statistics include *number of packets sent* and *number of packets received*, for example.

An additional valuable feature of OPNET is External Model Access (EMA), which provides an API (Application Programming Interface) with which the simulation model can be manipulated externally via code rather than the GUI. This feature was used in this study, for example, to generate a large number of nodes—i.e. 100 nodes. Likewise, another useful feature is the utility *op_cvov* that enables the user to extract results from the OPNET output file into, for example, a CSV (comma-separated values) file from which they can be imported to spreadsheets. This feature was used extensively in this study as it included extracting results for a large number of statistics, as discussed shortly.

5.2 Simulation model of the proposed design

Figure 5.2 illustrates the Network level view of the simulation model in OPNET, for a scenario involving 18 chain nodes and 2 terminal nodes (train and TCC) discussed in the subsequent chapters. The two terminal nodes are placed one at each side of the chain, as previously shown in Figure 3.4 and Figure 4.3.

Figure 5.2: Simulation model in OPNET: Network level view showing a train, a TCC, and 18 chain nodes

Figure 5.3 illustrates the node model of the proposed node design. The node model consists of three WLAN MAC radio modules (*wireless_lan_mac*), representing two side radios and one top radio. Each WLAN MAC module is connected to a transmitter module (*wlan_port_tx*), a receiver module (*wlan_port_rx*), and an antenna (*ant*). These three radio modules inside the node model represent a real-life node equipment with three radio cards installed in it. Each of these WLAN MAC modules is based on a modified version of the built-in OPNET WLAN module. They have been modified to function cooperatively and in ad-hoc mode, as defined in the proposed design. Note that the model shown in Figure 5.3 is of a terminal node. The model for a chain node looks very similar except that it does not include a *source* module—which is responsible for generating traffic—as a chain node merely forwards the packets it has received from another node.

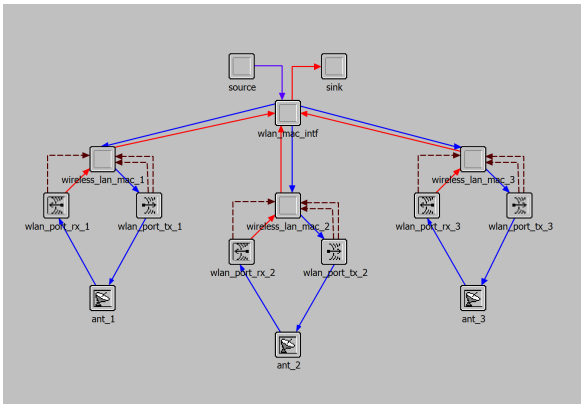

Figure 5.3: Simulation model in OPNET: Node level view showing, among others, three WLAN MAC modules inside the node

As seen, the three radio modules are connected to an interface module (*wlan_mac_intf*). This interface module implements the key functionality of the proposed node design, including delivering a packet to the correct side radio for further transmission (i.e. forwarding of the packet), duplicate packet handling, and calculating various statistics as discussed subsequently.

Figure 5.4 illustrates the underlying process model of the WLAN MAC module with a number of states and transitions between these states.

As discussed in Section 3.1.2 and illustrated in Figure 3.4, a TCC node in real-life will be connected to the last node in the chain with a wired connection. Nonetheless, when the simulation model was developed, there were still ambiguities involved regarding how the actual TCC node will function. Therefore, in the simulations, the same node model that represents a train node—shown in Figure 5.3—has been used for the TCC node as well. This is illustrated in Figure 5.5. Alternatively, it can be seen as a train transmitting to another train over a chain. This minor detail is not of significant relevance when the results are discussed. Note that this implies that transmissions between the last node in the chain (Node 5 in Figure 5.5) and the TCC will be slightly less reliable than that in real-life due to this lack of a wired connection. However, note that this decreased reliability is compensated by the duplicate packets the TCC will receive from Node 4, in contrast to real-life. An alternative was to make the last chain node function as the TCC. Since the last node in the chain will be wired to the TCC in real-life, the delay involved in transferring packets from that node to the TCC would be negligible anyway.

Once the development of the simulation model was completed, the model was first verified and validated with the help of various simple scenarios in which statistics such as *number of packets forwarded*, *number of duplicate packets received*, and *received power*

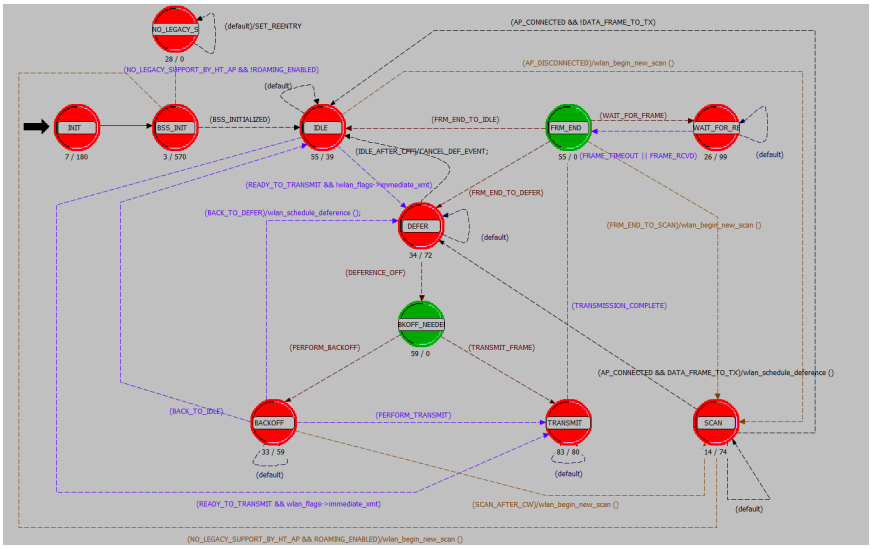

Figure 5.4: Simulation model in OPNET: Process level view showing the process model of the WLAN MAC module

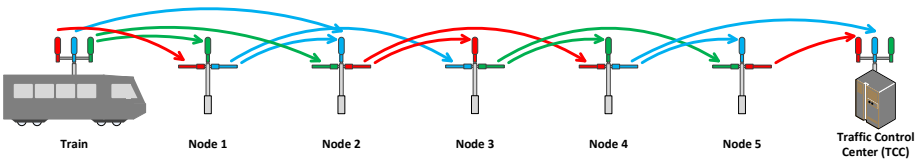

Figure 5.5: TCC node implemented with a node model identical to that of a train node

were studied. Note that the built-in OPNET modules—such as the WLAN MAC module used in this case—are extensively verified and validated during the process of the product development life cycle. Since the simulation model is based on these modules, this made the task of verification and validation of the overall model relatively less complicated.

Table 5.1 lists generic parameters and their values used in the simulations.

Note that the inter-node distance depends on the node's signal range which in turn depends on various factors including transmission power, gain and receiver sensitivity of the antenna, as discussed in Section 2.5.1.1. Nevertheless, an inter-node distance of 600 meters has been used in all experiments in this study, as it is consistent with the distance currently used in the Copenhagen S-train CBTC system, used as a reference point for this study. Additionally notable is that using a smaller inter-node distance implies that a greater number of nodes would have to be deployed, if the proposed design is to

Table 5.1: Generic simulation parameters

Parameter	Value
WLAN technology	IEEE 802.11a OFDM at 54 Mbps
Frequency channels (MHz)	5170, 5230, 5290
Transmission power (dBm)	7
Receiver sensitivity (dBm)	-76
Antenna gain (dBi)	14
Antenna height (m)	Train: 2, Chain node: 2 (side), 3 (top)
Packet size	Payload: 512 bytes, Headers: 297 bits
Inter-node distance (m)	600
Chain nodes	98
Track length (m)	58800
Packet rate (per second)	1000
Simulation time (s)	60

be tested on the existing Copenhagen S-train network. Thus, transmission power and receiver sensitivity were adjusted to transmit to a distance of 1200 meters (i.e. a 2-node range). As discussed previously in Section 2.5.1.1, the values of these parameters are highly dependent on the hardware equipment as well as the propagation conditions. Thus, while the values used for these parameters—i.e. 7 dBm and -76 dBm—are consistent with those used for real-life equipment, they might not always be sufficient in real-life environments where the propagation conditions are significantly worse.

Note that the table lists the default—and the shortest—simulation time of 60 seconds used in the study. Simulation times significantly longer than these were additionally used as noted in the subsequent chapters. Besides that, it is noted that it refers to the *simulated time* rather than the actual *simulation time*—i.e. the actual time that the simulation took to run. The actual time for running a complex scenario, for example a scenario involving multiple trains with bi-directional traffic or a network of 100 nodes, can easily range between 45 minutes to a couple of hours. An additional reason for this long time is that in various cases, results for a large number of statistics were collected for a scenario, even if only a limited number of these statistics were eventually used in the final results. Section 5.3 lists the six primary statistics that have been used when presenting the results in the following chapters.

As discussed in Chapter 1, one of the main objectives of this simulation study was to scale the network size beyond the limits that were experienced when carrying out the field experiment. Therefore, in the initial set of the simulations, a network size of 100 nodes (approximately 60 kilometers) has been used as this will more likely be the largest network size used in the actual CBTC deployments both in terms of the number of nodes and the actual length. As a comparison, the S-train network has a total track length

of approximately 170 kilometers. The length of the longest radial line (København H - Hillerød) is approximately 41.4 kilometers and that of the shortest radial line (København H - Klampenborg) is approximately 13.3 kilometers.

Furthermore, in actual deployments, the chain will be divided into much smaller segments as the network infrastructure available at train stations will be used to wire the two nearest nodes. Therefore, in the subsequent experiments, a smaller network of 18 nodes has been used, which corresponds to approximately 11 kilometers. As a comparison, there are 84 train stations in the S-train network, which gives an average of approximately 2 kilometers of distance between the stations. Since Copenhagen is a relatively small city, 11 kilometers serves as a reasonable inter-station distance for larger cities.

Likewise, the 5 GHz frequency band has been used in the simulations to remain consistent with that used in the S-train CBTC network, and a typical CBTC packet size (i.e. payload size) of 512 bytes has been used.

The proposed design relies on the assumption that the frequency separation provided by the three-frequency design is sufficient and signals from nodes beyond that distance will not interfere. However, this is far from reality. In this study, OPNET's default Free-Space Path Loss (FSPL) propagation model has been used. Since FSPL does not take into account obstructions between the transmitter and the receiver, the propagation phenomena that negatively impact the signal power—as discussed in Section 2.5.1.1—is not relevant. As a consequence, FSPL enables an exceptionally large signal range, which not only provides the worst case conditions to validate the proposed design but in a way is also consistent with the real-life railway environments where relatively insignificant changes in the propagation conditions have shown to dramatically increase the signal range, as discussed in Section 2.5. In other words, a large signal range is considered a disadvantage for the optimal performance of the proposed design, and a small range is considered an advantage.

Note that OPNET lacks support for a more comprehensive propagation model than the FSPL model. However, note that the objective of this study has primarily been focused on verifying and validating the fundamental idea behind the proposed design, for which the FSPL model serves the purpose. Using a more comprehensive propagation model will improve the conditions anyway, as signal power will diminish faster, resulting in lower interference. Developing such a model for OPNET involves a substantially large amount of time. Therefore, it was considered outside the scope of this study.

Nonetheless, to imitate more realistic propagation conditions, a random error is introduced in the system in which 2% of packets are dropped as erroneous. This number is based on the results from the field experiment discussed in Chapter 4, in which an average error rate of 1 to 2 percent was observed. Note, though, that a part of the reason of this high error rate in the field experiment was the low quality of the radio equipment. In real-life, an error rate lower than this is thus expected. Nonetheless, an error rate of 2% will otherwise account for the slightly less favorable propagation conditions in the real-life compared to the field experiment. The additional objective of introducing this

error rate is to study how the redundancy in the design guarantees a high number of packet transfer rate despite these errors.

5.3 Key performance indicators (KPIs)

While a vast number of statistics could be studied, the following six KPIs are focused in this study in particular:

1. **Total packets received**: This statistics represents the number of packets received at a node including duplicate packets. This number excludes any erroneous packets received.
2. **Unique packets received**: This statistics represents the number of unique packets received at a node, i.e. excluding any duplicate packets. This statistic serves as one of the most important KPIs for this study as it indicates how many packets were successfully transferred over the network.
3. **Duplicate packets received**: As discussed in Section 3.1.4, a duplicate packet is when multiple copies of the same packet are received at a node, from the same node or from different nodes.
4. **Number of packets lost**: The number of packets that, out of the original packets sent, were not received at the receiving end, for example due to errors.
5. **Erroneous packet**: The number of erroneous packets received at a node, mainly due to interference.
6. **Number of collisions**: The number of collisions experienced at a node.

Note that since a node forwards each unique packet received to the next nodes in the chain, the number of unique packets received for a node is essentially equivalent to the number of packets forwarded by that node.

There is a distinction between the number of erroneous packets received at a node and the number of collisions experienced at a node. In both cases, a node receives multiple transmissions simultaneously. However, the former refers to a situation where for some of these transmissions, the power level is below the minimum required level—i.e. receiver sensitivity—and thus these transmissions are considered noise. If the amount of this noise is large, the packet is declared erroneous. Otherwise, it is received successfully. The latter refers to the a situation where the power level for all of the transmissions is above the receive sensitivity.

Additionally interesting, at least initially, was the end-to-end delay. Namely, this is the delay that incurs from the time the packet is transmitted by the sending terminal node to the point it is received at the receiving terminal node. The long distance a packet must travel might result into a large delay and thus might impact the timely delivery of the

CBTC messages. However, later on, the simulation results revealed that the end-to-end delay was of a lower significance, as discussed further in Chapter 6.

As mentioned previously, the most decisive success criterion for this study is the number of packets successfully transferred from one terminal node to the other terminal node over the network. This criterion is represented by the *unique packets received* KPI listed above or, alternatively, by the *number of packets lost* KPI. Note that the values of the two KPIs are indirectly proportional to each other. Nonetheless, in this study, the use of *number of packets lost* is preferred when discussing the performance of the network.

Note that while discussing results in the following chapters, in certain scenarios, some of the KPIs might convey redundant information. For example, the number of duplicate packets received can be deduced by subtracting the number of unique packets received from the number of total packets received. Nonetheless, given that one key feature of the design is the redundancy—i.e. in form of duplicate packets—the performance of the design is highly dependent on this number. With the help of this number included in the figures, it can be quickly deduced how the network is performing. Furthermore, in some of the later experiments, a greater number of trains located at different positions relative to the chain are considered. As a consequence, it becomes increasingly difficult to comprehend the results without including the number of duplicate packets in the figures. The same applies to, for example, the total number of packets received, which can be likewise deduced based on the other two numbers. In short, with the help of these KPIs, it becomes increasingly straightforward to comprehend the results.

Besides the above listed six statistics, a vast number of additional statistics were either used from OPNET's predefined set of statistics or implemented to study the network performance and to validate the results. Results for these statistics are not included in the final results. For example, statistics such as *WLAN MAC queue size*, *WLAN MAC delay*, *number of WLAN MAC back-off slots*, etc., were examined to study the network congestion. Likewise, for example, the statistic *packets received directly from a train* was implemented to study the number of packets a node receives directly from the train, which indicates the interference a train caused on the nodes beyond its transmission range of two nodes. Likewise, the statistic *own packets received* was implemented to study the situation where a train receives the packets sent by itself, i.e. when forwarded by a chain node in the backward direction. Additionally, statistics such as *received power* and *Bit Error Rate (BER) per packet* were examined to study if the transmission power was sufficient. A number of the statistics were implemented for each of the three radios on a node, to study specifically how individual radios on a node perform. Besides the above listed six statistics, this includes *number of packets forwarded*, for example.

Note that while the results for the chain nodes are as well discussed, the results for the terminal nodes are of primary interest. Additionally note that—as is obvious from the above discussed six KPIs—while discussing results, packet rate has been used as a measure of data rate, as it facilitates in keeping track of the number of packets received at a node. As mentioned above, typical CBTC traffic only uses 20-100 kbps of data rate. Nonetheless, a higher data rate of 1000 packets per second, equivalent to $\approx$ 4.4 Mbps, has

been primarily used in this study to investigate how much bandwidth such a network can support, as any excessive bandwidth can be utilized for providing non-CBTC services. Table 5.2 presents a complete list of the data rates used in this study. Note that a payload size of 512 bytes has been used. On top of that, the overhead of the PLCP (Physical Layer Convergence Procedure) and MAC headers is 297 bits.

Table 5.2: Packet rates and equivalent data rates

Packet rate (per second)	Data rate
1000	4.393 Mbps ($\approx$ 4.4 Mbps)
500	2.1965 Mbps ($\approx$ 2.2 Mbps)
250	1.09825 Mbps ($\approx$ 1.1 Mbps)
125	549.125 kbps ($\approx$ 550 kbps)

5.4 Summary

Computer-based simulations are used to imitate a real-life system in the computer. A model of the real-life system is built inside the computer based on the characteristics of the real-life system. The performance of the real-life system can then be predicted by performing experiments with this model. Thus, simulations are highly cost-effective, less time-consuming, and enable a controlled environment for studying a real-life system. A simulation model of the proposed design was created using OPNET Modeler 17.1—a commercially available simulation tool—for this simulation study. This chapter provided a brief overview of the simulation modeling process, OPNET Modeler 17.1, and the simulation model of the proposed design developed for this study. The chapter further discussed the six key statistics (KPIs) used to measure the performance of the system in this study, and the simulation parameters and their values used. The values of a number of these parameters are based on those used in the Copenhagen S-train CBTC system.

CHAPTER 6

Simulation Phase 1: Preliminary Evaluation of the Design

A large number of simulation scenarios were carried out in the course of the simulation study. This chapter presents the results from the first phase of this study. These results have been published in [Farooq2017b]. The objective of this first phase was primarily to evaluate the design with simplistic scenarios. As with the field experiment, in these scenarios, only a stationary train located at one end of the chain was considered.

6.1 Scenario 1: A network with uni-directional traffic

In this scenario, the train node transmits packets which are then transferred to the TCC over a chain of 98 nodes. A packet rate of 1000 packets per second—equivalent to 4.4 Mbps—is used. Figure 6.1 presents a simplified visualization of the scenario.

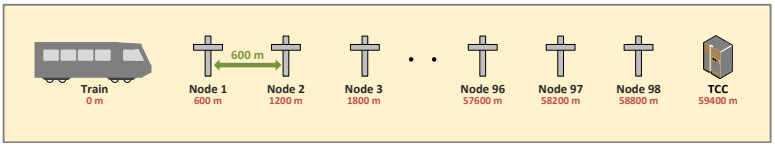

Figure 6.1: Illustration of the scenario, with 1 stationary train, 98 chain nodes, and 1 TCC

Figure 6.2 shows the results for the six KPIs discussed in Chapter 5 against a select set of nodes displayed on the x-axis. Note that the selection of nodes is not uniformly distributed. Specifically, first the five first nodes in the chain are listed—to highlight the interference the nodes near the train experience—and then every tenth node is listed. The y-axis shows the number of packets received in percentage.

Note that at the rate of 1000 packets per second and the simulation time of 60 seconds, the number of packets sent by a single radio on the train during the whole simulation run is 60,000. Thus, a 100% unique packets received for a node on the figure implies that it received all 60,000 packets. Note that the total number of packets sent by the train is thrice this number, i.e. 180,000, as it transmits three copies of the same packet via its three radios. Likewise note that ideally the total number of packets received by a chain

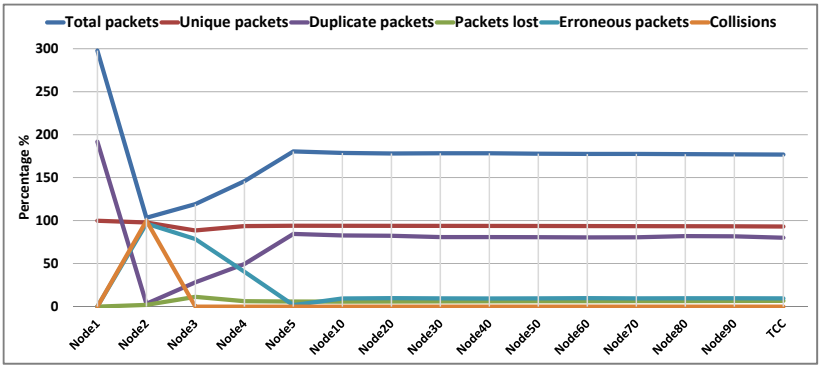

Figure 6.2: Results for Scenario 1: A network with uni-directional traffic

node is twice this number, i.e. 120,000, as a node is supposed to receive two copies of the same packet, one from its immediate neighbor node and another from the following node.

Figure 6.2 shows that 93.26% of the packets (red line) were successfully transferred to TCC, i.e. a packet loss of only 6.74% over a large network of 100 nodes. As seen, the large and stable number of duplicate packets (purple line) received at each node highlights the effectiveness of the redundancy in the design. Furthermore, the frequency separation successfully minimizes interference as the number of erroneous packets (light blue line) is minimum—except for at the first few nodes. As a result, only a negligible drop in the number of packets received—both total and unique—is seen at each subsequent node in the chain.

The results highlight a shortcoming of the design as well. As a train transmits on all frequencies in all directions in contrast to a chain node, the inherent frequency separation guaranteed otherwise in the chain is not fully achievable, resulting in interference on the nearby nodes. This is evident from the left part of Figure 6.2 where a dramatic increase in the number of erroneous packets—and as a result a drop in the number of total and duplicate packets—is seen at Nodes 2 to 4. The shortcoming is particularly critical due to the fact that as a train will be travelling along the chain, the effects currently seen on the first few nodes in the chain will be seen across each node in the chain.

At Node 2, train's transmissions result in collisions with those of Node 1. Note that Node 2 is the only node in this chain that is in the transmission range of two nodes transmitting on the same frequency, and thus the only node to experience collisions. As seen (orange line), nearly all transmissions from the train result in collisions on Node 2. Specifically, three copies of the same packet are received at Node 2, two from the train and one from Node 1. Out of these, the two packets received on the same frequency, i.e. packets from the train and Node 1 on blue frequency, as illustrated in Figure 5.5, result in collisions. However, the packet from the train received on green frequency is successfully

received. While Nodes 3 and 4 are outside the transmission range of the train, they are still in the interference range. For example, at Node 3, train's transmissions interfere with those of Nodes 1 and 2, i.e. all transmissions on the red and blue frequencies as illustrated in Figure 5.5. Nonetheless, as seen in Figure 6.2, due to the redundancy in the design, only a minor drop in the number of unique packets received (red line)—and thus a minor increase in the packets lost (green line)—is seen at these nodes, except for Node 3 for which the drop is slightly more significant. It is because while Nodes 2 and 4 suffer from interference primarily on only one of their radios, Node 3 does it on both of its radios.

Interference introduced by the train to Node 1's transmissions is particularly crucial. Due to the short distance between these two nodes (i.e. train and Node 1), the insignificant difference in the received power of the two signals at Node 3 results in very low signal-to-noise ratio (SNR). Results for individual radios showed that 83% of the erroneous packets at Node 3 were received on its left radio. Notably, this phenomenon occurs only in the beginning of the chain where two nodes with a short distance between them (i.e. train and Node 1) transmit on the same frequency. Nonetheless, it is an important observation as it indicates that in case of an increased signal range due to improved propagation conditions, additional nodes in the beginning of the chain might face this problem. Likewise, the erroneous packets seen at Node 4, for example, are because the train is still in the interference range (it interferes with the transmissions of Node 2), although in this case the SNR will be comparatively higher.

Nonetheless, beyond this problematic initial part of the chain, i.e. as the interference from the train dies off, a stable number of packets received is seen at each node from Node 5 onward. Additionally, this implies that a network of a smaller size of e.g. 20 or 50 nodes would have fared the same.

As discussed in Section 3.1.3, the exceptionally high number of total packets received (i.e. above 200%) at Node 1 is because Nodes 2 and 3, upon receiving packets directly from the train, forward them in the backward direction as well, thus arriving back on Node 1.

6.2 Scenario 2: A network with lower redundancy

The idea behind making the design redundant—i.e. by transmitting packets to two immediate neighbors in each direction—is to make it robust against random node failures. Failing a node and examining its impact on the network resiliency thus is an essential part of the evaluation. Thus in this scenario, first one node—out of the total 98 chain nodes—is purposely failed and its impact on the packet loss seen at TCC is studied. This is then repeated by increasing the number of failed nodes, one at a time, to a total of 10 nodes. Note that odd numbered nodes are failed, i.e. Node 1, 3, 5, and so on. Figure 6.3 presents the results. Note that it shows the number of failed nodes on the x-axis in contrast to Figure 6.2.

The results show that when one node is failed (Node 1), the packet loss seen at TCC

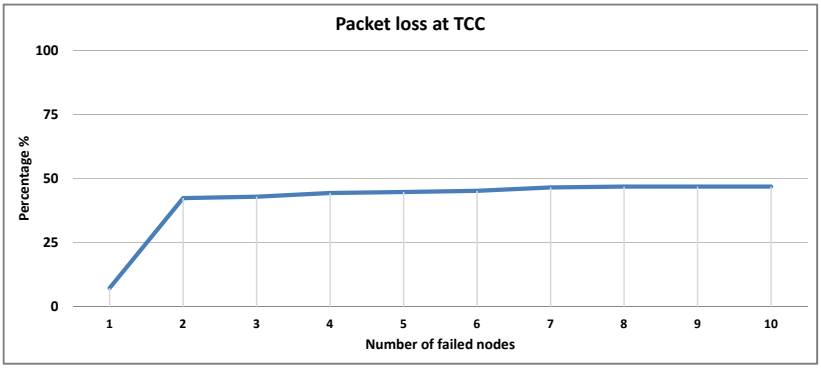

Figure 6.3: Results for Scenario 2: Packet loss for a network with up to 10 failed nodes

raises from the original 6.74% seen in Figure 6.2 to 7.26%. The increase is insignificant due to the redundancy in the design, as train's transmissions are received not only by Node 1 but also Node 2. However, as one more node is failed next (Node 3), the packet loss increases sharply to 42.4% (i.e. an increase of approximately 35%). This is because as in Scenario 1 (Figure 6.2), Node 4 receives around 40% erroneous packets from Node 2 due to the interference from the train. In Scenario 1, the redundant packets that Node 4 received from Node 3 compensated for this large number of erroneous packets. However, as Node 3 is not functional in this scenario, these erroneous packets result in lost packets, and this loss is not recovered throughout the chain. The shortcoming identified in Scenario 1 related to a train's transmissions thus reappears here with a more pronounced impact. Nonetheless, after this point, as the interference from the train dies off, only a slight increase in the packet loss is seen at TCC as the number of failed node is increased incrementally to 10. A packet loss of only 0.93% is seen at each node on average.

Next, to present with the worst possible case, every second node in the chain is failed—i.e. 48 failed nodes. This essentially makes it a network with zero redundancy. The results are presented in Figure 6.4. As expected, the number of duplicate packets has fallen to zero for all nodes—except for Node 2 that receives type 2 duplicate packets from the train. Thus, the number of total and unique packets has become equal for each node. As a consequence, a sharp drop in the number of packets received is seen at each subsequent node. Similarly, a sharp increase in the number of packets lost is seen, accumulating to 71.8% at TCC. However, as discussed above, the packet loss at Node 4 makes a large fraction of this number. Results presented later in Figure 7.15 in Chapter 7 show how reduced interference from the train will lower this packet loss.

The results show that due to the redundancy in the design, the network sustains the failure of a remarkably large number of nodes (48 out of 98) as it still manages to transfer packets across the chain. Note that in an ordinary chain network without redundancy, a

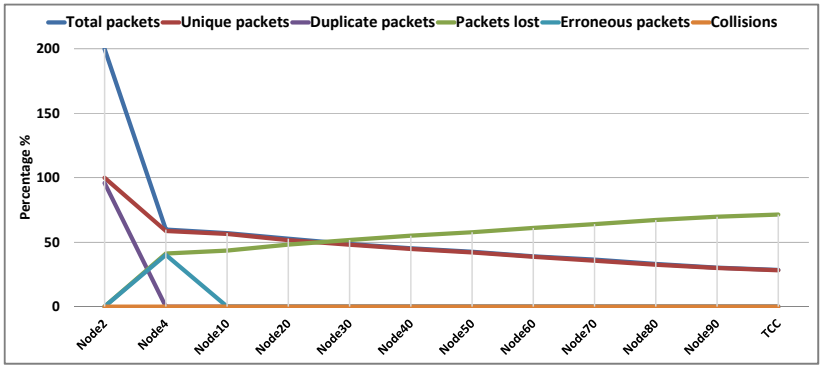

Figure 6.4: Results for Scenario 2: A network without redundancy (i.e. every second node failed)

single failed node can break the whole chain.

For the sake of comparison, Figure 6.5 illustrates the number of unique packets received for the scenario with redundancy (Figure 6.2) and the scenario without redundancy (Figure 6.4). It emphasizes how the redundancy in the design ensures a stable number of packets received—on average 93.74% of packets—across the 100 nodes in the former, while in the latter, it sees a sharp drop. If the large drop seen at Node 4 due to the reasons discussed above is briefly ignored, the drop seen from Node 4 to TCC (a drop of approximately 30%) highlights how a network with no redundancy built into its design will perform.

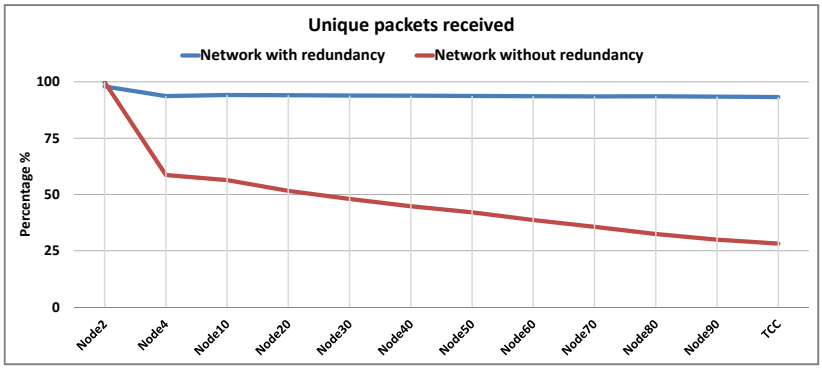

Figure 6.5: Unique packets received: network with redundancy vs. network without redundancy

6.3 Scenario 3: A network with bi-directional traffic

In this scenario, Scenario 1 is extended with two flows, one in each direction, i.e. from train to TCC and vice-versa. Note that this is equivalent to transmitting with a data rate of 8.8 Mbps. The results are presented in Figure 6.6. Note that a significantly higher number of total and duplicate packets—on average 40.4% more packets, specifically—is received at each node in this scenario compared to the scenario with uni-directional traffic. These excessive packets are those flowing in the opposite direction. Nonetheless, for brevity, the figure shows an average of these numbers for the two flows.

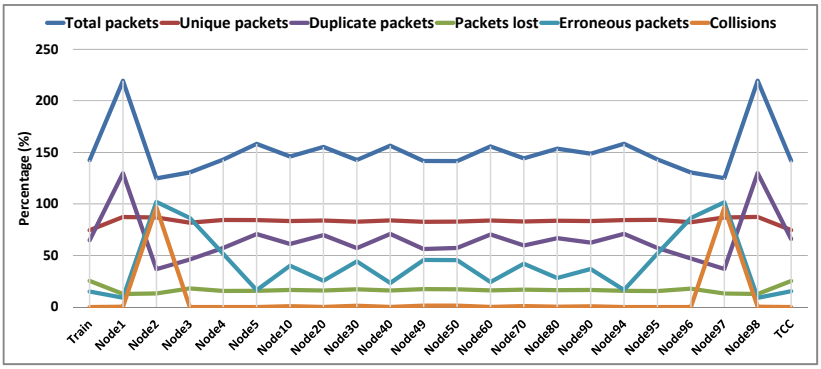

Figure 6.6: Results for Scenario 3: A network with bi-directional traffic

As seen in Figure 6.6, a stable number of unique packets received is maintained throughout the chain. Nonetheless, a significantly increased packet loss of on average 25.42% is seen at the two terminal nodes. Note that since traffic is flowing in both directions now, each top radio faces interference from nodes on its both sides. This leads to increased interference as seen from the significantly higher number of erroneous packets at each node compared to the scenario with uni-directional traffic in Figure 6.2. Specifically, on the middle nodes (Nodes 10 to 90), on average 17.21% erroneous packets are received per flow compared to 9.63% in Figure 6.2.

Additional results showed an end-to-end delay of 2.67 milliseconds at the terminal nodes, which is well below the typical end-to-end delay of 500 milliseconds specified in the IEEE CBTC standard, as discussed in Section 2.6.1. Since transmissions are separated by frequencies, there can be at most one node—in a uni-directional flow scenario—and two nodes—in a bi-directional flow scenario—contending for the medium on one frequency at a given location in the chain. Thus, MAC contention delay and queueing delay are irrelevant. Likewise, as stated in Chapter 3, no MAC layer retransmissions are made in this design. An additional component that impacts the delay is the processing delay at each node, particularly the delay involved when a radio on a node, upon receiving a packet, performs duplicate handling and delivers the packet to the appropriate side radio

for further transmission. This delay is highly dependent on the processing power of the node's hardware, and is considered to be negligible with the high-performance hardware available today. Given these reasons, end-to-end delay is not of particular interest for this study.

Note that the 25.42% packet loss over a large distance of approximately 60 kilometers is still acceptable additionally due to the following facts:

1. The CBTC traffic is redundant in nature as the train control information sent both ways (i.e. train to TCC and vice-versa) is repeated at regular intervals. Each of these CBTC messages includes the distance that the train is permitted to travel, i.e. the *limit of movement authority* (LMA) as discussed in Section 2.1. While the train is completing this distance, the loss of CBTC messages can be tolerated.

2. The less favorable propagation conditions in the real word will lower the transmission range and thus the interference.

3. In real world, Quality of Service (QoS) differentiation will be applied to ensure that the CBTC traffic experiences lower packet loss.

Continuing the first argument above, as discussed in Section 2.1.2, a CBTC radio communication system can typically tolerate a failure of radio communication for 5 or more seconds. Let's suppose it is 5 seconds. If the CBTC messages are sent every 100 milliseconds, as discussed in Section 2.1.3, it implies that after receiving a CBTC message successfully, a train can tolerate the loss of the following 50 or more CBTC messages. In other words, a train running at a speed of 120 kilometers per hour can travel a distance of 166.67 meters (i.e. distance travelled in 5 seconds) without receiving a CBTC message.

Nonetheless, the results imply that if exceptionally favorable propagation conditions are assumed, distant nodes might still be able to interfere despite the frequency separation, i.e. the interference range becomes larger than the 2-node transmission range and thus exceeds the 3-node frequency separation distance discussed in Section 3.1.2.

Additionally notable in Figure 6.6 is the increased number of erroneous packets received at the two terminal nodes compared to Figure 6.2. Note that the packets forwarded backward by e.g. Nodes 1 and 2 upon receiving from the train, prove to be a major source of interference for the packets of the other flow, i.e. flowing from TCC to the train.

Overall, the results show that due to the inherent frequency separation and redundancy in this design, significantly large numbers of packets can be transferred across large networks with an acceptable packet loss. Nonetheless, simultaneously it is noted that the design is still highly sensitive to interference, and relies on the assumption that the interference range is equal to the transmission range, as discussed previously in the context of Figure 6.2, which is far from the truth in real-life. It further highlights an interesting observation. Suppose, just as a hypothetical scenario, that in Figure 5.5, the interference range of the transmissions from Node 1's right radio (blue) reach past Node 4. Node 4's right radio (blue), being unable to hear this transmission due to its uni-directional

antenna pointing in the opposite direction, will continue to transmit, and, as a result, the transmissions will interfere with each other at Node 5 top. This presents with another sort of hidden node problem.

Nonetheless, at the same time, it is emphasized that this exceptionally large transmission and interference range is also due to the simplistic FSPL propagation model used in this study, as discussed in Chapter 5.

6.4 Summary

This chapter presented the results from the first of the four phases of the simulation study. In this phase, a large network of 100 nodes (approximately 60 kilometers) was simulated, with a stationary train as in the field experiment. The results showed that compared to a regular network without redundancy, due to the inherent redundancy in this design, significantly large numbers of packets can be transferred across large networks with an acceptable packet loss. Reduced interference as a result of frequency separation further minimizes the packet loss. Likewise, end-to-end delay is minimum as frequency separation guarantees reduced contention for the wireless medium.

The chapter additionally presented results for a scenario in which a number of nodes in the chain were purposely failed to study how a lowered redundancy impacts the network performance. The results showed that due to the redundancy in the design, the network can sustain the failure of a remarkably large number of nodes—up to 48 nodes out of the total 98 nodes—as it still managed to transfer packets across the chain.

The results for the scenario with bi-directional traffic showed that due to the increased interference each chain node experiences from its both sides, the packet loss at the terminal nodes increased substantially, to 25.42%. The chapter further discussed why this packet loss can still be acceptable in CBTC due to a number of reasons.

Nonetheless, the results identified two shortcomings of the design as exposed by the results:

1. The terminal node (i.e. a train) undermines the frequency separation guaranteed by the chain nodes as it is required to transmit on all frequencies. This results in excessive interference at the first few nodes in the chain, i.e. at the train's *entry point in the chain*. It is an important observation as it indicates that in case of an increased signal range of the train, e.g. due to improved propagation conditions, additional nodes in the beginning of the chain might experience this interference.

2. The design under-estimates the interference produced by distant nodes in ideal propagation conditions despite the inherent frequency separation. This results in interference throughout the chain nodes, i.e. interference *inside the chain*.

CHAPTER 7

Simulation Phase 2: Identifying Improvements to the Design

This chapter presents the subsequent set of simulations carried out to identify potential solutions to the shortcomings of the design identified in the previous chapter. These results have been published in [Farooq2017d]. To summarize, the following two shortcomings were identified.

1. A train's transmissions cause interference on the nearby nodes, as contrary to a chain node, a train transmits on all three frequencies in all directions, thus undermining the frequency separation otherwise guaranteed inside the chain. The impact of this shortcoming is seen on the nodes near the train, or in other words, at the train's *entry point in the chain*.

2. In favorable propagation conditions, transmissions from nodes outside the transmission range still manage to interfere beyond the frequency separation distance. The impact of this shortcoming is seen throughout the chain, or in other words, *inside the chain*.

A number of potential solutions to minimize the above two shortcomings are thus studied in the following scenarios. Note that the solutions are studied in isolation from each other, to clearly identify the improvements that each solution can offer.

Note that the first of the two shortcoming is not particularly problematic if 100% redundancy is ensured in the chain, as seen in Scenario 1 (Figure 6.2). However, the problem intensifies when there are failed nodes in the network, as discussed in the results for Scenario 2 (Figure 6.3 and Figure 6.4). The problem is particularly critical due to the fact that as a train will be travelling along the chain, the effects currently seen on the first few nodes in the chain will be seen across each node in the chain. Multiple trains in close proximity will further worsen the situation. Thus, potential solutions for this shortcoming are studied first.

7.1 Scenario 4: Lower transmission power on the train

One potential solution is to use a different, lower transmission power on the train compared to that on a chain node. A lower power will reduce the interference as the transmissions

will reach fewer nodes. Thus, Scenario 1 is repeated but this time with lower power values of 4, 5 and 6 dBm, in contrast to the original 7 dBm. Figure 7.1 compares the number of erroneous packets received at each node for all four power values. It shows that as expected, compared to 7 dBm, the lower power values result in reduced interference on the nearby nodes. Likewise, as expected, the lowest power value (4 dBm) results in the lowest interference.

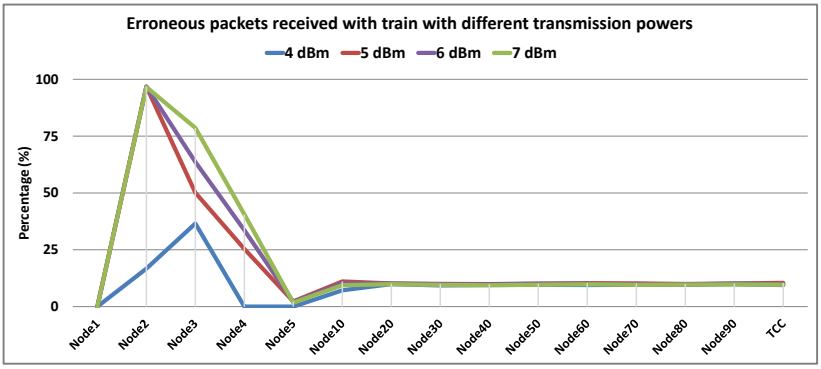

Figure 7.1: Results for Scenario 4: Erroneous packets received with different transmission powers on the train

The results for the 5 dBm transmission power—which yielded the lowest packet loss at TCC—are presented in Figure 7.2. Compared to Figure 6.2, an increase in the number of total and duplicate packets received is seen in the figure for Nodes 3-4 as a result of lower interference from the train. As a result, the packet loss at TCC has decreased from the original 6.74% in Figure 6.2 to 2.18%.

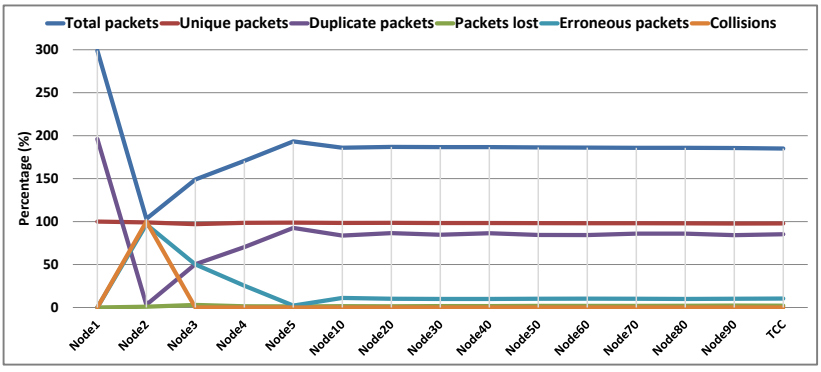

Figure 7.2: Results for Scenario 4: Packet loss with 5 dBm transmission power on the train

The results for the 4 dBm transmission power are presented in Figure 7.3. They show that train's transmissions cannot reach Node 2 with this power. This is evident from, for example, the lack of collisions seen at Node 2 and the resulting drop in interference, compared to in Figure 7.2. It is further evident from a lowered number of total and duplicate packets received at Node 1 compared to in Figure 7.2, as now Node 1 does not receive packets forwarded by Node 2 in the backward direction. Nonetheless, the results show a packet loss of 7.99% at TCC, which is only slightly higher than the original 6.74% seen in Figure 6.2. While 4 dBm transmission power further lowers the interference, the slight increase in the packet loss is due to the lowered redundancy as Node 2 is not able to receive redundant copies of the packets from the train. Nonetheless, as discussed subsequently, this implies that a design with a 1-node transmission range for the train might as well be feasible.

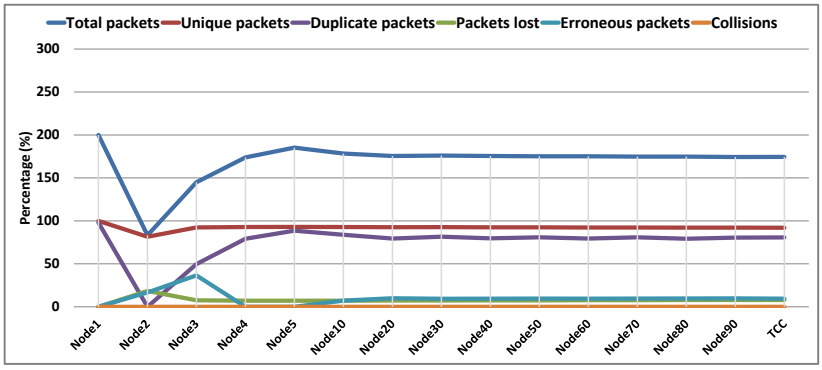

Figure 7.3: Results for Scenario 4: Packet loss with 4 dBm transmission power on the train

7.2 Scenario 5: Fewer radios on the train

As discussed in Section 3.1.2, as a train approaches a chain node, at most only two radios on the node will be able to receive train's transmissions because the third radio will be facing opposite. Thus, the design required that a train must transmit on minimum two frequencies to ensure that a chain node was able to receive from it. Nonetheless, to further maximize the availability, it was decided to enable the train to transmit on all three frequencies. However, now that the problem caused by a train's transmissions is evident, in this scenario, the number of radios (or frequencies) on the train is reduced first to two and then to one. Note that chain nodes still use three radios.

7.2.1 Train with two radios

First, the feasibility of using two radios on the train is studied. As shown in Figure 7.4, two frequencies on a train node will result in three different combinations relative to the frequencies on the nearest two chain nodes.

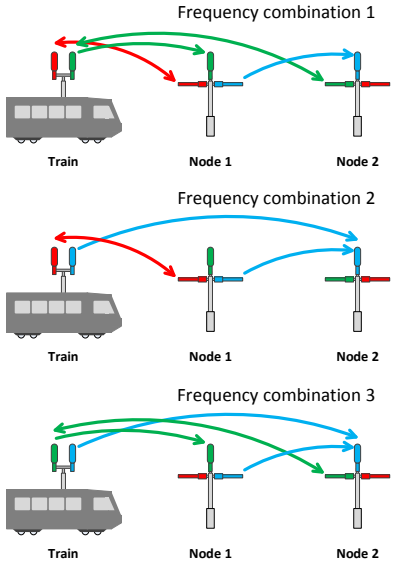

Figure 7.4: Train with two radios and the three frequency combinations

The figure shows the combinations in the order—from most favorable to least favorable—as per the probability with which the chain nodes, preferably the first chain node, can receive transmissions from the train. As seen, for all three combinations, both chain nodes (Node 1 and Node 2) will be able to receive transmissions from the train. For frequency combinations 1 and 3, a total of three radios on the two nodes will be able to receive, in contrast to only two radios for the frequency combination 2. In the opposite direction, i.e. traffic flowing from the chain nodes to the train, in frequency combination 1, the train will be able to receive from two nodes, in contrast to one for frequency combinations 2 and 3.

Figure 7.5 and Figure 7.6 show the number of duplicate and erroneous packets received at each node, respectively, for the three frequency combinations.

As seen in Figure 7.5, frequency combination 1 results in the highest number of duplicate packets received at each node. As seen in Figure 7.6, a major contributor is the significantly lower interference at the nodes near the train (i.e. Nodes 2 and 3) compared to Figure 6.2, particularly because the top radio on Node 2 does not receive transmissions from the train and thus does not experience interference (collisions) from

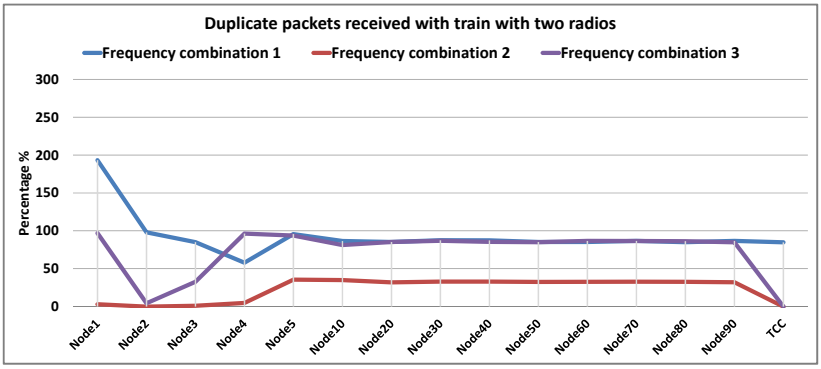

Figure 7.5: Train with two radios: Duplicate packets received for the three frequency combinations

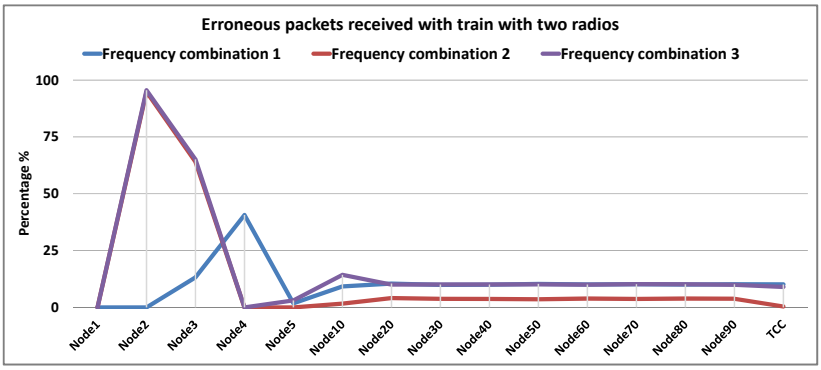

Figure 7.6: Train with two radios: Erroneous packets received for the three frequency combinations

the transmissions from Node 1. Figure 7.5 shows that frequency combination 2 results in the lowest number of duplicate packets received at each node. As seen from the large number of erroneous packets at Node 2 in Figure 7.6, it is due to the fact that nearly all (100%) transmissions from the train received at the top radio of Node 2 experience interference from the transmissions from Node 1. Since Node 2 does not receive any redundant copies of the packets from the train (i.e. on its left radio), these erroneous packets result in lost packets. Figure 7.5 further shows that no duplicate packets are received at TCC for frequency combinations 2 and 3, as discussed above in the context of Figure 7.4. Thus, it is noted that while a design with a reduced number of radios on the train decreases the interference at the nearby nodes, it decreases the ability of receiving duplicates for a train at the receiving end as well. Overall, from Figure 7.5 and Figure 7.6, it is concluded that frequency combination 1 is the most favorable and

frequency combination 2, rather than 3, is the least favorable.

Figure 7.7 presents the complete results for the most favorable frequency combination 1 for the scenario with uni-directional traffic, for a comparison with Figure 6.2. It shows that the packet loss at TCC drops to 1.36% from the original 6.74%. Figure 7.8 presents the results for the equivalent scenario with bi-directional traffic. It shows a drop in packet loss from 25.42% seen in Figure 6.6 to 21.57%.

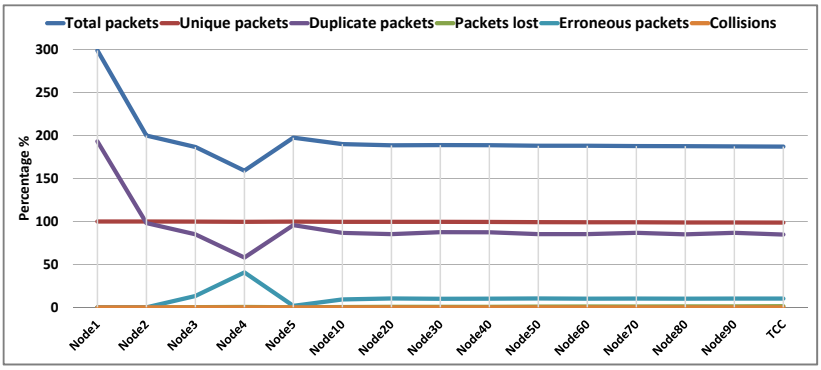

Figure 7.7: Results for Scenario 5: Train with two radios and the most favorable frequency combination (combination 1)

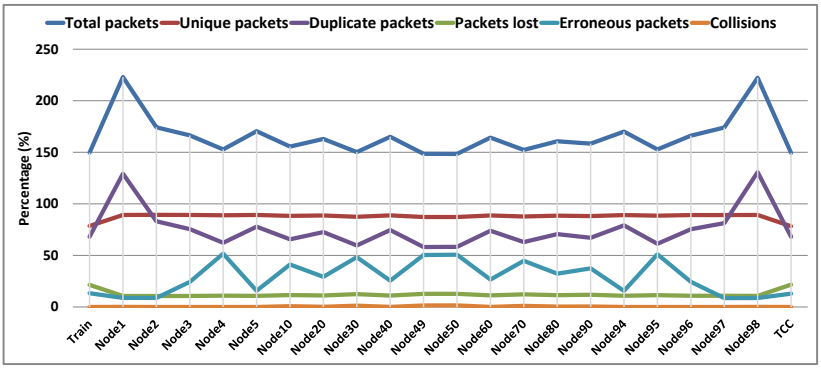

Figure 7.8: Results for Scenario 5: Train with two radios and the most favorable frequency combination (combination 1), with bi-directional traffic

Figure 7.9 presents the complete results for the least favorable frequency combination 2 for the scenario with bi-directional traffic, for a comparison with Figure 6.6. As discussed above, due to the interference experienced at the second node at each side

(Node 2 and Node 97), and a lack of duplicate packets received due to the reduced number of radios on the terminal nodes, a substantially high packet loss of 67.36% is seen at the terminal nodes compared to the original 25.42%. Thus, continuing from the discussion above, it is concluded that when the top radio is the only radio on a node that receives transmissions, in the absence of redundant packets, the impact of the interference from the transmissions of the preceding node increases dramatically.

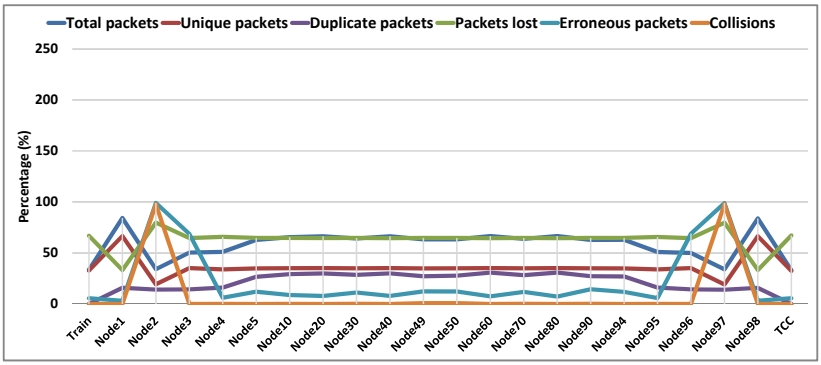

Figure 7.9: Results for Scenario 5: Train with two radios and the least favorable frequency combination (combination 2), with bi-directional traffic

The results show that the performance of the network depends on which two frequencies are used on the train. Nonetheless, on the other hand, note that a train will be moving along the chain and thus will regularly encounter nodes with the favorable frequency combinations.

7.2.2 Train with one radio

As discussed in Section 3.1.2, the design requires that the train transmits on minimum two frequencies. Nonetheless, in this scenario, results for a train node with only one radio are presented to highlight the impact of using three frequencies on the interference experienced at the nodes near the train. Figure 7.10 illustrates the three possible frequency combinations for a train with one radio. Note that in all combinations, at least one of the two chain nodes will be able to receive transmissions from the train. Combination 2 is particularly favorable as here both Node 1 and Node 2 will be able to receive from the train. For the same reason, it is the only combination in which Node 2 will receive duplicates. In the opposite direction, however, the train will be able to receive transmissions only in the first two combinations. This highlights the fact that while a train with one radio will be able to send packets to the chain, it might not always be able to receive from the chain.

Figure 7.11 compares the number of duplicate packets received at each node for the three frequency combinations. It shows that frequency combination 3 is the least favorable

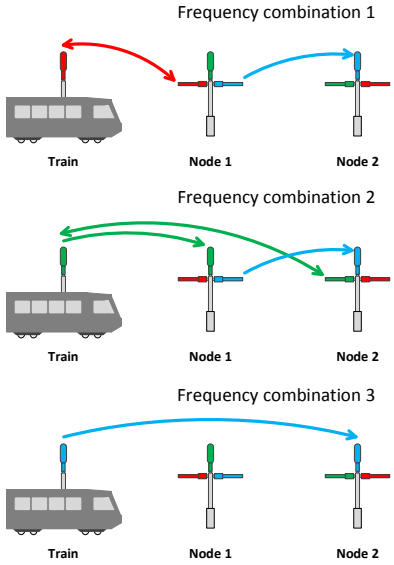

Figure 7.10: Train with one radio and the three frequency combinations

as no duplicate packets are received at any node before Node 4. This is because this is the only frequency combination where Node 1 does not receive train's transmissions, and thus does not send duplicate copies of packets to Node 2. Note that the duplicate packets seen at Node 1 for frequency combination 2 are due to the backward forwarded packets from Node 2. Furthermore, no duplicate packets are received at TCC for any of the combinations as it has only one radio.

Figure 7.12 shows the number of erroneous packets received for the three combinations. Note that due to the small numbers, the figure uses a smaller scale on the y-axis. As expected, the erroneous packets seen on the first four nodes in Figure 6.2 previously have disappeared as a result of the lower interference from the train.

Figure 7.13 presents the complete results for the most favorable frequency combination 1, for a comparison with Figure 6.2, and shows that the packet loss at TCC drops to 5.27% from the original 6.74% due to the reduced interference at the nodes near the train. Results for the equivalent scenario with bi-directional traffic—not presented here—showed a drop in packet loss from 25.42% seen in Figure 6.6 to 24.78%.

Note that the interference seen throughout the chain caused by the transmissions from the nodes outside the frequency separation distance (i.e. shortcoming 2) is comparatively a larger contributor of the high packet loss than the interference caused by a train's transmissions (i.e. shortcoming 1). Furthermore, as discussed above, reducing the number of radios to one also means that a terminal node is not able to receive any duplicates.

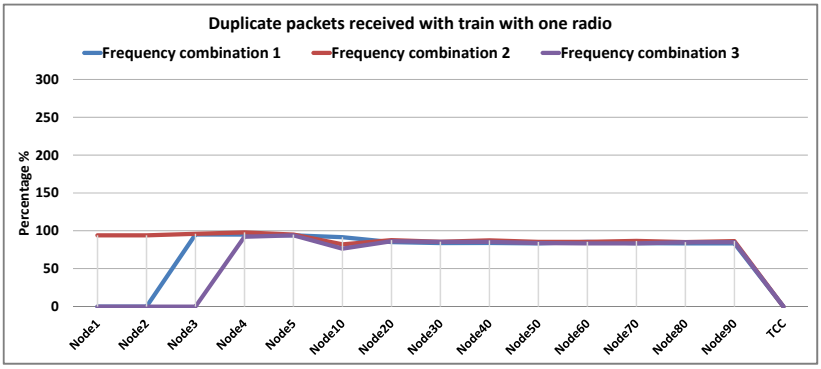

Figure 7.11: Train with one radio: Duplicate packets received for the three frequency combinations

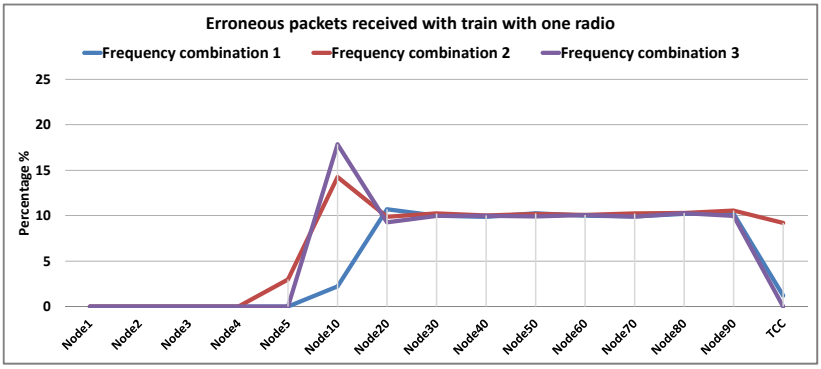

Figure 7.12: Train with one radio: Erroneous packets received for the three frequency combinations

Therefore, reducing the number of radios on the terminal node alone does not offer significant improvements to the packet loss.

Figure 7.14 presents results for the least favorable frequency combination 3, for a comparison with Figure 6.6. As discussed above, no packets are received at either of the terminal nodes. Nevertheless, note that the chain is still able to transfer packets as seen from the average packet loss of 23.97% at the last node at each chain end (i.e. Node 1 and Node 98).

In the results for Scenario 2, in which every second node in the chain was purposely failed (Figure 6.4), a packet loss of 71.8% was seen at TCC, mainly as a result of the 40% occurred already at Node 4 due to the interference from the train. For the sake of comparison, Figure 7.15 shows the packet loss seen in the original scenario together with that seen when a 5 dBm transmission power is used on the train (as discussed in Scenario

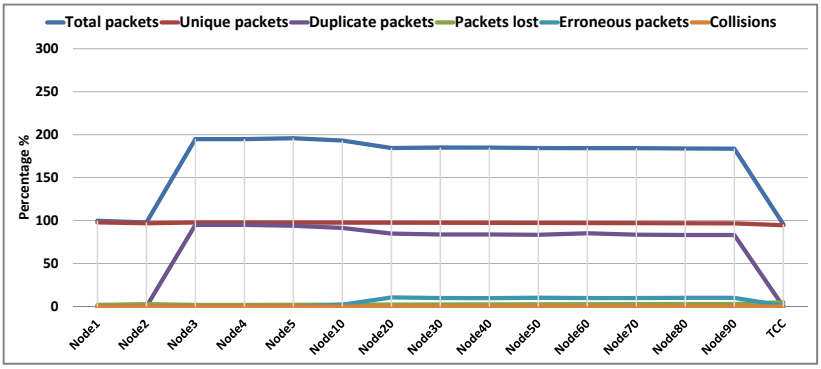

Figure 7.13: Results for Scenario 5: Train with one radio and the most favorable frequency combination (combination 1)

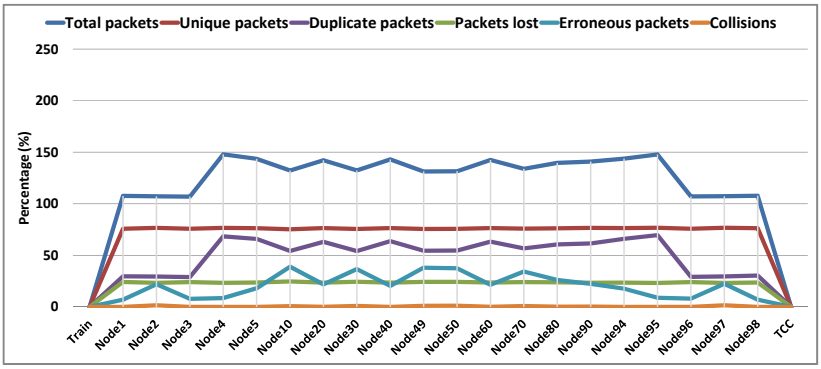

Figure 7.14: Results for Scenario 5: Train with one radio and the least favorable frequency combination (combination 3)

4 in Section 7.1), and, when one radio is used on the train (as discussed in Scenario 5 in Section 7.2). It shows that when a lower transmission power is used on the train, the packet loss at TCC drops to 63.9%—as the number of erroneous packets at Node 4 drops to 25%. When one radio is used on the train, the results show that the packet loss drops to 54.88%—as the number of erroneous packets at Node 4 drops to only 3.89%—which implies that about 17% packet loss seen at TCC in Figure 6.4 is a direct result of the interference received at a single node (Node 4) due to train's transmissions. Thus, it is concluded again that the impact of interference caused by a train is more pronounced in a network with lower redundancy.

The results assert that a train node does not necessarily have to have three radios. A

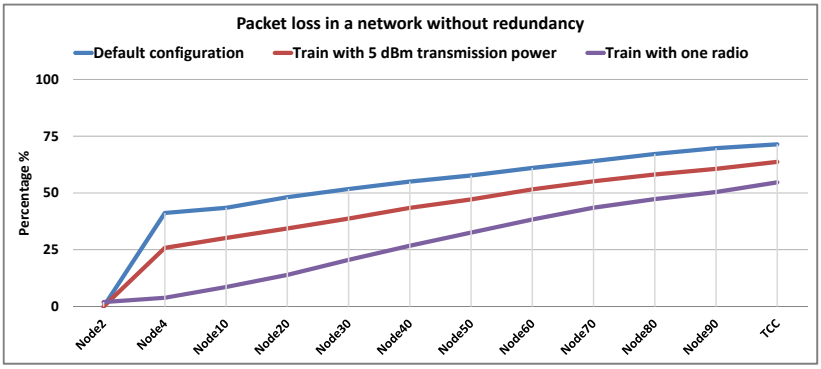

Figure 7.15: Packet loss in a network without redundancy, with different train configurations

design in which the train has two radios, or even one, is likewise feasible. This is again with a note that a train will be moving along the chain and will nonetheless encounter a node with a favorable frequency combination two out of three times. However, for a standing train, the case of one radio and frequency combination 3 (Figure 7.14) presents a problem as the train will not able to receive packets from the chain, unless it is in the range of multiple chain nodes. An alternative approach can be to still have three radios on the train such that all three are used for receiving but only one for transmitting—a variation of this solution is investigated later in Section 8.3. Another workaround could be to deploy nodes of all three frequency combinations on train stations, or maybe a specialized chain node with three omni-directional antennas like on a train in the original design.

7.3 Scenario 6: A more robust modulation and coding scheme

The default data rate used in this simulation study is 54 Mbps—as listed previously in Table 5.1—which uses 64-QAM (Quadrature Amplitude Modulation) as the modulation scheme and a coding rate of 3/4. In this scenario, a more robust modulation and coding scheme is used for transmissions as it helps in coping with the impact of interference. Note that the solution is studied in isolation from the solutions in the previous scenarios, i.e. default transmission power and number of radios on the train is used. Table 7.1 lists the modulation and coding schemes and the corresponding data rates.

First, the coding rate of 2/3, yielding a data transmission rate of 48 Mbps is used. Note that as seen in Table 7.1, this transmission rate still uses the 64-QAM modulation scheme. The results, presented in Figure 7.16, show a dramatic decrease in the number of erroneous packets, both near the terminal nodes and throughout the chain, and as a result, a drop in the packet loss from 25.42% seen in Figure 6.6 to 14.39%.

Next, the most robust, QAM-based modulation and coding scheme, namely 16-QAM

Table 7.1: A comparison of data rates supported by different IEEE 802.11 technologies per modulation and coding scheme

Modulation scheme	Coding rate	Data rate (Mbps)		
		802.11a	**802.11n**	**802.11ac**
16-QAM	1/2	24	240	780
16-QAM	3/4	36	360	1170
64-QAM	2/3	48	480	1560
64-QAM	3/4	54	540	1755

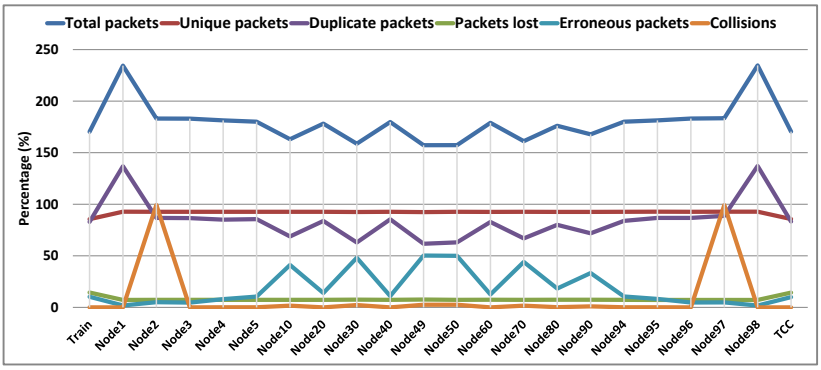

Figure 7.16: Results for Scenario 6: Transmissions with the 64-QAM 2/3 modulation and coding scheme

1/2, is used. The results are presented in Figure 7.17. The results show a further drop in the number of erroneous packets throughout the chain, as is evident from the "smoothed out" lines for the total and duplicate packets received, resulting in a packet loss of 13.07%.

Note that this simulation study were carried out with IEEE 802.11a as (1) it is the technology officially approved by Siemens A/S for the hardware for its CBTC project, and, (2) to be able to relate to the results from the field experiment in which the available hardware was limited, as discussed in Chapter 4. As seen in Table 7.1, more advanced IEEE 802.11 technologies such as 802.11n and 802.11ac support substantially high data rates with the same two combinations of the modulation and coding schemes, specifically, data rates of up to 480 and 1560, and, 240 and 780 Mbps, respectively.

7.4 Scenario 7: Combined adjustment of multiple parameters

In this scenario, the impact of using various combinations of modulation and coding scheme, receiver sensitivity, and train's transmission power, are studied. Figure 7.18 presents results for a combination of the 16-QAM (1/2) modulation and coding scheme,

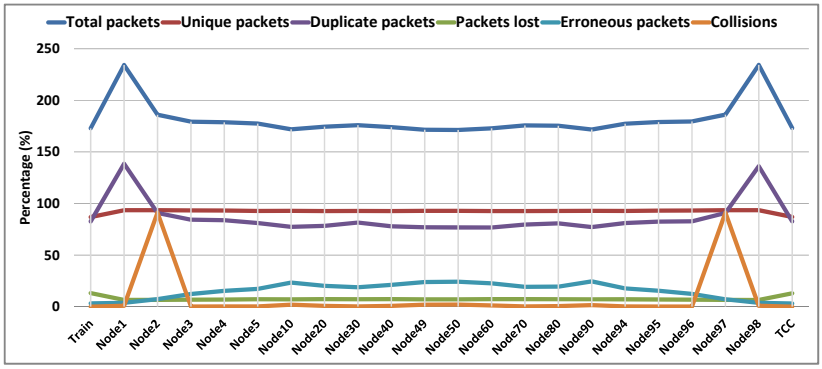

Figure 7.17: Results for Scenario 6: Transmissions with the 16-QAM 1/2 modulation and coding scheme

5 dBm transmission power on train, and receiver sensitivity of -75 dBm. As seen, the packet loss drops further to 12.73%, the lowest seen until now.

As seen from the drops in the number of total and duplicate packets received at Node 2 and Node 97 compared to Figure 7.17, these parameter values reduce the transmission range of the terminal node to one node. For the same reason, no jumps in the number of total and duplicate packets received are seen at the preceding two nodes (Node 1 and Node 98) as Node 2 and Node 97 do not forward packets backward.

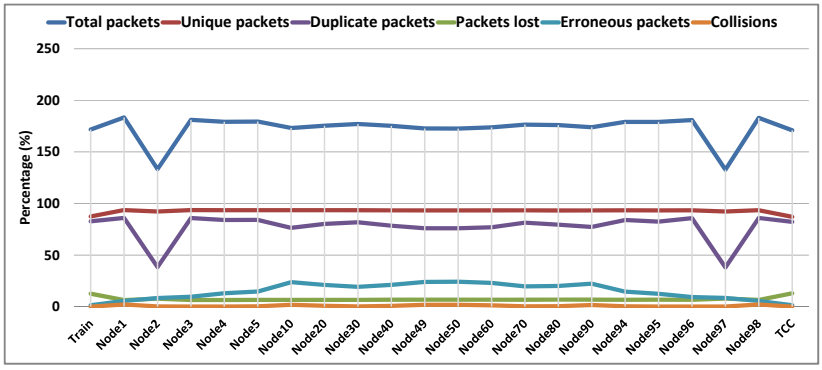

Figure 7.18: Results for Scenario 7: Transmissions with the 16-QAM (1/2) modulation and coding scheme, -75 dBm receiver sensitivity, and 5 dBm transmission power on train

Thus, together with the results discussed in Scenario 4 where a 4 dBm transmission power on the train resulted in a 1-node range, the results show that the presumption that a minimum 2-node range is required at the train is not valid. In fact, a 1-node transmission

range at the train together with the assurance that minimum two radios are able to receive from the train—i.e. two radios on the nearest node—will both result in lower interference on the nearby nodes and at the same time guarantee the redundancy aimed by the design.

7.5 Summary

This chapter presented the results from the second of the four phases of the simulation study. In this phase, a number of potential solutions to address the two shortcomings identified in the first phase were investigated in isolation from each other.

To minimize the interference caused by a train node due to its transmissions on all frequencies (i.e. shortcoming 1), a number of scenarios were performed to investigate the impact of decreasing the transmission range of the train node or using a reduced number of radios on the train instead of the three radios in the default design.

The results showed that when the transmission range of the train was decreased from two nodes to one node, it minimized the interference as now only the first node in the chain experienced the interference and not the second node. The results further showed that the presumption that a minimum 2-node transmission range is required at the train is not valid. In fact, a 1-node transmission range at the train—together with the assurance that minimum two *radios* (in contrast to *nodes*) are able to receive from the train—will both result in lower interference on the nearby nodes and at the same time guarantee the redundancy aimed by the design.

The results showed that when a reduced number of radios is used on the train, there will be both favorable and unfavorable frequency combinations in relation to the alignment of the train's antennas to those on the nearest chain nodes.

The results showed that using a reduced number of radios on the train minimized the interference at the nearby nodes. However, it is noted that it decreased the train node's ability of receiving duplicates from the chain nodes as well.

The results showed that if the train is equipped with only two radios, a less favorable frequency combination is when only the top radio on the second node receives from the train. Due to the lack of duplicate packets received on the side antenna, the impact of the interference from the transmissions of the preceding node increases sharply.

Note that the interference seen inside the chain caused by an interference range larger than the frequency separation distance—i.e. shortcoming 2—is comparatively a larger contributor of the high packet loss than shortcoming 1. Therefore, the results showed that when a reduced number of radios was used on the train, the improvement seen in packet loss in the scenarios with bi-directional traffic was less significant compared to that seen in the uni-directional scenarios. The results showed that when two radios were used on the train, the packet loss dropped from the original 25.42% to 21.57%. Likewise, when one radio was used, the packet loss dropped from 25.42% to 24.78%. Thus, it was concluded that reducing the number of radios on the train alone does not offer significant improvements to the packet loss. Nonetheless, at the same time, it is noted that no increase

in packet loss is seen either, despite that using a reduced number of radios on the train reduces the redundancy as well.

The results showed that when train used only one radio, in the least favorable combination, no packets were received at either of the terminal nodes, as the respective antenna on the nearest chain node was pointing in the opposite direction. However, it was noted that the chain was still able to transfer packets, with a packet loss of 23.97% at the last node at each end.

To address shortcoming 2, scenarios involving the use of more advanced IEEE 802.11 technologies with more robust modulation and coding schemes were investigated. The results showed that dramatic decrease in the interference can be achieved, both for the interference at the train's entry point in the chain and the interference inside the chain. Specifically, with the most robust modulation and coding scheme (16-QAM 1/2), the packet loss dropped from 25.42% to 13.07%.

The chapter further presented the results for the scenarios in which multiple parameters were adjusted simultaneously. The results showed that when train's transmission power was lowered from the default 7 dBm to 5 dBm—the lowest power to enable a 2-node range—and receiver sensitivity was increased to -75 dBm, the packet loss dropped to 12.73%.

CHAPTER 8

Simulation Phase 3: Proposing Extension to the Design

This chapter presents the additional set of scenarios carried out to identify potential solutions to the shortcomings of the design discussed in the Chapter 6. These results have been published in [Farooq2017e] and [Farooq2018b]. Additionally, a patent application ([Farooq2017f]) covering the solution presented in Section 8.3 has been filed. Note that these solutions are studied in isolation from those presented in Chapter 7.

8.1 Scenario 8: Optimizing the frequency separation distance

As discussed in Chapter 6, despite the frequency separation distance enabled by the design, nodes beyond this distance still interfere due to their large interference range in ideal propagation conditions (i.e. shortcoming 2). To minimize this interference, in this chapter, an improved design is proposed that extends the frequency separation distance by increasing the total number of frequencies used, and employing them in an interleaving fashion at each node. The total number of frequencies is increased to four, five and six in steps, to examine closely how it affects the interference. A chain node still uses three frequencies but now each subsequent node uses a different set of three frequencies instead of repeating the same set. That is, at each node, one of the existing three frequencies is replaced with a new one by iterating over the total number of frequencies. Figure 8.1 illustrates the mechanism.

The top part of Figure 8.1 shows the original three-frequency design. Here, for example, the blue frequency is used by Node 1 and Node 4, i.e. a frequency separation distance of three nodes. The bottom part of the figure uses one additional frequency (black—used by Nodes 2, 3 and 4). As seen, this extends the frequency separation distance from three nodes to four nodes as the blue frequency is now repeated at Node 5 instead of Node 4. Increasing the number of frequencies to five and six further extends the frequency separation distance likewise.

Note that as seen in Figure 8.1, no modifications are required to be made to the chain node's equipment as it is still equipped with three radios. On the contrary, the train node is now required to be equipped with additional radios, because, as discussed in Section 3.1.2, it must use all frequencies to be able to transmit to the chain and receive from it. Note that as discussed in Section 2.5.3, it is normal to employ various—e.g. up to

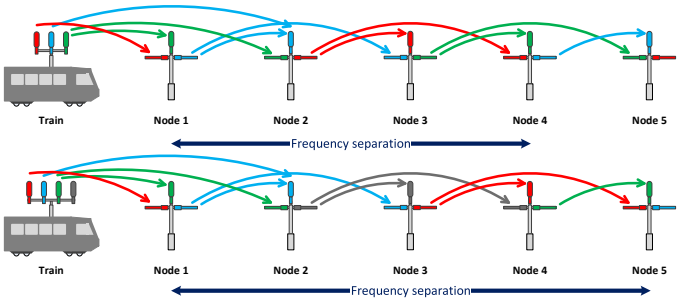

Figure 8.1: Mechanism of optimizing the frequency separation distance: 3 vs. 4 frequencies

four—radios per train in conventional CBTC systems in order to ensure high availability. Thus, this additional radio on the train does not necessarily increase the system's cost. Besides the default three frequencies listed in Table 5.1, the additional three frequencies used are 5735, 5795 and 5815 GHz.

The results for the scenario with four frequencies are presented in Figure 8.2. The results show that when compared to Figure 6.2, which shows results for the three-frequency scenario, an extended frequency separation has resulted in a lowered number of erroneous packets (light blue line) on the middle nodes due to the lowered interference. The result is that the number of packets transferred to the terminal nodes has increased from 74.58% to 82.77%. In other words, the packet loss has dropped from 25.42% to 17.23%.

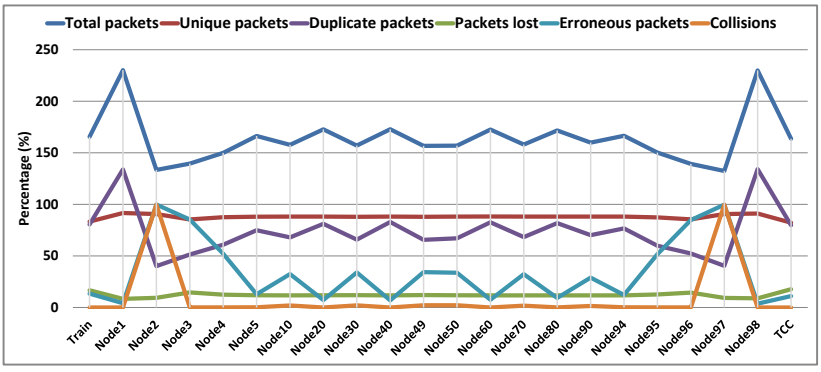

Figure 8.2: Results for Scenario 8: A design with 4 frequencies

The results for five frequencies are presented in Figure 8.3. They show a further drop in the interference, as is also evident from the "smoothed out" lines for erroneous, total and duplicate packets received. For example, the number of total packets received by a

middle node has increased to 170.6% on average, compared to 149.36% seen in Figure 6.2. As a result, the packet loss seen at the terminal nodes has further dropped to 16.22%.

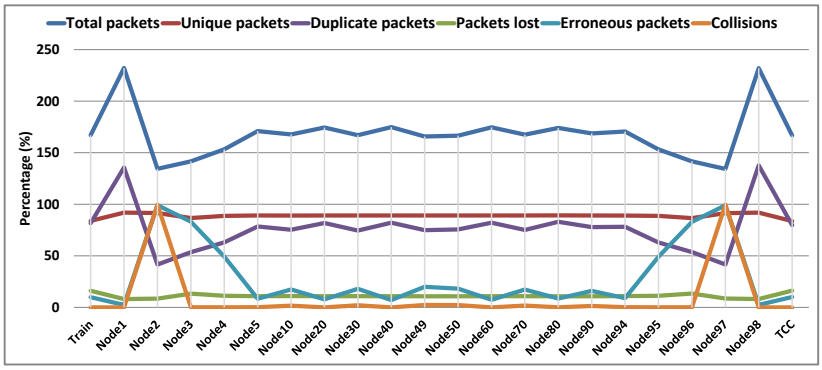

Figure 8.3: Results for Scenario 8: A design with 5 frequencies

Finally, Figure 8.4 shows the results for the six-frequency design. As expected, a significant further drop in the erroneous packets is seen. Specifically, on the middle nodes, on average only 1.93% erroneous packets are received compared to 17.21% seen in Figure 6.2). As a result, the packet loss at terminal nodes drops to 14.54%, a significant drop from 25.42% seen in Figure 6.2.

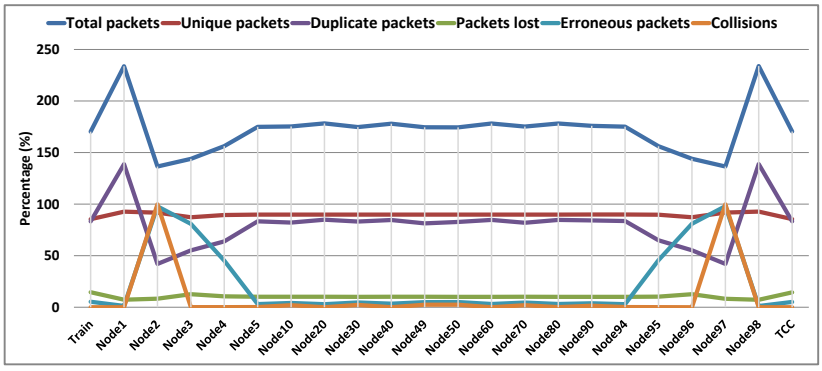

Figure 8.4: Results for Scenario 8: A design with 6 frequencies

Notably, despite that now the number of erroneous packets caused by the chain nodes due to the insufficient frequency separation has dropped to only 1.93% per node, as discussed above, the total packet loss seen at a terminal node is still 14.54%. This reveals that the interference caused by the terminal nodes at their nearby nodes (Nodes 2-4 and

95-97)—i.e. shortcoming 1—is a in fact a greater contributor of the total packet loss, contrary to the conclusion reached in Chapter 7. Specifically, the results indicate that out of the 25.42% packet loss seen in the original three-frequency scenario, approximately 10.88% was introduced by the interference from the nodes inside the chain and 14.54% by the terminal node. Thus, employing additional frequencies might thus not improve the situation significantly unless the interference from the terminal nodes is also minimized.

For the sake of comparison, Figure 8.5 and Figure 8.6 present the number of total and erroneous packets received for the different number of frequencies used, respectively.

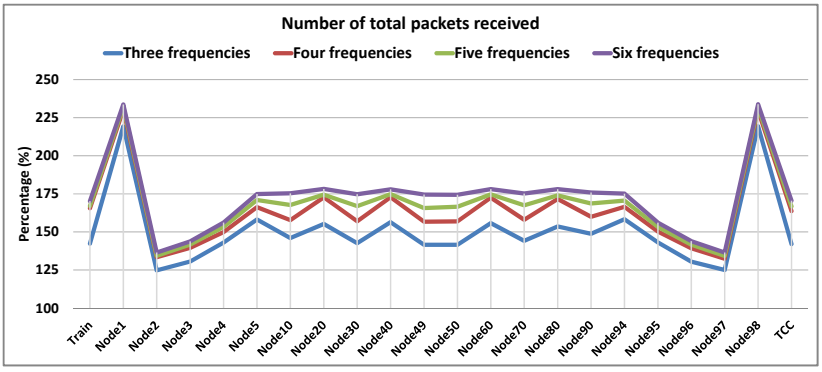

Figure 8.5: Results for Scenario 8: Total packets received for different number of frequencies

As seen in Figure 8.6, increasing the frequency separation distance minimizes the amount of interference dramatically. As a result, the number of total packets received is increased, as seen in Figure 8.5.

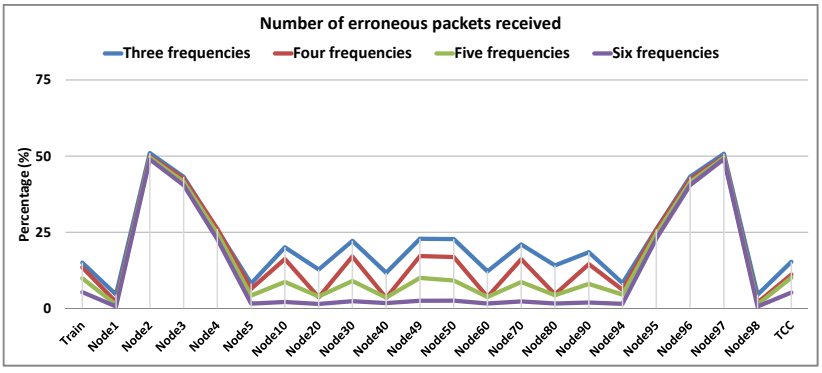

Figure 8.6: Results for Scenario 8: Erroneous packets received for different number of frequencies

Additionally noteworthy in Figure 8.6 is that despite the number of frequencies a terminal node transmits on is increased, no significant difference is seen in the interference at the nearby nodes. The reason is that a chain node still transmits on only two frequencies. Thus, the total number of frequencies interfering with a terminal node's transmissions has not changed. Finally, Table 8.1 summarizes the results.

Table 8.1: Performance comparison of different number of frequencies

Frequencies	Number of packets received at middle nodes (%)			Packet loss at terminal nodes (%)
	Total	Duplicate	Erroneous	
3	149.36	63.93	17.21	25.42
4	164.4	74.21	10.67	17.23
5	170.6	78.6	6.5	16.22
6	176.5	83.67	1.93	14.54

The results emphasize that the interference is a function of distance between nodes transmitting on the same frequency—or in other words, their signal ranges—and demonstrate the effectiveness of the design as it allows to extend this distance by employing additional frequencies. Note that as discussed in Section 2.5.3, the large number of frequencies used is not of a particular concern here as the conventional CBTC systems are already known to employ multiple frequencies to improve availability. Additionally, a vast majority of the CBTC systems in operation today work in the license-free ISM frequency band, as discussed in Section 2.3.3. Furthermore, the objective here primarily is to demonstrate that such a solution is feasible. As discussed in Section 5.2, the simplistic FSPL propagation model has been used for this simulation study. The results show that more realistic, less favorable propagation conditions will improve the performance by negatively affecting the signal range and thus lowering the interference. Thus, a design with a fewer number of frequencies, e.g. four, might as well yield the desired results.

8.2 Scenario 9: Preliminary evaluation of a chain of smaller size

As discussed in Section 5.2, smaller chain segments will be used in actual deployments as the network infrastructure available at train stations will be used to wire the two nearest nodes. Given that, in this phase of the study, the scenarios for the preliminary evaluation of the design presented in Chapter 6 were repeated with a smaller chain size of 18 nodes, which corresponds to approximately 10 kilometers. The simulations in the rest of the study use the same size. This section presents the results for the two scenarios presented in Chapter 6, namely the scenario with uni-directional traffic (Section 6.1, Figure 6.2) and the scenario with bi-directional traffic (Section 6.3, Figure 6.6), repeated with the small chain size, in order to provide a reference point for the discussion of the rest of the results.

Figure 8.7 presents the results for the scenario with the uni-directional traffic, i.e. in which the train transmits packets which are then transferred to the TCC over a chain of 18 nodes. Note that in contrast to the figures presented previously that displayed only a select set of nodes on the x-axis, Figure 8.7 displays all nodes on the x-axis.

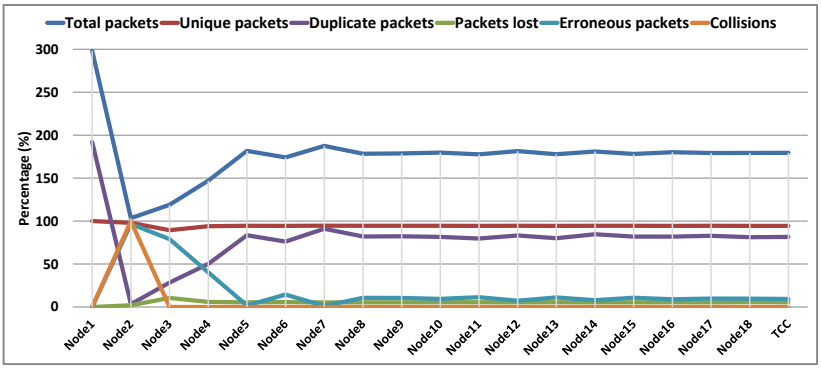

Figure 8.7: Results for Scenario 9: A network with uni-directional traffic, repeated for a smaller chain size

The results show that 94.37% of the unique packets (red line) were successfully transferred to TCC, i.e. a packet loss of 5.63% over a network of 20 nodes. It is noteworthy that only a slight drop in the packet loss is seen compared to 6.74% seen in Figure 6.2, despite that the network size has been reduced to one-fifth—i.e. 20 nodes compared to 100 nodes.

Figure 8.8 shows the results for the scenario with bi-directional traffic, i.e. both the train and the TCC transmit packets to each other, which results in two traffic flows, one in each direction, and a combined data rate of 8.8 Mbps.

The results show that only 59.48% of packets were successfully delivered to the terminal nodes at the each end. In other words, a packet loss of on average 40.52% is seen. This represents a substantial increase from the 25.42% packet loss seen in Figure 6.6 for the scenario with a network size of 100 nodes. Thus, these results prove the obvious misconception held earlier—that a small chain size will result in a lower packet loss—wrong. The reason is that because of the smaller distance between the nodes now, in particular between the terminal nodes, the interference has a more pronounced impact. Unlike in the scenario with 100 nodes, the distance is not large enough to allow the interference to die off. As a result, compared to Figure 6.6, a significant increase in the number of erroneous packets is seen at all nodes, especially Nodes 8-11. This again highlights the interference the chain nodes cause as their interference range exceeds the frequency separation distance. Specifically, at Nodes 5-14, the average number of erroneous packets received ranges as high as 25.59%. As a result, the number of total packets received at these nodes is less than 150%. This is a low number given that a node

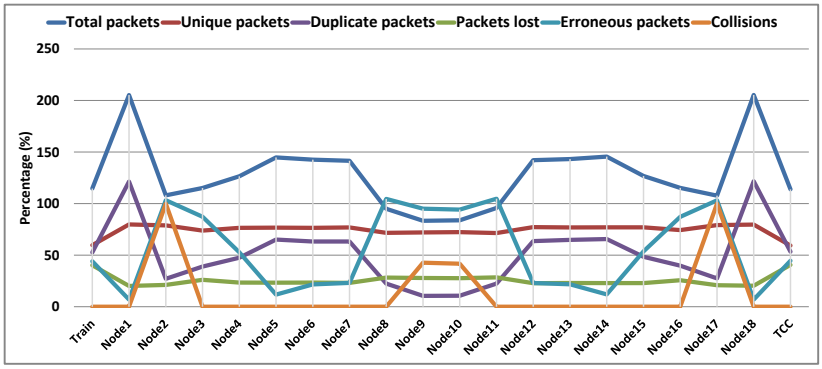

Figure 8.8: Results for Scenario 9: A network with bi-directional traffic, repeated for a smaller chain size

shall ideally receive two copies of the same packet, i.e. 200%. Likewise, the number of duplicate packets received is less than 65%, a much lower number than the ideal 100%.

8.3 Scenario 10: Introducing frequency separation for the train

As discussed in Section 8.1, the interference caused by a train at its nearby nodes proves to be a greater contributor of the high packet loss than the interference caused by the nodes inside the chain. Thus, this section presents an extension to the design in which a dedicated new frequency is employed for the train-to-trackside (i.e. train to chain) communication. Figure 8.9 illustrates the mechanism where the yellow color represents the new frequency.

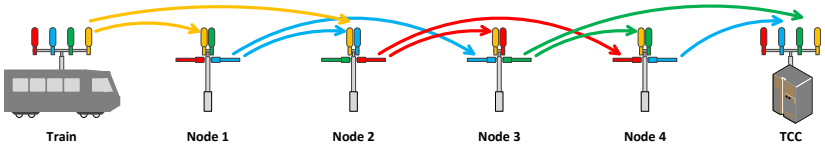

Figure 8.9: Mechanism of using a separate frequency for train-to-trackside communication

Each node in this design is equipped with an additional radio that operates on this dedicated frequency. All the transmissions from train to chain are now made on this new dedicated frequency. On the other hand, a chain node, upon receiving a packet from a train, still uses the original three frequencies for forwarding the packet to the other chain nodes as in the original design. Thus, in this way, the transmissions from the train do not

interfere with those from the chain nodes. Note that the transmissions from chain to train are also made on the existing three frequencies, as before.

Figure 8.10 shows the results for the proposed extension for the scenario with uni-directional traffic. The effectiveness of the new design is evident as the erroneous packets seen at Nodes 2-4 in Figure 8.7 have disappeared and so has the drop in the total and duplicate packets received at these nodes. As a result, the packet loss at the TCC has dropped from 5.63% to only 0.41%.

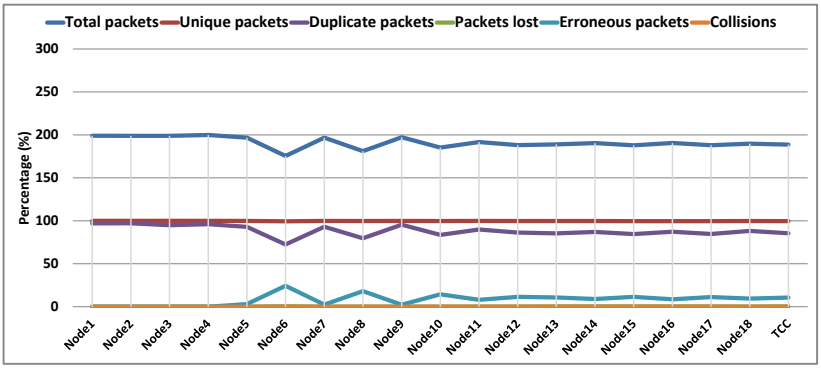

Figure 8.10: Results for Scenario 10: Separate frequency for train-to-trackside communication with uni-directional traffic

Figure 8.11 shows the results for the scenario with bi-directional traffic. As expected, the erroneous packets have disappeared at both ends of the chain and the packet loss at the two terminal nodes has dropped from 40.52% seen in Figure 8.8 to 17.85%. This confirms, as concluded above, that the major part of the packet loss—22.67% out of 40.52%—was caused by the terminal nodes' transmissions. As it is observed subsequently, the rest 17.85% packet loss is caused by the interference between the chain nodes, due to their interference range being larger than the frequency separation distance.

It is worth noting that while the original objective of introducing the additional radio on the train is to employ a separate frequency for the train-to-trackside communication, alternatively, it can as well be used to employ a separate radio technology. For example, a combination of radio technologies can be employed such that LTE or IEEE 802.11p is used for the train-to-trackside communication, and Wi-Fi for the in-chain communication.

Note that one drawback of using one separate frequency for train-to-trackside communication is the loss of redundancy, as now train only transmits one copy of a packet in contrast to three copies as in the original design. One potential solution is to increase the number of frequencies for train-to-trackside communication to, e.g. two or three. However, a drawback of that would be the increased number of total frequencies—and thus, radio equipment—involved. An alternative solution could be to transmit each packet

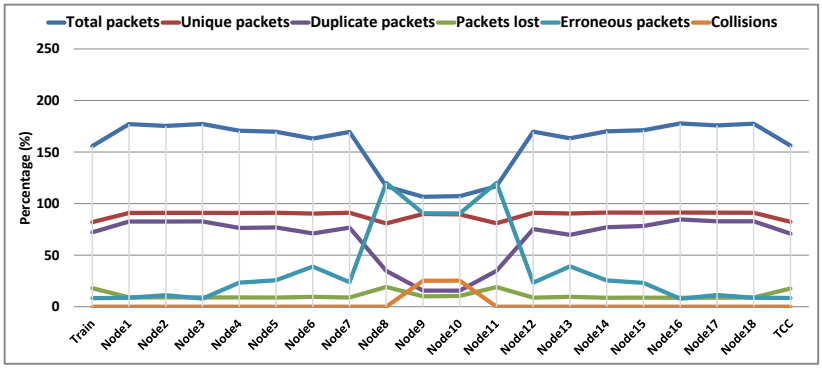

Figure 8.11: Results for Scenario 10: Separate frequency for train-to-trackside communication with bi-directional traffic

multiple times. Nonetheless, a drawback of that would be that the bandwidth will be halved.

8.4 Scenario 11: Combined frequency separation optimization

To further minimize the packet loss of 17.85% seen in Figure 8.11, in this scenario, the extension proposed in Section 8.1—in which additional frequencies are employed by the chain nodes to extend the frequency separation distance—is combined with the extension involving a separate frequency for the train-to-trackside communication discussed in Section 8.3. Note that Section 8.1 discusses configurations involving a total of four, five, and six frequencies. However, only the configuration involving four frequencies is considered in this scenario.

Figure 8.12 illustrates the mechanism when the two extensions are combined, i.e. the yellow frequency is used for train-to-trackside communication and the black frequency is used for communication between chain nodes in addition to the original three frequencies.

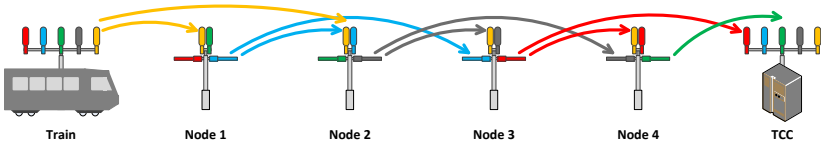

Figure 8.12: Separate frequency for train-to-trackside communication combined with extended frequency separation

The results for the design with the combined extensions are presented in Figure 8.13.

As seen, when compared to Figure 8.11, the extended frequency separation has resulted in a lowered number of erroneous packets at Nodes 5-14. Thus, a significant drop is seen in the number of packets lost at each node and consequently, an increase in the number of unique packets received. As a result, the packet loss has dropped from 17.85% seen in Figure 8.11 to only 1.1%.

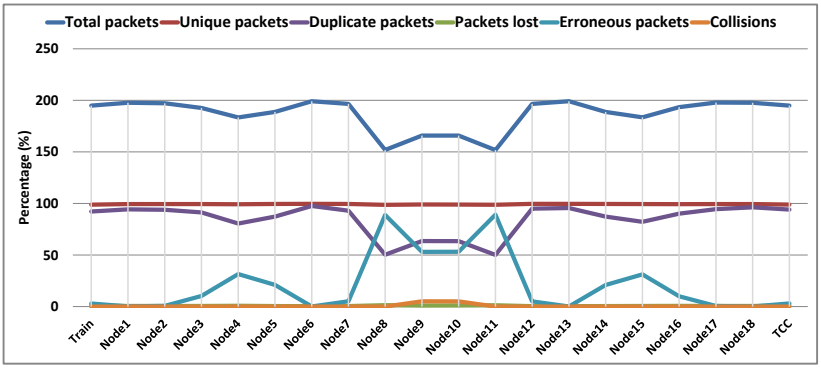

Figure 8.13: Results for Scenario 3: Separate frequency for train-to-trackside communication combined with extended frequency separation

The results further confirm that the interference caused by the terminal nodes at their nearby nodes is a greater contributor to the total packet loss. Specifically, out of the 40.52% packet loss seen in the default scenario (Figure 8.8), 22.67% was introduced by the terminal nodes, and 16.89% out of the rest 17.85% was introduced by the interference between the chain nodes.

The results demonstrate the effectiveness of the design as it allows to optimize frequency separation by employing additional frequencies, both for train-to-trackside and in-chain communication.

8.5 Summary

This chapter presented the results from the third phase of the simulation study which continued to investigate additional solutions to the two shortcomings discussed earlier. The chapter discussed two extensions to the design to address these shortcomings.

To minimize the shortcoming that deals with the interference produced by the nodes inside the chain despite the frequency separation, the proposed extension employs additional frequencies in order to optimize the frequency separation distance. In this solution, the number of total frequencies used is increased from the default three to four, five and six, such that introducing each additional frequency extends the frequency separation distance. The results showed that the packet loss dropped from the original 25.42% to

17.23%, 16.22%, and 14.54%, as the number of frequencies were increased from three to four, five and six, respectively.

It is noted that in this extension, a chain node still uses three frequencies, i.e. no changes are required to be made to the node hardware. However, these frequencies are now used in an interleaving fashion, i.e. each subsequent node uses a different set of the three frequencies instead of repeating the same set as in the original design. It is simultaneously noted that using a large number of frequencies is not of a particular concern as the conventional CBTC systems are already known to employ multiple frequencies to improve availability. Additionally, a vast majority of the CBTC systems worldwide operate in the ISM frequency band which is license-free. It is further emphasized that the simplistic FSPL propagation model has been used for this simulation study. In real-life, less favorable propagation conditions will improve the performance by decreasing the interference range, and thus, a design with a fewer number of frequencies, e.g. four, might as well yield the desired results.

The scenarios performed in Chapter 6 for the preliminary evaluation of the design were repeated at this stage with a smaller chain size of 18 nodes, in contrast to the original 98 nodes. Interestingly, the results showed that the packet loss increased—from 25.42% to 40.52%—instead of dropping. The results proved the misconception that a small chain size will result in a lower packet loss wrong. The reason is that because of the smaller distance between the nodes now, interference caused by the transmissions of the terminal nodes—as well as that caused by the chain nodes inside the chain—has a more pronounced impact. Furthermore, the distance is not large enough to allow the interference to die off.

To minimize the interference caused by a train node due to its transmissions on all frequencies, an extension was proposed in which an additional, dedicated frequency is employed for the train-to-trackside communication to introduce frequency separation. The results showed that the proposed extension successfully eliminated the interference caused by the train and as a result, the packet loss dropped from 40.52% to only 5.63%.

It is noted that with the help of this extended design, besides employing a separate frequency for the train-to-trackside communication, a separate radio technology can as well be used, e.g. a combination of technologies can be used such that LTE or IEEE 802.11p is used for the train-to-trackside communication, and Wi-Fi for the in-chain communication.

Finally, the results for a scenario in which the two extensions were combined showed that the packet loss dropped to only 1.1%.

CHAPTER 9

Simulation Phase 4: Extended Evaluation of the Design

This chapter presents the results from the extended evaluation of the design in which the impact of parameters such as number of trains, train speed, train's location on the track, headway distance, train direction, and track layouts are investigated. Note that except for Section 9.1, which evaluates the backward forwarding mechanism, all the scenarios discussed in this chapter involve moving trains. These results have been disseminated in [Farooq2018c].

As discussed in Chapter 1, the focus of this study is open lines (or tracks) in contrast to train stations. Therefore, the scenarios presented in this chapter involve a maximum of three trains, as a number greater than this within a certain distance is less likely. The track-to-chain distance has been set to 10 meters, a typical distance in real CBTC networks. Table 9.1 lists a number of additional parameters as well as updated values of the parameters listed earlier in Table 5.1.

Table 9.1: Simulation parameters

Parameter	**Value**
Transmission power (dBm)	Train: 1 (default), 7, Chain node: 1
Track-to-chain distance (m)	10
Chain nodes	18
Track length (m)	10800
Number of trains	1-3
Train speed (km/h)	60, 90, 120, 180
Headway (m)	100, 200, 300, 600, 3000
Packet rate (per second)	1000 (default), 500, 250
Simulation time (s)	60 (default), 145, 192, 288, 576

The practice of presenting the results for the scenarios with uni-directional traffic (i.e. train to TCC) first and then the results for the scenarios with bi-directional traffic is followed in this chapter. It facilitates in discussing the results in isolation from whatever impact bi-directional traffic may have on the results.

Note that in addition to the large headway distances listed in Table 9.1, a number of

scenarios in this chapter use smaller headway distances of 100, 200 and 300 meters to consider the worst case scenarios. For example, in the congested areas such as train stations and depot and parking areas, it is common for the trains—moving or stationary—to have short distances between them. Additional reason why short distances are interesting is the shortcoming 1 discussed in the previous chapters. Namely, that the since a train transmits on all frequencies, it undermines the frequency separation otherwise guaranteed in the chain. In the scenarios discussed in the previous chapters, the impact of this shortcoming was seen as increased interference on the nearby chain nodes. In the scenarios in this chapter, since multiple trains are involved, the impact of this shortcoming will be seen on the trains, as they will interfere with each other's transmissions—if the distance between them is small. Note that the typical headway distances in the real CBTC networks are much larger. For example in the Copenhagen S-train CBTC network, the highest train speed is 120 kilometers per hour (km/h) and the minimum headway interval is 90 seconds—i.e. a headway distance of 3000 meters. To assist in discussing the results, Table 9.2 lists trains speeds and the distance traveled in the headway interval of 90 seconds, as well as in the typical simulation time of 60 seconds used in this study.

Table 9.2: Example train speeds and distances covered

Train speed		**Distance traveled (m) in**	
(km/h)	**(m/s)**	**60 s (simulation time)**	**90 s (typical headway)**
60	16.6	1000	1500
90	25	1500	2250
120	33.33	2000	3000
150	41.67	2500	3750
180	50	3000	4500

Nonetheless, note that at lower speeds, for example, at 60 km/h, a train's actual stopping distance is much smaller than 1500 meters shown in Table 9.2. The minimum separation between the trains depends on the stopping distance of the train, which is based on a safe braking model. Besides the speed, there are a number of parameters that influence the stopping distance, including, for example, deceleration rate, geometry of the track, train mass, and braking delay. Table 9.2 lists approximate stopping distances for the S-train trains running at different speeds [160]. As seen, two trains running at the speed of 30 km/h can run as close as 100 meters. Thus, the small headway distances used in this study take into account the trains running at low speeds.

It is noteworthy that the objective of the scenarios presented in this chapter is to evaluate the original design. Due to the fact that the development of the actual product was already in its relatively advanced stages by the time, and that a preliminary version of the product was already being tested on a real railway line, adopting the improvements discussed in Chapter 7 and Chapter 8, especially those involving equipment modification, was not feasible. Therefore, the scenarios presented in this chapter are carried out in

Table 9.3: S-train speeds and approximate stopping distances

Train speed (km/h)	Stopping distance (m)
30	100
60	240
90	460
120	790

isolation from these improvements.

Further note that the results presented until now used the constant distribution for data traffic generation, which causes increased interference as the probability that the trains transmit at the exact same time increases. As the following scenarios involve a greater number of traffic flows—six for the scenarios with three trains and bi-directional traffic—normal distribution has been used from now onward. Normally distributed traffic generation is additionally consistent with real-life where there will be more variations in the propagation delay as well as in the traffic generation patterns of different trains.

9.1 Scenarios involving stationary trains

Figure 9.1 shows the results for the scenario with stationary terminal nodes and bi-directional traffic, as previously presented in Section 8.2 (Figure 8.8).

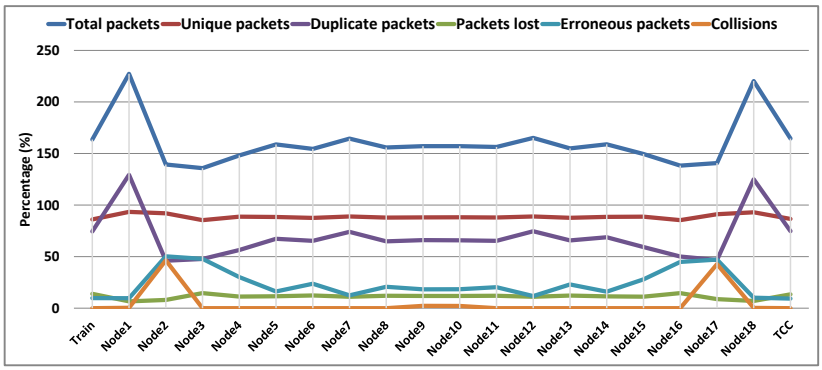

Figure 9.1: Results for scenario with bi-directional traffic

Note that in the results presented until now, the figures showed an average of the numbers for each statistic except for the number of erroneous packets received and the number of collisions. This helped observing, for example in Figure 8.8, that all (i.e. 100%) transmissions from the train resulted in collisions at Node 2, and likewise on Node 17. However, from now onward, since a greater number of traffic flows is involved, these

two numbers are also averaged. This implies that, for example, the actual number of collisions experienced at Node 2 and Node 17 are still 100%, despite shown as 50% in Figure 9.1.

The most significant observation from Figure 9.1 is that when the traffic is generated in a normally distributed fashion, the probability that transmissions interfere with each other drops dramatically. Specifically, compared to Figure 8.8 in which a packet loss of 40.52% was seen at the terminal nodes, a substantially lower packet rate of 13.66% is now seen. This is evident from the substantial decrease in the number of erroneous packets received at the chain nodes, particularly at Nodes 8-12, in Figure 9.1. This implies that the degree of variations in the traffic generation patterns of the terminal nodes—and as a consequence, of the chain nodes—will greatly influence the interference produced. This emphasizes the fundamental characteristic of this design in which chain nodes are supposed to forward the packet immediately after receiving and thus the probability of interfering with each other depends greatly on the data rate of the terminal nodes. Likewise, it shows that if a higher data rate was used—i.e. higher than the default 1000 packets per second or 4.4 Mbps used in this study—the outcome will be less promising.

In the following scenario, a stationary train is placed in the middle of the chain—at 5700 meters—as shown in Figure 9.2. The objective is to verify that the same number of packets is received regardless of which end of the chain the TCC is located. Recall that a chain node, upon receiving from a train, forwards packets in both directions, as described in Section 3.1.3.

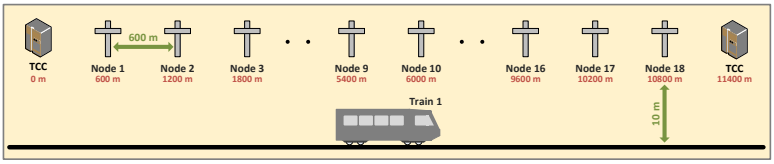

Figure 9.2: Scenario with 1 stationary train in the middle of chain

Train's transmission power is set to 1 dBm, sufficient enough to reach two nodes at each side from this distance—this change is power is further explain later in Section 9.2. Note that with this power, only one radio (i.e. the side radio) on the second node is supposed to receive from the train, and not the top radio. This is consistent with the intended design in real-life where the top radio will have lower gain due to its omni-directional antenna, and thus lower receive sensitivity compared to the side antenna. Note that since the track-to-chain distance is 10 meters, this means the transmission range with this power is 610 meters.

In the first part of the scenario, TCC is located at the right end of the chain and in the other, at the left end. Figure 9.3 illustrated the results for the first part of the scenario. The results for the scenario with TCC located at left are not presented here as they look very similar (i.e. symmetrical).

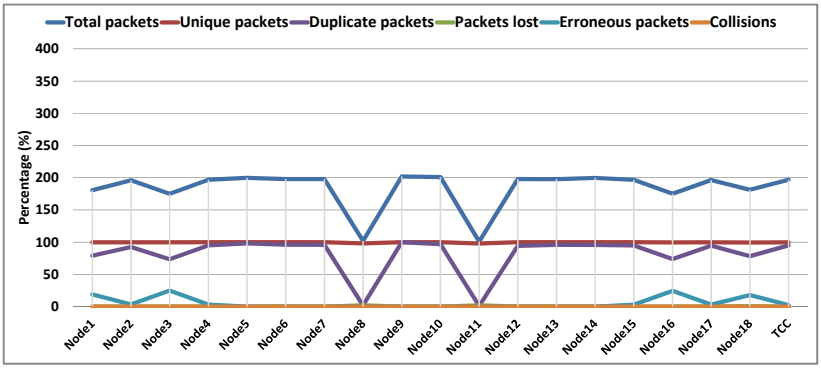

Figure 9.3: Results for 1 stationary train in the middle and TCC located at the right of the chain

As seen from the number of total packets received, the TCC receives an equivalent number of packets in both cases. The average packet loss seen at TCC in the two cases is 0.21%. Note that the number of total packets received at Nodes 8 and 11 is only 100% compared to 200% received at the other nodes. As seen, this is due to the fact that the number of duplicate packets received at these nodes is zero. These drops in the number of total and duplicate packets are because as noted above, only the side radios on these nodes receive packets form the train.

Additionally, a noteworthy observation is the increase in the number of erroneous packets further in the chain at both sides, namely at Nodes 1, 3, 16 and 18. As discussed in Section 3.1.3, in the proposed design, a chain node, upon receiving a packet directly from a train, forwards the packet in both directions. These large numbers of erroneous packets are a result of the additional interference produced by this backward forwarding. That is, packets forwarded by Node 9 in the right direction and by Node 10 in the left direction. Note that these erroneous packets are not seen in Figure 8.7—i.e. the scenario in which the train is located at one end of the chain. It is due to the fact that in that case, the packets are forwarded in the backward direction (i.e. left) by Nodes 1-2 but since there are no nodes located at the left side of these nodes, this phenomenon cannot be seen. The backward forwarding mechanism is discussed in further detail shortly.

In the next scenario, two stationary trains located at the middle of the chain transmit packets. The objective is to study how the trains interfere with each other's transmissions. Recall from the discussion in the context of Figure 8.7 and Figure 9.1 that since a train transmits on all frequencies with omni-directional antennas, there is a lack of frequency separation otherwise guaranteed between the chain nodes. Additional objective is to verify that the backward forwarding mechanism performs as expected. The headway is set to 600 meters, which means the trains are positioned at the 5400 and 6000 meters positions in the chain. Each train transmits to a TCC located at the opposite end of the

chain. Figure 9.4 illustrates it in a simplified way to aid the understanding.

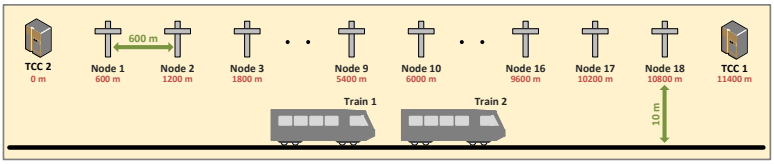

Figure 9.4: Scenario with 2 stationary trains in the middle of chain

Figure 9.5 presents the result for the scenario shown in Figure 9.4. Here, a averaged packet loss of 4.76% is seen at the two TCCs.

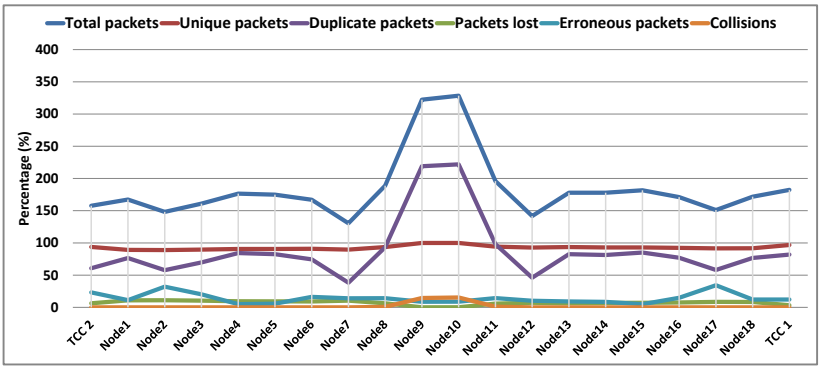

Figure 9.5: Results for 2 stationary trains in the middle of chain

However, when in the next scenario the locations of the two TCCs are swapped, as shown in Figure 9.6, a substantial increase in the packet loss is seen. The packet loss now jumps to 15%. The results are shown in Figure 9.7.

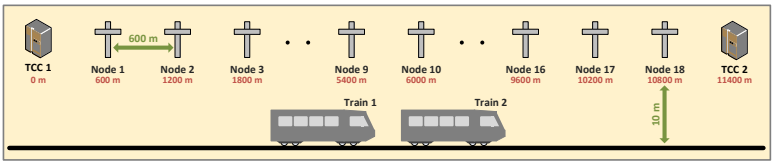

Figure 9.6: Scenario with 2 stationary trains in the middle of chain and TCCs swapped

Noticeably, while the results for the number of unique packets received and packets lost in the two figures look identical for the chain nodes, a significant change is seen in the results at the TCCs compared to in Figure 9.5. Specifically, there is now a lower number

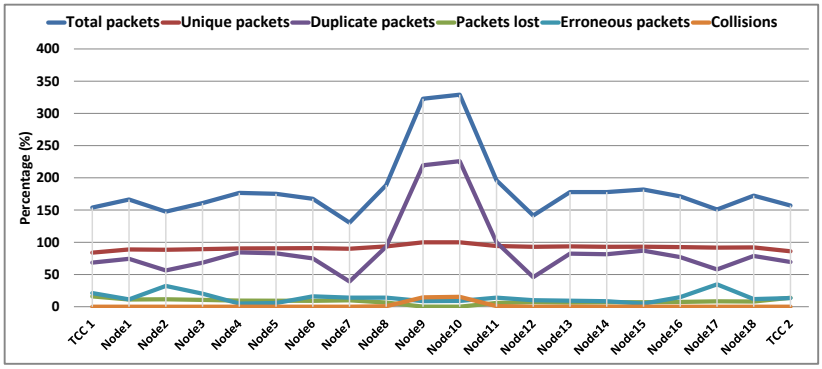

Figure 9.7: Results for 2 stationary trains in the middle of chain amd TCC swapped

of unique packets received (red line) and a higher number of packets lost (green line) at the TCCs. This implies that for a given train, there is a larger number of packets travelling through the chain in one direction than in the other direction. Additionally noteworthy is that in each scenario, the results for the two trains are not identical. Specifically, in Figure 9.5, the two trains experience a packet loss of 6.26% and 3.26% (average 4.76%) and in Figure 9.7, the two trains experience a packet loss of 16.08% and 13.92% (average 15%). The reason behind this phenomenon is discussed next.

As discussed in Section 3.1.3, in the proposed design, a chain node, upon receiving a packet directly from a train, forwards the packet in both directions. In the original design presented in Chapter 3, the top radio on the node performs this two-direction forwarding. This is illustrated in Figure 9.8 (a) where the top radios on Node 2 and Node 3 forward the packet received from the train in both directions (via their side radios). On the contrary, a side radio delivers the packet received from the train only to the other side radio inside the node for forwarding, as illustrated in Figure 9.8 (b). This means, the node forwards the packet only in one direction, i.e. forward direction. For example, Node 3's left radio (blue) delivers the packet to its right radio (green) where it is transmitted in the forward (i.e. right) direction to Node 4.

Note that a train's transmission range is 2-node in reality, i.e. Train 1's packets will be received at Node 1 and Train 2's packets will be received at Node 4 as well. However, for simplicity, Figure 9.8 only shows train's transmissions with a 1-node range.

There are two problems with this approach. First, normally packets are received first on a side radio of a node and then on its top radio, due to the greater gain of the side radio (a directional antenna) compared to the top antenna (an omni-directional antenna). First, since this approach relies only on the top radio to forward in the two directions, if the packet on the top radio turn out to be erroneous, for example due to the interference from another train, the packet might be discarded and thus not forwarded. One will

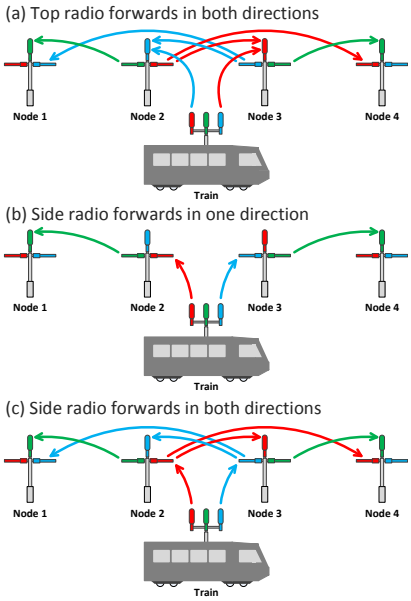

Figure 9.8: Forwarding mechanism, default (a & b), improved (a & c)

assume that then the side radio on the node at the other side (i.e. left) of the train (right radio on Node 2 in Figure 9.8) will forward the packet in the other direction (i.e. right) anyway. However, if the trains are located close to each other, the packets received on the other node might also turn out erroneous, as discussed further in this section. Thus, to overcome this shortcoming, an improvement to the mechanism is proposed in which a side radio upon receiving a packet from a train, both delivers it to the other side radio for transmission and transmits it itself as well. This enables additional redundancy as an additional copy of the packet is transmitted. This is illustrated in Figure 9.8 (c).

As a further explanation of the problem, Figure 9.9 illustrates the scenario where two stationary trains located close to each other transmit. As shown in Figure 9.9 (a), the transmissions of the two trains on the red and blue frequencies interfere with each other at Node 2's top and right radios and Node 3's top and left radios, resulting in erroneous packets. Thus, the top radio on the two nodes are unable to forward the packet in either direction. For the same reason, the right radio on Node 2 and the left radio on Node 3 are unable to forward the packets in the opposite directions, i.e. left and right directions, respectively. Figure 9.9 (b) omits the erroneous transmissions and illustrates only the successful transmissions for simplicity. As seen, the packets from Train 1 are correctly received at Node 2 left (green), which delivers it to the right radio (red), which transmits the packet. Similarly, Train 2's packets are correctly received at Node 3 right (green)

and are forwarded via its right radio (blue). However, as seen in Figure 9.9 (b), the consequence is that trains' packets are now flowing only in one direction, i.e. Train 1's packets are flowing to the right and Train 2's packets are flowing to the left. No packets are transmitted in the opposite direction for either of the train. Now suppose the destination TCC for a train was located in the other end, as shown in Figure 9.6. It will result in none of the packets arriving at the correct TCC, i.e. a packet loss of 100%. If the improved forwarding mechanism is used, Node 2's left radio will transmit the packet again, thus flowing in the left direction. Likewise, Node 3's right radio will transmit in the right direction.

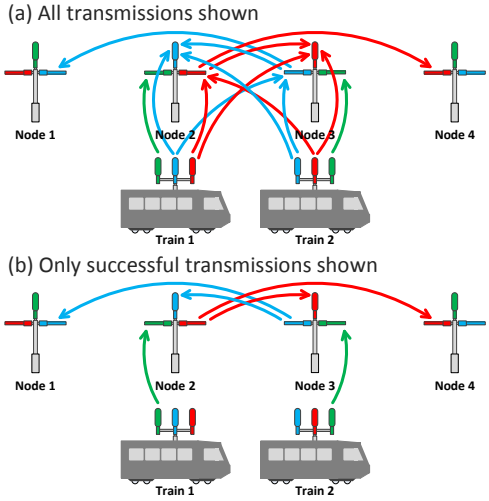

Figure 9.9: Performance of the original backward forwarding mechanism when two trains are located close to each other

Note that even if the top radios on Nodes 2 and 3 had received the packets correctly, they would have dropped as duplicates as the packets had already been received on their side radios (Node 2's left radio and Node 3's right radio) correctly. Further note that as with Figure 9.8, Figure 9.9 only shows train's transmissions with a 1-node range. Nonetheless, for a scenario with trains running this close, the probability of them interfering at Nodes 1 and Nodes 4 is likewise high.

Figure 9.10 presents results for the improved backward forwarding mechanism. It shows that a significantly higher number of packets is received, particularly on Nodes 7-12, compared to in Figure 9.7. Additionally, the drops in the number of total and duplicate packets received at Nodes 7 and 12 seen in Figure 9.7 have disappeared. This is a result of packets forwarded by the side radios of Nodes 9 and 10 in the backward direction. The packet loss seen at the TCCs has now dropped to 7.65%, compared to 15%

in Figure 9.7. Note that although the improved mechanism creates additional interference—as an additional transmission is made for each packet received—the additional redundancy achieved compensates for it. This increased interference is evident in Figure 9.10, seen by the greater number of collisions and erroneous packets at Nodes 1-3, 9-10 and 16-18 compared to in Figure 9.7.

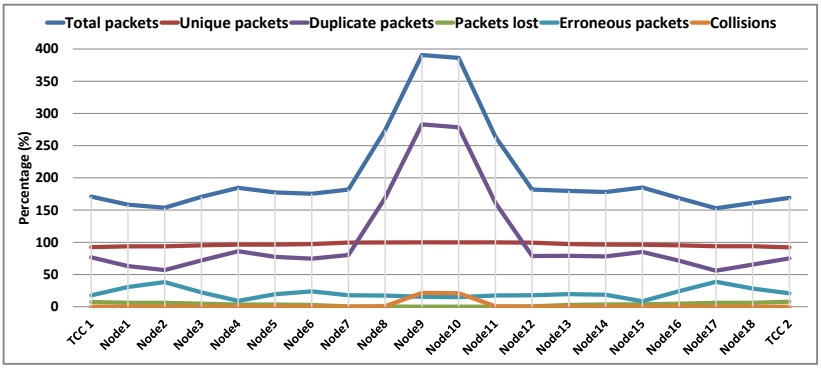

Figure 9.10: Results for 2 stationary trains in the middle of chain, with improved backward forwarding mechanism

Finally, results for the scenario in Figure 9.3 but with the improved backward forwarding mechanism are presented in Figure 9.11. The greater (300%) number of total and duplicate packets received at Nodes 9-10 is because now each of these nodes receives three copy of each packet. For example, Node 9 receives two copies directly from the train on its right and top radios and one copy forwarded backward (i.e. left direction) by the left radio of Node 10. For the same reason, the drops in the number of total and duplicate packets at Nodes 8 and 11 seen Figure 9.3 have disappeared as these nodes now receive packets forwarded by Nodes 9-10 in the backward direction. As with Figure 9.10, a greater number of erroneous packets is seen at the nodes at the two ends—Nodes 1-3 and 16-17—compared to in Figure 9.3 is due to the packets forwarded backward by Nodes 9 and 10.

9.2 Scenarios involving trains running on the same track

In this section, scenarios involving one or more moving trains are presented. In the first scenario, results against a train running at the speed of 60 and 180 km/h are compared to study the impact of speed on the amount of interference seen on the chain nodes. The train moves from left to right and TCC is located at right. Figure 9.12 illustrates the scenario.

The train starts running from the position of 0 meters as shown in Figure 9.12. The train's transmission power is set back to 7 dBm for this particular scenario, as in Section

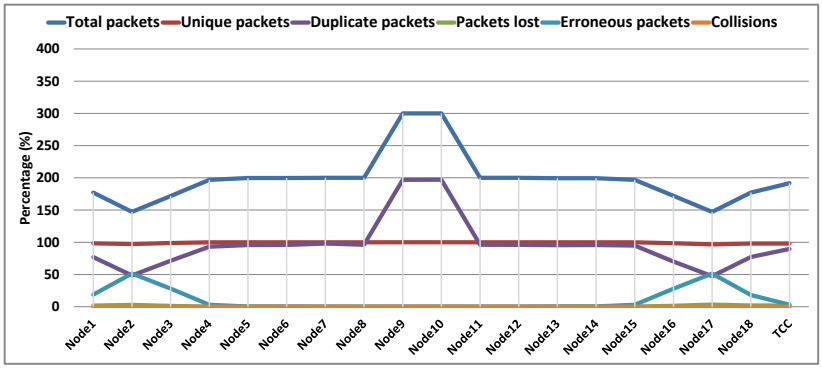

Figure 9.11: Results for 1 stationary train in the middle and TCC located at the right of the chain, with improved backward forwarding mechanism

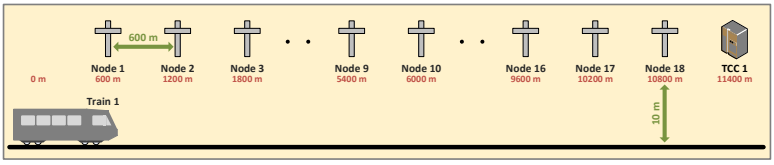

Figure 9.12: Scenario with 1 train running from left to right

9.1, to be able to reach Nodes 1-2 from that position. As seen in Table 9.2, at the speeds of 60 km/h and 180 km/h, the train will travel a distance of 1000 and 3000 meters, respectively, in the simulation time of 60 seconds. Thus, as shown in Figure 9.12, for 60 km/h, it will stop 200 meters before Node 2 and for 180 km/h, it will stop next to Node 5. Figure 9.13 and Figure 9.14 show the results for the two speeds.

The results show that the packet loss seen at the TCC for the two speeds is 10.14% and 13.1%, respectively. It shows that the slower the train speed, the greater the interference as more transmissions will interfere with the exact same arrival time. This is evident from the greater number of erroneous packets and collisions on Nodes 2-4 for 60 km/h (Figure 9.13) compared to for 180 km/h (Figure 9.14). This is further evident as Figure 9.13 is more similar to Figure 8.7—that showed results for the scenario with the stationary train—than Figure 9.14 is to Figure 8.7.

The large number of total and duplicate packets received for certain nodes in the figures presented—e.g. for Nodes 1-2 in Figure 9.13 and Nodes 1-5 in Figure 9.14—indicate how far the train traveled. Recall that as discussed in Section 3.1.3, these large numbers are because the two nodes nearest the train forward the packets received directly from the train in the backward direction as well.

Note that in the scenarios presented thus far—except for the scenarios in Section 9.1

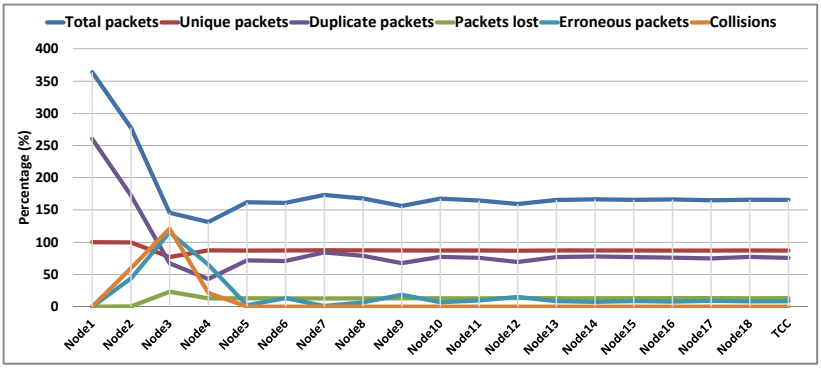

Figure 9.13: Results for 1 train running left to right at a speed of 60 km/h and transmission power of 7 dBm

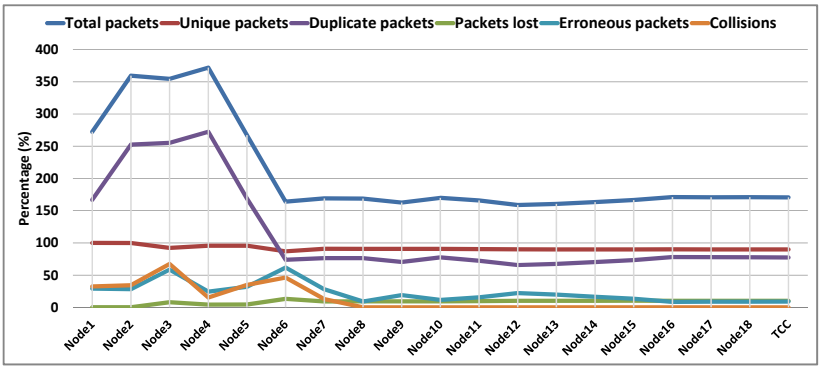

Figure 9.14: Results for 1 train running left to right at a speed of 180 km/h and transmission power of 7 dBm

discussing the backward forwarding mechanism—the train was positioned at 600 meters from the first node in the chain (Node 1)—i.e. position 0 meters—as shown in Figure 3.4. It served the purpose then as train movement was not considered and the objective mainly was to verify the design with stationary nodes. In other words, train acted just like a chain node. However, now that the train movement is involved, this distance is not realistic. Note that a typical track-to-chain distance in real CBTC networks is in the range of 5-20 meters.

Further note that since the train transmits with a transmission power of 7 dBm like any chain node, which guarantees a range of 1200 meters, it implies that in certain situations, its transmissions reach three nodes instead of two nodes (i.e. in one direction) required by the design. For example, when train reaches next to Node 1, it's transmissions will be

heard at Nodes 1-3. This also explains that large amount of interference—i.e. number of erroneous packets and collisions—seen in Figure 9.13 and Figure 9.14. For these reasons, in the next scenario, the train moves at the same two speeds except that now it starts moving from the position of 600 meters rather than 0 meters. Note that this means the train will start from a position parallel to Node 1. Since the track-to-chain distance has been set to 10 meters, the train's transmission power is now lowered from 7 dBm to 1 dBm. Note that as per the outcome of the discussed in Section 7.1, in which train's transmission power was lowered to decrease the interference on the nearby nodes, this power value (1 dBm) represents the absolute minimum power required to reach two nodes from this distance.

Figure 9.15 and Figure 9.16 show the results for the two speeds, respectively. As seen, there is a substantial decrease in the interference compared to Figure 9.13 and Figure 9.14 that has resulted in a low packet loss of 1.79% and 1.85% at TCC, respectively.

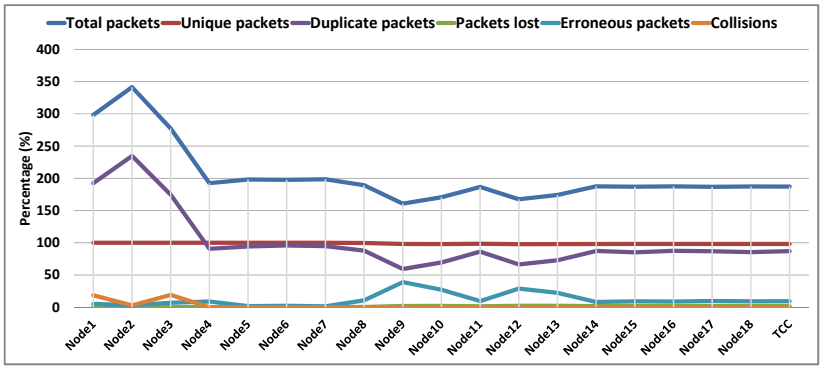

Figure 9.15: Results for 1 train running left to right at a speed of 60 km/h

In the next scenario, the TCC is moved to the left of the track. This means that the TCC is located only 600 meters from the train when the train starts running. The results showed a packet loss of only 0.28%, which presents a significant drop given that now the TCC is placed much closer to the train.

Next, the scenario in Figure 9.16 is repeated except that now only TCC transmits. The results, presented in Figure 9.18, show that a negligible amount of packet loss is seen at the train—0.18%. Note that the greater number of total and duplicate packets received at the train in comparison to the chain nodes is because train receives packets on all three frequencies. Thus, the train will receive at least two copies of the packet. Occasionally, it will receive three copies of a packet at certain locations where it is within in the transmission range of three chain nodes. This explains the 250% number of total packets received shown in Figure 9.18. In the subsequent scenario, when the TCC is moved to the left side, as shown in Figure 9.17, the results—not presented here—showed

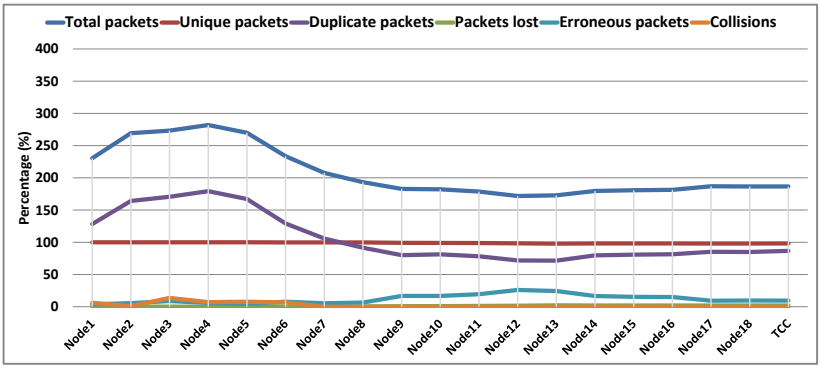

Figure 9.16: Results for 1 train running left to right at a speed of 180 km/h

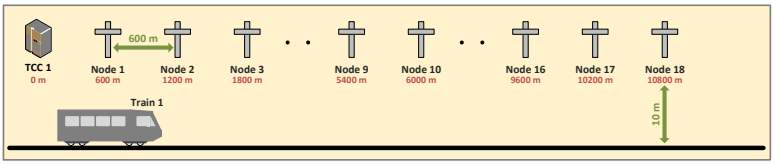

Figure 9.17: Scenario with 1 train running from left to right at TCC located at left side

that the packet loss at the train dropped further to 0.045%.

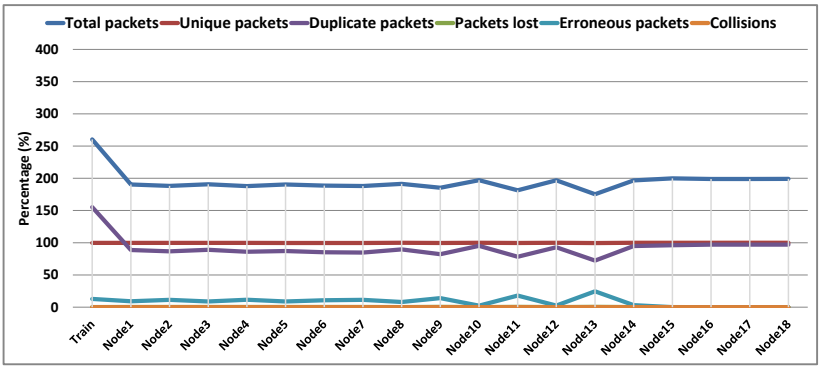

Figure 9.18: Results for 1 train running left to right at a speed of 180 km/h, only TCC transmits

Figure 9.19 shows results for a scenario where both train and TCC transmit packets to each other, i.e. bi-directional traffic, which results in a combined data rate of 8.8 Mbps.

Since the TCC also transmits now, a significant increase in amount of interference—i.e. in the number of erroneous packets—is seen in Figure 9.19 compared to Figure 9.16. Note that as the traffic is flowing in both directions, the top radio on each node faces interference from nodes on its both sides. As a result, a slightly higher packet loss of 7.65% and 2.53% is seen at the TCC and the train, respectively, compared to 1.85% in Figure 9.16. The results imply that the train loses a greater number of packets due to its movement compared to the TCC which is stationary.

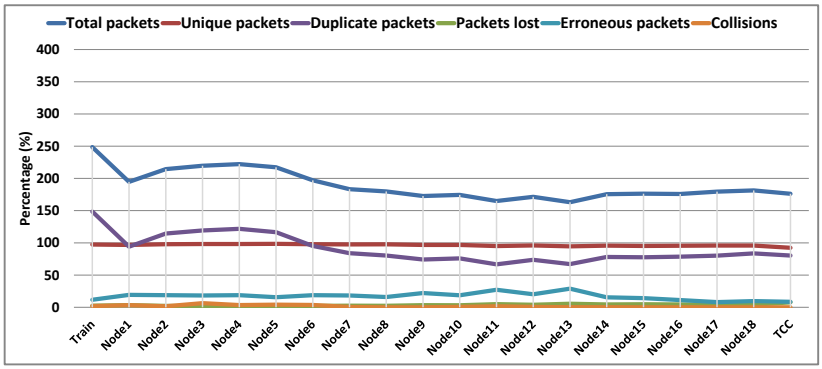

Figure 9.19: Results for 1 train running left to right at a speed of 180 km/h and bi-directional traffic

In the next scenario, two trains run on the same track from left to right as illustrated in Figure 9.20, with a 100, 200, 300 and 600 meters headway. TCC is located at the end of the track at right.

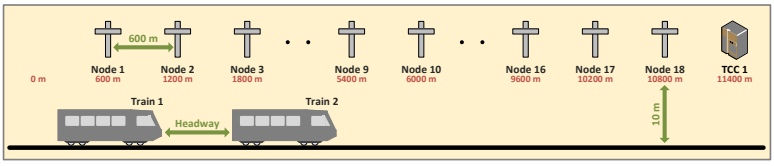

Figure 9.20: Scenario with 2 trains running left to right on the same track

The resulting average packet loss seen at TCC for the two trains for the four headway distances are 13.57%, 11.8%, 10.12% and 6.04%, respectively. As expected, it shows that the greater the headway, the lower the packet loss, as the trains interfere less with each other's transmissions. Results for the 100 m and 600 m headway scenarios are presented in Figure 9.21 and Figure 9.22.

Note that although the two trains transmit to the same TCC, the figures display the values for the two trains (i.e. at TCC) separately. This helps in observing that the front train (Train 2) experiences a slightly higher packet loss—7.67%—compared to the rear

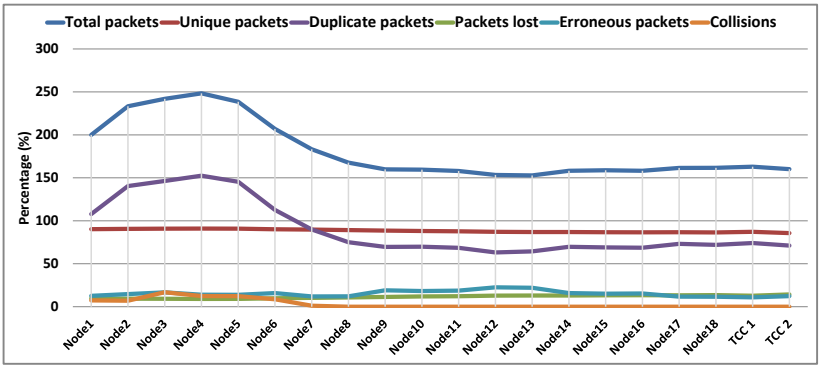

Figure 9.21: Results for 2 trains running left to right on the same track at 180 km/h and 100 m headway

train (Train 1)—4.42%. This is due to the fact that the rear train produces interference for the front train on the left radios of the chain nodes. Note that since the trains are running from left to right, the left radios on the chain nodes are critical as they receive the packets from the train before the top and the right radios, and thus forward the packets first.

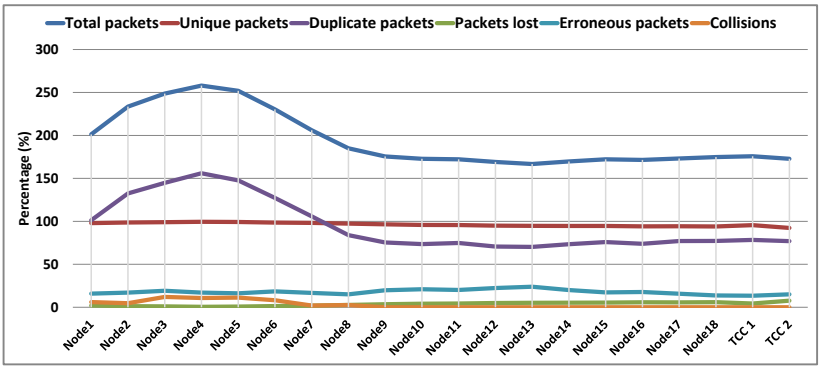

Figure 9.22: Results for 2 trains running left to right on the same track at 180 km/h and a 600 m headway

The impact of this phenomenon is more evident and worse if the original backward forwarding mechanism is used which does not forward packets in the backward direction. Figure 9.23 shows results for the scenario in Figure 9.22 but with the original backward forwarding mechanism. As seen, Train 2 now experiences nearly twice—190% to be specific—the amount of packet loss, i.e. 14.55%.

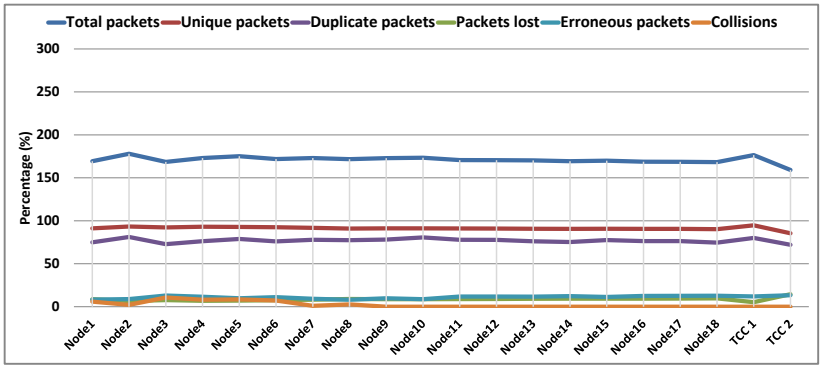

Figure 9.23: Results for 2 trains running left to right at 180 km/h and a 600 m headway, with the original backward forwarding mechanism

In an alternative version of the above scenario, TCC is moved to the left side of the chain instead of the right side. As expected, the results—not presented here— showed that the packet loss for the two trains was reversed, i.e. Train 1 now experienced the higher packet loss (12.68%) than Train 2 (4.48%). This implies that always the train closer to the TCC experience the high loss even when they are running away from TCC.

Figure 9.24 presents the results for the scenario as in Figure 9.22 with bi-directional traffic. A much higher packet loss of 29.37% and 38% is now seen at the TCCs and the trains, respectively. As discussed in Section 5.2, in this simulation study, it is assumed that the TCC also behaves as a train in that it also has three radios. As with a train, the TCC's transmission power has been set to 1 dBm, which enables a 1-node range. In this way, the interference seen at Nodes 16-17 in Figure 9.1 due to the 2-node range is avoided. Thus, in Figure 9.24, the drop seen in the number of total and duplicate packets at Node 17 is because it only receives a packet from its preceding node (Node 18) and not the duplicate copy from the TCC. This is additionally consistent with the real-life where TCC will be wired to only the last node in the chain. In other words, the link between Node 18 and Node 17 is non-redundant unlike the rest of the chain. This is one of the reasons why the packet loss for TCCs (38%) is greater than that for the trains (29.37%).

Besides that, the high packet loss is because the trains now produce greater interference for each other as now their outgoing transmissions interfere with the incoming transmissions from the chain nodes. This indicates that the 600 meters separation between the trains is not sufficient. Thus, next the same scenario is repeated with the train speed of 120 km/h and a headway distance of 3000 meters, as in the Copenhagen S-train CBTC as discussed in the beginning of this chapter. The results are presented in Figure 9.25

The peaks in the number of total and duplicate packets seen at Nodes 2-4 and Nodes 8-11 in Figure 9.25 indicate the position of each train and the distance it has traveled. As seen, there is a greater separation between the two peaks compared to that in Figure 9.24

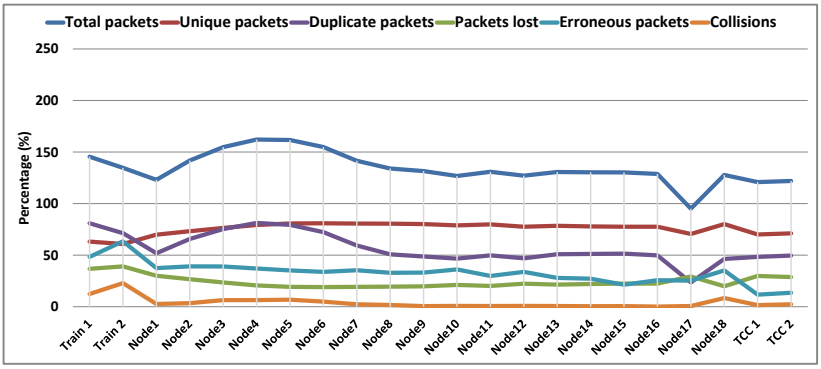

Figure 9.24: Results for 2 trains running left to right at 180 km/h, a 600 m headway, and bi-directional traffic

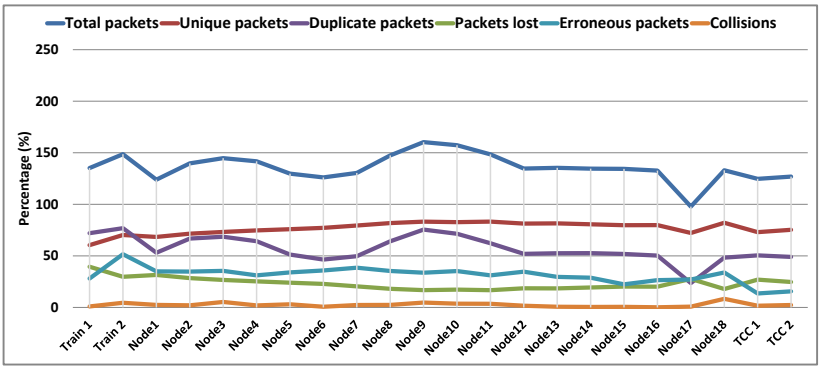

Figure 9.25: Results for 2 trains running left to right at 120 km/h, a 3000 m headway, and bi-directional traffic

due to the larger headway. The packet loss is 25.86% and 34.65% at the TCCs and the trains, which is lower compared to 29.37% and 38% seen in Figure 9.24. It is noted that the packet loss experienced by the front train (Train 2) is lower compared to the the rear train (Train 1), namely 24.7% and 27%. Accordingly, the peaks for the number of total and duplicate packets received for the two trains indicate that the front train receives a greater number of packets than the rear train.

Recall from the discussion in Section 3.1.3, when a chain node receives packets directly from a train, it forwards the packet in both directions. This implies that in this scenario with four flows (2 trains and 2 TCCs), at any location in the chain—not just in the direction of the train's movement—there are four flows being transferred by the chain. This additionally implies that a train receives its own packets sent back to itself by the

chain node. Thus, each train receives packets from four flows. Out of these, two flows are addressed from the TCCs to the trains and the rest two in the opposite direction. Out of these, a train discards three flows and processes only the packets addressed to itself by the TCC.

Four traffic flows result in 4.4 Mbps $\times\ 4 = 17.6$ Mbps of total traffic. Thus, a major reason behind the above high packet loss is that the network is saturated. Recall that the packet rate of 1000 packets per second (4.4 Mbps) is adopted in this study to be able to use any excessive bandwidth for non-CBTC traffic. As discussed in Section 2.1.3, the actual CBTC traffic requirement is only 20-100 kbps. Thus, next, the scenario in Figure 9.25 is repeated with the data rate per node cut to half, i.e. 500 packets per second (2.2 Mbps), resulting in a total traffic of 8.8 Mbps. Results are presented in Figure 9.26 and show a packet loss of 9.62% and 17.45% at the TCCs and the trains, which presents a significant drop compared to the 25.86% and 34.65% in Figure 9.25.

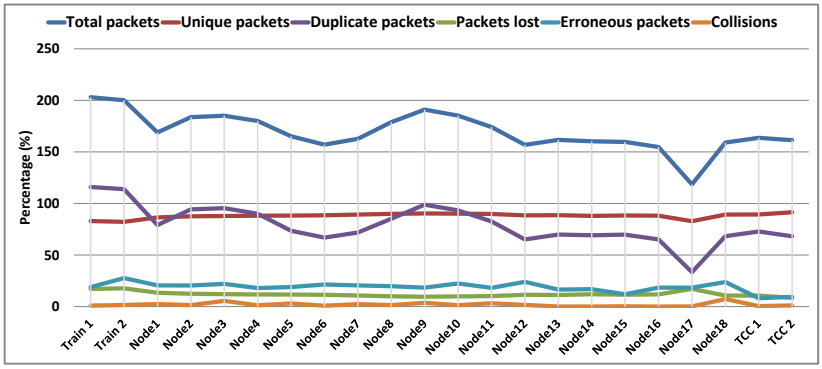

Figure 9.26: Results for 2 trains running left to right at 120 km/h, a 3000 m headway, bi-directional traffic, and 2.2 Mbps data rate (per terminal node)

Next, the traffic load is further cut into half, i.e. 250 packets per second or 1.1 Mbps per node. Figure 9.27 shows the results in which a further significant drop is seen in the packet loss. The packet loss is now 6.5% and 5.64% at the TCCs and the trains, respectively. This is evident from the significantly lower interference seen compared to e.g. in Figure 9.24, and the resulting improvement in the number of total and duplicate packets received. Additionally noteworthy is that now the two trains receives more or less the equal number of packets compared to in Figure 9.25.

The results show that for example, if the number of trains has to be increased to four with a data rate of 1.1 Mbps per node—i.e. $1.1 \times 8 = 8.8$ Mbps—, the packet loss will be in the range of 9.62% and 17.45% at the TCCs and the trains, respectively. Note that as previously discussed in Chapter 6, this packet loss is considered less critical as the train control information sent in CBTC is redundant in nature and is repeated at regular intervals.

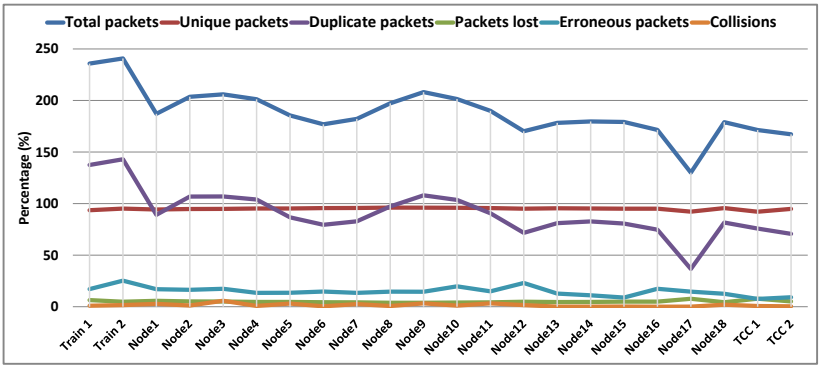

Figure 9.27: Results for 2 trains running left to right at 120 km/h, a 3000 m headway, bi-directional traffic, and 1.1 Mbps data rate (per terminal node)

It can be further concluded that if a high data rate, i.e. higher than 1.1 Mbps per node, or a greater number of trains, i.e. greater than two trains, is required to be supported, an alternative solution is to use a smaller chain size, i.e. smaller than 18 nodes. Using a smaller chain size will minimize the probability that a large number of trains coexist in a specific simultaneously. Furthermore, as the results discussed shortly show, packet loss is a function of the chain length.

In the next scenarios, the number of trains is increased to three. They run on the same track from left to right and TCC is placed at right side of the chain as before. Likewise, the train speed is 180 km/h and the headway is 600 meters as before. Figure 9.28 illustrates the scenario.

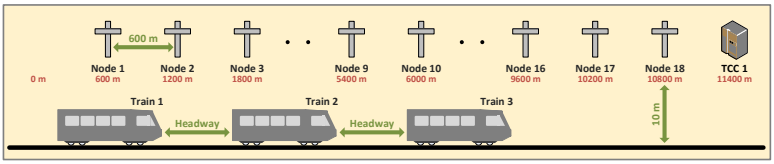

Figure 9.28: Scenario with 3 trains running left to right on the same track

Figure 9.29 presents the results for a train speed of 180 km/h and the headway of 600 meters, and uni-directional traffic. The result show that the three trains experience a packet loss of 8.4%, 21.88% and 14.35%, respectively, which is a significant increase compared to 4.42% and 7.67% seen in Figure 9.22 for the two-train scenario. Notably, the train in the middle (Train 2) experiences the highest, given that it faces interference from trains at its both sides.

In the next scenario, the simulation time is extended so that the trains travel a larger

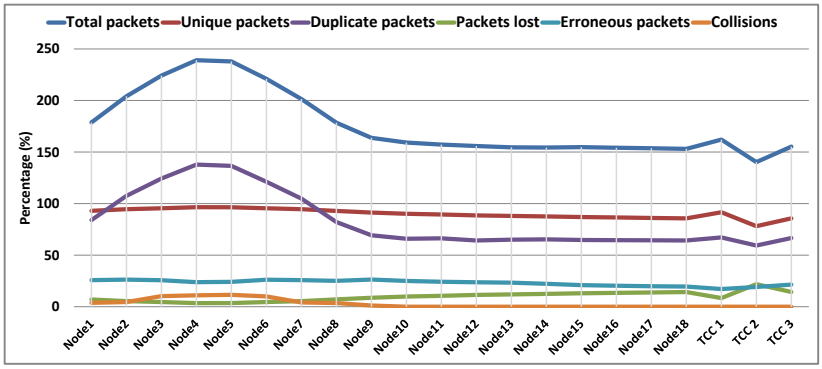

Figure 9.29: Results for 3 trains running left to right on the same track at 180 km/h and a 600 m headway

distance of 9600 meters. Since the starting position of the front train (Train 3) is 1200 meters, the simulation time is set to 192 seconds to allow Train 3 to travel a distance of 9600 meters—the full track length is 10800 meters. This implies that Train 3 reaches the TCC, upon which, the simulation is ended. In this way, it is ensured that no train gets idle time after reaching TCC—which will allow it to transmit packets standing right next to TCC—and thus have an advantage over the other trains. The results for the train speed of 180 km/h and a headway of 600 meters are presented in Figure 9.30 which shows a packet loss of 5.5%, 18.6% and 10.86% for the three trains. The lowered packet loss compared to seen in Figure 9.29 is because as the trains now reach closer to the TCC, the packets now have to travel a shorter distance over the chain to reach the TCC.

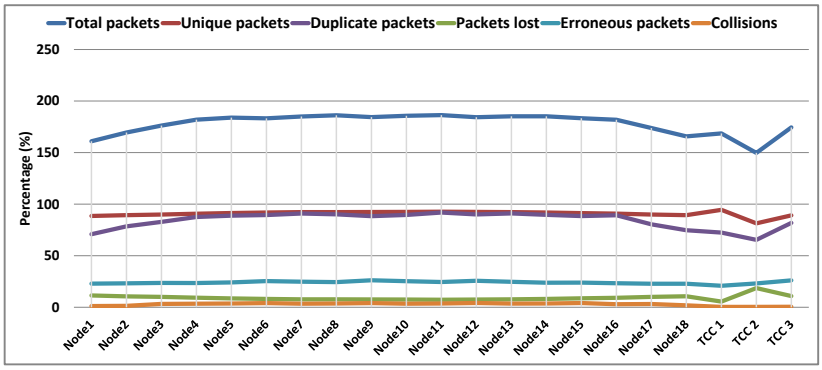

Figure 9.30: Results for 3 trains running left to right on the same track at 180 km/h and a 600 m headway, and travel a longer distance

Figure 9.31 presents the results for the scenario with the train speed of 120 km/h and a headway of 3000 meters. An extended simulation time of 145 seconds is set in the same fashion as above—note that this implies that the starting position of the front train (Train 3) is now 6000 meters. As seen, the packet loss is now 14.07%, 15.3% and 7.38% for the three trains, respectively. Note that the front train now experiences the lowest packet loss given that it has to travel a very short distance ($10800 - 6000 = 4800$ meters) to reach the TCC.

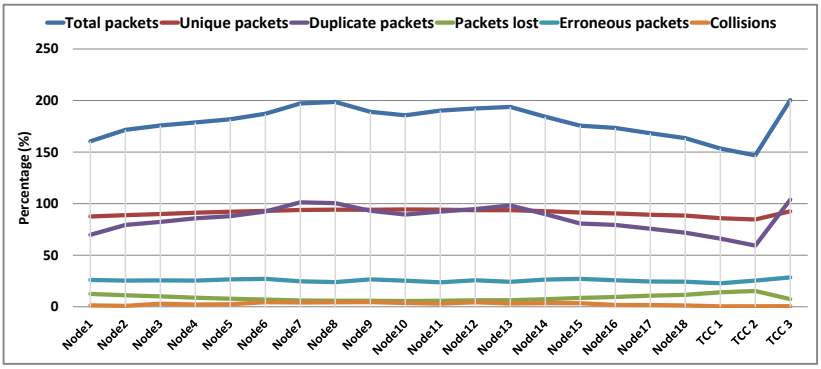

Figure 9.31: Results for 3 trains running left to right on the same track at 120 km/h and a 3000 m headway, and travel a longer distance

9.3 Scenarios involving trains running on parallel tracks

Two trains running in parallel, as shown in Figure 9.32, is a common scenario where the tracks are used mainly for trains running in the opposite directions, and occasionally in the same direction. Scenarios with more than two parallel track is not of particular interest for this study as it rarely occurs, except for the situations where the third track is used for parking purposes. Thus, in the following scenarios, two trains run left to right on two parallel tracks, one at the each side of the chain. The two tracks are separated by 20 meters. The trains start at the same position (0 meters). This is illustrated in Figure 9.32.

This scenario is additionally important because the trains transmit on the same three frequencies with omni-directional antennas and thus, the probability of them interfering with each other increases if the distance between them is small.

Figure 9.33 shows the results for the scenario with 180 km/h speed. As seen, the average packet loss seen for the two trains at TCC is 15.21%. This packet loss is much higher compared to 1.85% seen in Figure 9.16 for the one-train scenario because of the interference the two trains produce for each other. This interference is evident from a

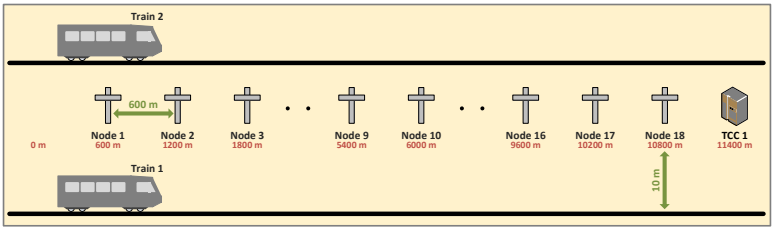

Figure 9.32: Scenario with 2 trains running left to right parallel on parallel tracks

larger number of collisions seen at Nodes 1-5 and of erroneous packets seen at all nodes in Figure 9.33.

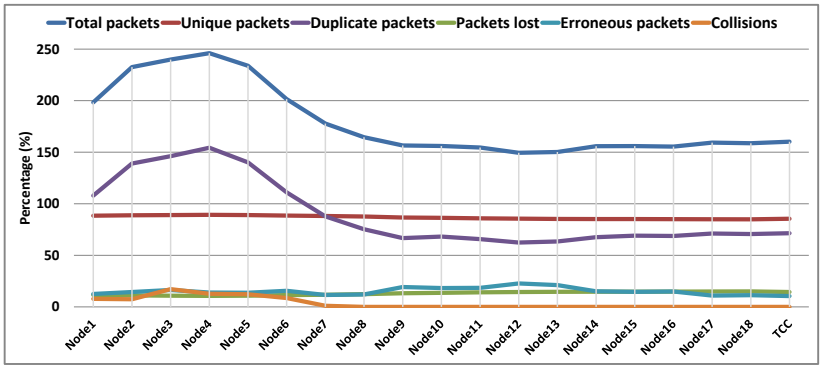

Figure 9.33: Results for 2 trains running left to right on parallel tracks at 180 km/h, starting from the same position

Nonetheless, in real-life scenario, it is relatively rare for two trains on two parallel tracks to run at the same speed and thus to maintain the same distance from each other. Thus, in the next scenario, the two trains run at different speeds. Note that while they still start at the same position, the distance between them increases subsequently due to the difference in speeds. Figure 9.34 shows results for the scenario in which the two trains run at the speeds of 60 km/h and 180 km/h and Figure 9.35 for the scenario in which the two trains run at the speeds of 150 km/h and 180 km/h.

As seen in Figure 9.34 and Figure 9.35, the packet loss seen at TCC in the two cases is 7.71% and 11.14%, respectively. Thus, as expected, the greater the distance between the two trains—or in other words, the faster this distance increases—, the lower the packet loss. The lower interference is evident from the lower number of collisions compared to that seen in Figure 9.33. Note that the lower number of total and duplicate packets received at Nodes 1-5 in Figure 9.34 compared to in Figure 9.33 and Figure 9.35 is

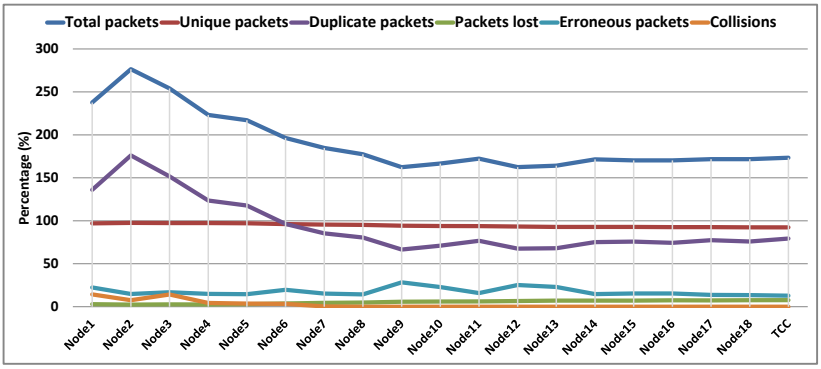

Figure 9.34: Results for 2 trains running left to right on parallel tracks at 60 km/h and 180 km/h

because Train 1 manages to travel only a very short distance (1000 m) due to its low speed.

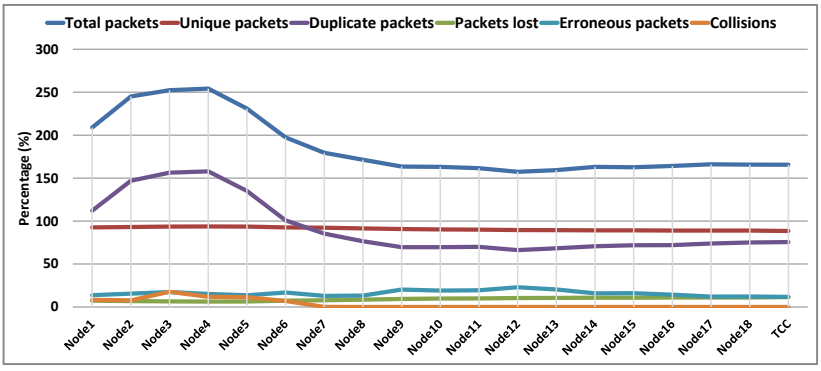

Figure 9.35: Results for 2 trains running left to right on parallel tracks at 150 km/h and 180 km/h

9.4 Scenarios involving trains running in opposite direction

In the next scenario, two trains start from the two ends on two parallel tracks and travel in the opposite direction. Train 1 and Train 2 send packets to TCC 1 and TCC 2, located at the opposite end of the chain, respectively. Figure 9.36 illustrates the scenario. Train 1 starts from 1800 meters position and Train 2 starts from 9600 meters position.

Figure 9.37 shows the results for the speed of 180 km/h. A packet loss of on average 8.59% is seen, compared to only 1.85% in Figure 9.16 for the one-train scenario.

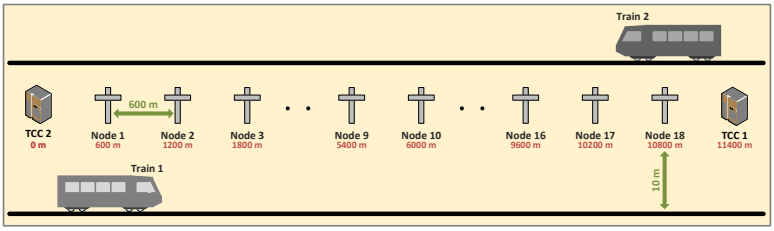

Figure 9.36: Scenario with two trains running in opposite direction on two tracks

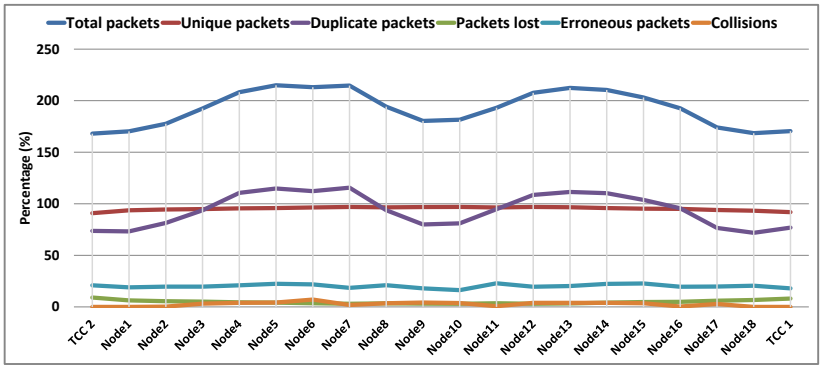

Figure 9.37: Results for 2 trains running in opposite direction on two tracks at 180 km/h

As with the previous scenarios with two or more trains, compared to Figure 9.16, a significant increase in the number of erroneous packets is seen throughout the chain, resulting in a lower number of total and duplicate packets received. Note again that the traffic is flowing in both directions and the top radio on each node faces interference from nodes on its both sides.

Likewise, results for the speeds of 120 km/h and 60 km/h—not presented here—showed a higher packet loss of 9.53% and 10.19%, respectively. However, it is noteworthy that this increased packet loss is not due to the lower train speeds. Since these simulation were run for a fixed time interval (60 seconds), this packet loss is due to the relatively smaller distance that a train travels towards the TCC due to its lower speed, and as a result, the larger distance that its packets must travel to reach the TCC. As seen in Table 9.2, at the speed of 60, 120 and 180 km/h, the train travels a distance of 2, 4 and 6 chain nodes, respectively.

To disregard the impact of the distance traveled, in the next scenario, the simulation time is extended to enable the trains to reach the end of the track for the all three speeds. In other words, the trains now travel the same distance and thus meet the same number

of chain nodes. Additionally, the objective is to study the impact of trains crossing each other.

The results show that now an identical average packet loss of 6.27% is seen for all three speeds. This is noteworthy, as it indicates that the network performance is a function of the number of chain nodes a train meets—or a packet flows through—and is independent of the train speed. Only the results for 180 km/h are presented in Figure 9.38, in which the average packet loss at the TCCs is 6.38%.

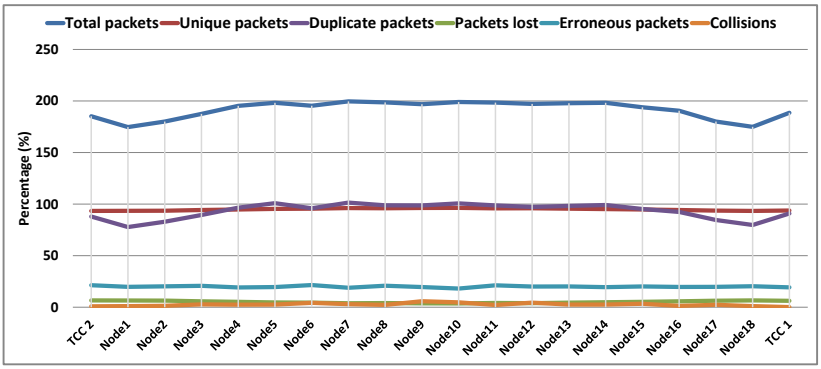

Figure 9.38: Results for 2 trains running in opposite direction on two tracks at 180 km/h and reaching the end of track

Figure 9.39 shows the results for a scenario in which the two trains run at different speeds, 180 km/h (Train 1) and 120 km/h (Train 2). The packet loss for Train 1 is 3.34% compared to 6.54% for Train 2. The reason why Train 1 experiences a lower packet loss is that now it reaches the end of the track earlier and has more time transmitting directly to TCC without any intermediate chain nodes. This is evident from the greater number of total and duplicate packets received at TCC 1 than at TCC 2 in Figure 9.39.

Figure 9.40 shows the results for the scenario in Figure 9.37 but with bi-directional traffic. A much higher packet loss of 34.2% and 24.6% is now seen at the TCCs and the trains, respectively. This is in contrast to Figure 9.24 (two trains running in the same direction) in which the loss seen at the trains was greater than that seen at the TCCs. The reason is that since the trains run in the opposite directions now and the TCCs are also located in the opposite ends, each train now faces two flows in the direction opposite to its direction of movement. As in Figure 9.24, the drops seen in the number of total and duplicate packets at Nodes 2 and 17 are because these nodes do not receive duplicate packets from the TCCs.

As discussed in the context of Figure 9.24, note again that in this study, it is assumed that the TCC also behaves as a train in that it uses radio communication for transmissions. For this reason, as stated in the beginning of this section, in these scenarios, the starting location of the train has been changed from 600 meters to 1800 meters from the track end.

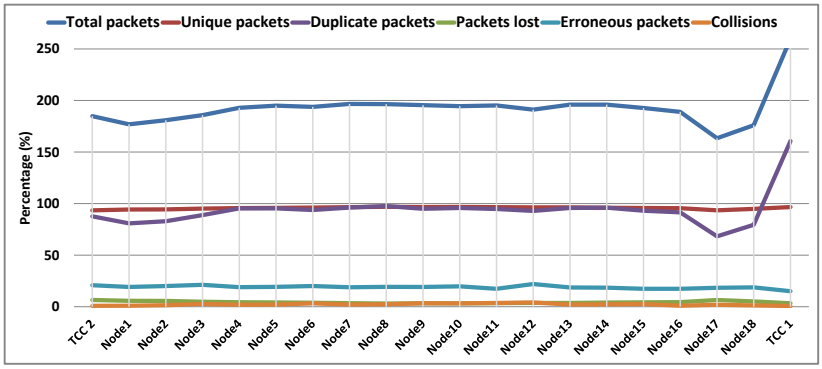

Figure 9.39: Results for 2 trains running in opposite direction on two tracks at 180 and 120 km/h and reaching the end of track

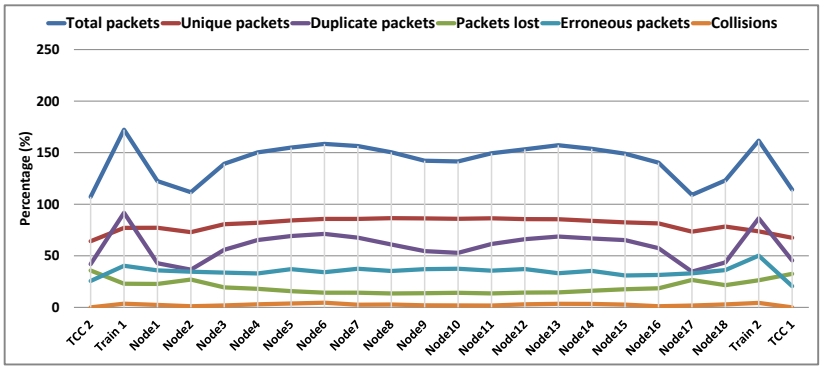

Figure 9.40: Results for 2 trains running in opposite direction on two tracks at 180 km/h and bi-directional traffic

This is done to minimize any interference caused by the train and the TCC for each other. Thus, the drops seen in the number of total and duplicate packets at Nodes 2 and 17 are because these nodes only receive a packet from their preceding nodes (Nodes 1 and 18) and not the duplicate copy from the TCC due to the TCC's shorter range.

Results for a scenario with trains running at the speed of 120 km/h—not presented here—showed an almost identical packet loss of 34.5% and 27.53% for the TCCs and the trains, respectively.

As discussed above, the packet loss is a function of the number of chain nodes a packet has to travel through. When the locations of the TCCs are swapped in the scenario in Figure 9.40—i.e. TCCs were moved closer to their respective trains—, the results

showed that the packet loss dropped to 21.66% and 15.3% for the TCCs and the trains, respectively.

In the next scenario, the data rate per terminal node is cut to half, i.e. 2.2 Mbps (i.e. 8.8 Mbps total load). Figure 9.41 presents the results. As seen, the packet loss has dropped significantly, to 12.2% and 15.2% at the TCCs and the trains, respectively. Compared to Figure 9.40, a significant drop is now seen in the number of erroneous packets due to the lowered interference.

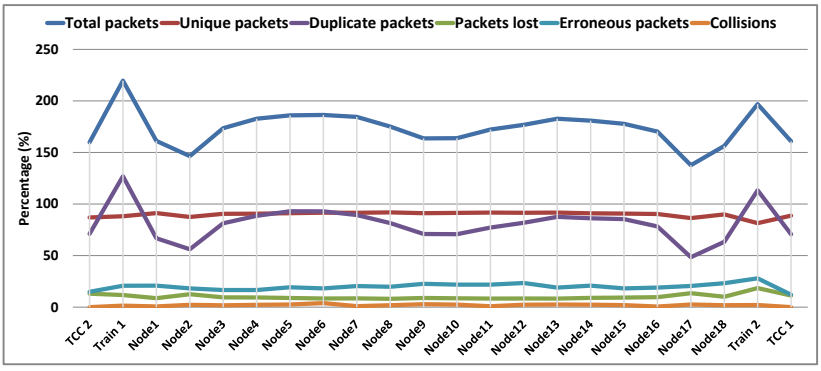

Figure 9.41: Results for 2 trains running in opposite direction on two tracks at 180 km/h, bi-directional traffic, and 2.2 Mbps data rate (per terminal node)

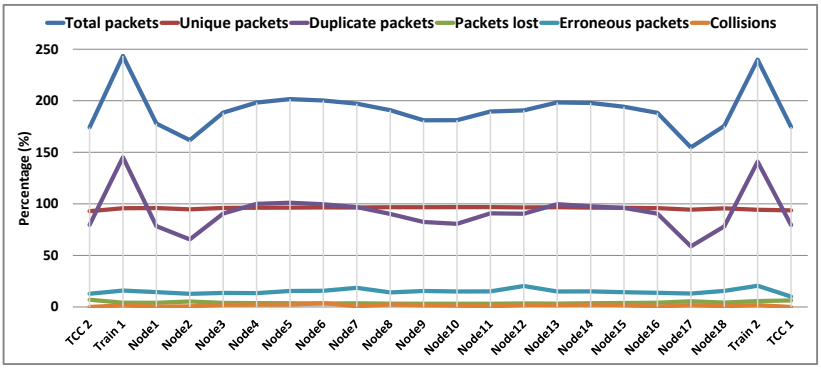

Figure 9.42: Results for 2 trains running in opposite direction on two tracks at 180 km/h, bi-directional traffic, and 1.1 Mbps data rate (per terminal node)

Likewise, results for the data rate of 1.1 Mbps presented in Figure 9.42 show a packet loss of only 6.72% and 4.94%, respectively. Additionally note how this packet loss is very

similar to 6.5% and 5.64% seen in the results for the two-train scenario in Figure 9.27. The scenarios with the train speed of 120 km/h produced identical results.

9.5 Scenarios involving fewer radios on the train

In the beginning of this chapter, it was noted that the scenarios in this phase were carried out without the improvements discussed in the previous chapters. Nonetheless, this last section of the chapter presents the results for scenarios involving one train equipped with a fewer number of radios—one of the potential improvements presented in Section 7.2. The objective is to verify the conclusions made in Section 7.2, in which the same scenario was done with a stationary train. Figure 9.43 and Figure 9.44 presents the results for a train equipped with two radios and one radio, respectively. The train runs at the speed of 180 km/h.

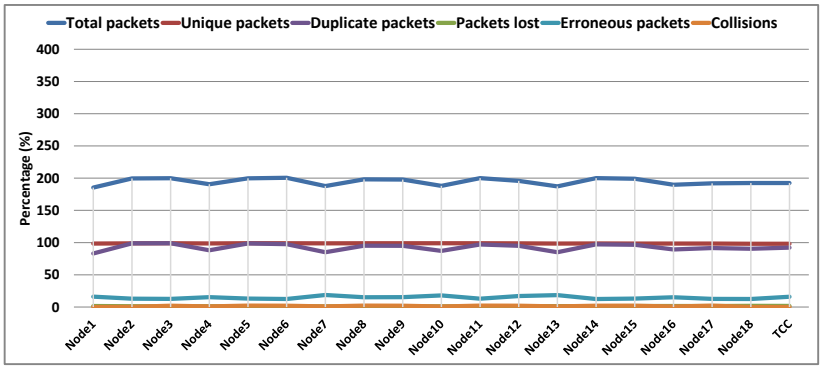

Figure 9.43: Results for 1 train running left to right at a speed of 180 km/h, equipped with only two radios

Note that in Figure 9.16, which presented the results for the equivalent scenario but with the train equipped with three radios, a packet loss of 1.85% was seen at the TCC. The results in Figure 9.43 show that when the train is equipped with two radios, it does not have a significant impact on the packet loss, which is now 1.77%. On the other hand, Figure 9.44, which shows the results for a train equipped with only one radio, shows that only a minor increase in the packet loss is seen, which is now 8.7%. Note that the peaks seen at Nodes 1-7 in Figure 9.16 are not seen in Figure 9.43 and Figure 9.44 because these scenarios were run for an extended simulation time to allow the train to travel the complete track distance, i.e. 10800 meters, and thus, to meet all nodes in the chain. Results for the equivalent scenarios but with the speed of 60 km/h—not presented here—showed a packet loss of 1.69% and 8.6% for the scenarios with two and one radios, respectively.

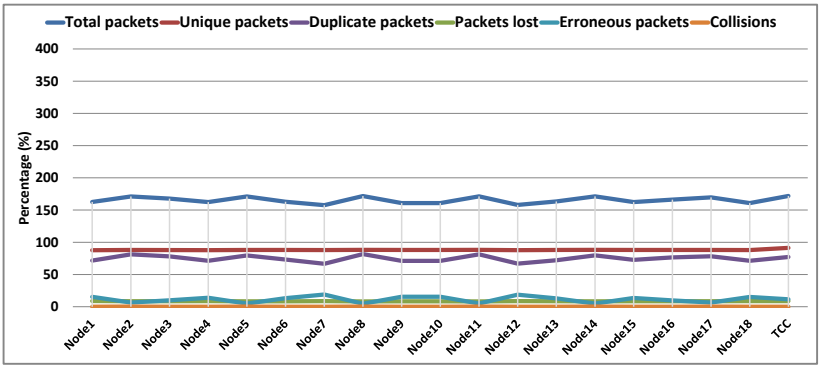

Figure 9.44: Results for 1 train running left to right at a speed of 180 km/h, equipped with only one radio

This verifies the conclusions presented in Section 7.2 that, (1) reducing the number of radios on the train minimizes the interference seen on the nearby chain nodes, (2) the train does not necessarily have to be equipped with three radios, and, (3) less favorable frequency combinations will not have a significant impact for a moving train as it will regularly meet the chain nodes of both favorable and unfavorable combinations.

9.6 Summary

This chapter presented results for a large number of scenarios involving multiple trains and tracks, where different train speeds, train locations and directions, and headway distances were considered.

The results showed the important conclusion that when the traffic is generated in a normally distributed fashion, the probability that transmissions interfere with each other drops dramatically. Specifically, in the stationary scenario with the two terminal nodes located at the two ends of the chain, and bi-directional traffic, packet loss dropped from 40.52% to 13.66%. This implies that the degree of variations in the traffic generation patterns of the terminal nodes—as well as the data rate—will greatly influence the interference produced.

The initial scenarios presented in this chapter investigated the behavior of the backward forwarding mechanism. In the original backward forwarding mechanism discussed in Chapter 3, only the top radio is supposed to forward a packet in both directions. A side radio only forwards a packet in one (opposite) direction. The results highlighted a shortcoming of the mechanism when two trains located close to each other transmitted. Since the two trains produced interference for each other, the packets received on the top radios of the nearby chain nodes turned out to be erroneous. Thus, the top radio did not

forward the packets. As a consequence, the train's packets were only forwarded in the direction opposite to that where the TCC was located, resulting in a high packet loss. To address this shortcoming, an improvement to the mechanism is proposed in which a side radio upon receiving a packet from a train, also forwards it in both directions. The results showed that this improvement in the design decreased the packet loss from 15% to 7.65%.

A comparison of the results for scenarios in which a train runs at different speeds of 60 km/h and 180 km/h showed that the slower the train speed, the greater the interference as more transmissions will interfere with the exact same arrival time. Additionally, the results showed that compared to at the TCC, a greater packet loss is seen at the trains due to their movement.

The chapter presented the results for the scenario in which two trains run close to each other on the same track, from left to right, such that the TCC was located at right end of the chain. The results showed that the front train experienced a slightly higher packet loss compared to the rear train, because the rear train produced interference for the front train on the left radios of the chain nodes, which were supposed to forward the packets in the right direction. In the next scenario, as the TCC was moved to the left side of the chain, the results showed that the packet loss for the two trains was reversed, which implies that always the train closer to the TCC experience the high loss even when they are running away from TCC.

The scenario with a 600 meters headway between the two trains and bi-directional traffic yielded a high packet loss of 29.37% and 38% at the TCCs and the trains, respectively. As discussed in Section 5.2, this simulation study assumes that a TCC also uses radio communication like a train. However, since the transmission range of the TCC has also been set to one node, this results in a certain packet loss at Node 17 because it only receives one copy of a packet from Node 18 and not the duplicate copy from the TCC. This is an additional reason why the packet loss for TCCs (38%) is greater than that for the trains (29.37%). Another reason behind this high packet loss is that the trains produce greater interference for each other due to the small distance between them. Nonetheless, when the headway distance was increased to 3000 meters, the packet loss dropped only marginally, to 25.86% and 34.65%, respectively. It is noted that since a chain node upon receiving packets from a train, forwards them in both directions, in this scenario with four flows (2 trains and 2 TCCs), there are four flows being transferred by the chain, resulting in 4.4 Mbps $\times\ 4 = 17.6$ Mbps of total traffic. In the next scenario, when the data rate per node was cut to half i.e. 500 packets per second or 2.2 Mbps, the packet loss dropped to 9.62% and 17.45%. Thus, the results concluded that a major reason behind the above high packet loss was that the network was saturated. These results further provide an estimated packet loss for, for example, a scenario in which four trains share this bandwidth (8.8 Mbps), with a data rate of 1.1 Mbps per node. Cutting the data rate further to half, i.e. 250 packets per second or 1.1 Mbps per node, decreased the packet loss to 6.5% and 5.64%.

The results for a scenario with three trains running in the same direction, at a speed of 180 km/h and a headway distance of 600 meters, showed that the train in the middle

experienced the highest packet loss, given that it faces interference from trains at its both sides. In the next scenario, the simulation time was extended in a way that the trains traveled longer distance, and that no train got idle time after reaching TCC and thus had an advantage over the other trains. The results showed a significant drop in the packet loss for all three trains. It is because as the trains now reached closer to the TCC, the packets now had to travel a shorter distance to the TCC.

The results for a scenario in which two trains ran on parallel tracks, at the same speed (180 km/h), and starting at the same position, showed that the average packet loss for the two trains at TCC was 15.21%, which represented a significant increase from the 1.85% packet loss for the one-train scenario, and was because of the interference the two trains produced for each other. In the next scenario, when the trains were run at different speeds (60 km/h and 180 km/h), the packet loss dropped to 7.71%. Thus, as expected, the faster this distance between the two trains increases, the lower the packet loss.

The chapter further discussed the scenarios with trains running in opposite direction (on two tracks), such that they started from one end of the track and their TCC was located at the other end. The results showed that when they ran at the speed of 180 km/h, a packet loss of on average 8.59% was seen, compared to only 1.85% for the one-train scenario. When the train speed for the two trains was decreased to 120 km/h and 60 km/h, the results showed that the packet loss increased to 9.53% and 10.19%, respectively. To disregard the impact of the distance traveled, in the next scenario, the simulation time was extended to enable the trains to reach the end of the track for the all three speeds. In other words, all trains now traveled the same distance. The results showed that now an identical average packet loss of 6.27% is seen for all three speeds, which indicated that the increase in packet loss is not due to the lower train speeds but that it is more a function of the number of chain nodes a train meets. In the next scenario, the two trains run at different speeds, namely, 180 km/h and 120 km/h. The packet loss for the two trains now dropped to 3.34% and 6.54%, respectively. The reason behind the lower packet loss for the first train is that now it reached the end of the track earlier and had more time transmitting directly to TCC.

The results for the scenario with 180 km/h speed but with bi-directional traffic showed a packet loss of 34.2% and 24.6% at the TCCs and the trains. As discussed above, the packet loss is a function of the number of chain nodes a packet has to travel through. When the locations of the TCCs were swapped—i.e. TCCs were moved closer to their respective trains—, the results showed that the packet loss dropped to 21.66% and 15.3%, respectively. As in the scenarios with two trains running in the same direction, when the data rate per node was next cut to half, i.e. 2.2 Mbps, the results showed that the packet loss dropped to 12.2% and 15.2%. Likewise, results for the data rate of 1.1 Mbps showed a packet loss of only 6.72% and 4.94%, respectively.

The results indicate that the packet loss is a function of the number of chain nodes a packet has to travel through, or in other words, the length of the chain. If a high data rate or a greater number of trains is required to be supported, an alternative solution is to use a smaller chain size. The results additionally emphasize that a major obstacle when the

trains run close to each other, in particular when the number of trains is increased, is the shortcoming 1 discussed in the previous chapters, in which a train produces interference due to its use of all frequencies for transmission.

CHAPTER 10

Conclusions

Communications-Based Train Control (CBTC) is a modern signalling system that uses radio communication to enable the exchange of high resolution and real-time train control information between the train and the wayside infrastructure. A vast majority of the CBTC systems worldwide use IEEE 802.11 Wi-Fi as the radio technology mostly due to its cost-effectiveness. The trackside networks in these systems are mostly based on conventional infrastructure Wi-Fi. To ensure a continuous wireless connectivity, hundreds of Wi-Fi Access Points (APs) are installed at the trackside. These APs are connected to the wayside infrastructure via optical fiber cables that incurs huge costs. Additionally, the train must associate (i.e. perform handshake) with these APs as it moves from one AP to another (i.e. roaming). This is a time-consuming process associated with a certain delay.

Siemens' current CBTC solution is likewise based on the infrastructure Wi-Fi, and therefore, is prone to the same problems. Therefore, a new design of the CBTC trackside network was proposed at Siemens. In this design, trackside nodes function in the ad-hoc Wi-Fi mode, which means no associations have to be performed with them prior to transmitting. A train simply broadcasts packets. A node upon receiving these packets forwards them to the next node and so on, forming a chain of nodes. Following this chain, packets arrive at the destination. To minimize the interference, in the proposed design, transmissions are separated on multiple frequencies. Each node is equipped with three radios—one top radio and two side radios—operating on one frequency each, such that only one frequency is used to transmit in one direction. Furthermore, redundancy is introduced in the design as a node forwards packets to not only one but two of its neighbors in each direction.

The objective of this PhD project was to evaluate the proposed design, in particular the resiliency, redundancy and scalability supported by the design, using computer-based simulations, which are highly cost-effective, less time-consuming, and enable a more controlled environment for experimentation. An extensive number of simulation scenarios were carried out in this study, and large network sizes of up to 100 nodes—equivalent to approximately 60 kilometers—were investigated. The performance of the network was evaluated with the help of a number of Key Parameters Indicators (KPI), all based on the number of packets received at the destination node—i.e. a train or a TCC (Traffic Control Center). The Copenhagen S-train CBTC system was used as a reference point when designing the simulation scenarios. Although the data rate required for typical CBTC traffic is only in the range of 100 kbps, substantially high data rate of 1000 packets per second (4.4 Mbps) was used in this study, with the objective of utilizing any excessive

bandwidth to support non-CBTC applications, e.g. remote diagnostics and maintenance. The simulation study spanned four phases.

The results for scenarios in the first phase of the study—involving a stationary train located at one end of the chain and transmitting packets to TCC over a chain of 98 nodes—showed that due to the frequency separation and redundancy inherent in this design, significantly large numbers of packets can be successfully transferred across large networks. Furthermore, due to the redundancy enabled by the design, the chain network can tolerate a large number of node failures without significant degradation in the performance. Nonetheless, the results exposed the following two shortcomings of the design as well.

1. A train node undermines the frequency separation guaranteed by the chain nodes as it is required to transmit on all frequencies. This results in excessive interference, at the first few nodes in the chain, i.e. at the train's *entry point in the chain*.

2. The design under-estimates the interference produced by distant nodes in ideal propagation conditions despite the inherent frequency separation. This results in interference throughout the chain nodes, i.e. interference *inside the chain*.

As the results indicated, the design is highly sensitive to the interference and relies on the assumption that the transmission range of a node is equal to its interference range, which is far from the truth in real-life. Furthermore, as discussed in Chapter 2, relatively insignificant changes in the propagation conditions can result in extending these ranges.

Nonetheless, as a consequence of the above shortcomings, a packet loss of 25.42% was seen at the TCC. It is noted that CBTC systems can typically tolerate high packet losses. It is because the train control information sent to the train is repeated at regular intervals, and since the *limit of movement authority* (LMA) allows the train to travel a specific distance, a certain loss of the CBTC messages can be tolerated during this time period. It is additionally noted that the simulation model used in this study employs the FSPL (Free-Space Path Loss) propagation model, which enables exceptionally large transmission ranges. In real-life, less favorable propagation conditions will lower the transmission range and thus the interference.

Furthermore, the results showed a negligible end-to-end delay at the TCC, which was well below the recommended end-to-end delay as specified in the IEEE CBTC standard. Note that the frequency separation results in reduced contention for the wireless medium, as only a limited number of nodes contend for the medium on a given frequency. Thus, the MAC contention delay and queueing delay are irrelevant. Likewise, the processing delay involved when the radios on a node process the packet is considered to be negligible with the high-performance hardware available today. Given these reasons, end-to-end delay was not of particular interest for this study afterwards.

A large number of potential solutions to minimize these shortcomings were subsequently investigated. To address the first shortcoming, the impact of decreasing the

transmission range of the train node or using a reduced number of radios on the train—instead of the three radios in the default design—was studied. The results showed that when the transmission range of the train was decreased from two nodes to one node, it minimized the interference significantly on the nearby nodes. The results further showed that the presumption that a minimum 2-node transmission range is required at the train is not valid. In fact, a 1-node transmission range at the train—as long as the transmissions are received at minimum two *radios* (in contrast to *nodes*)—will both lower the interference and at the same time, will guarantee the desired redundancy.

Likewise, the results showed that using a reduced number of radios on the train successfully decreased the interference at the nearby nodes. At the same time, it was noted that it decreased the train node's ability of receiving duplicates from the chain nodes as well. The results further indicated that with the reduced number of radios used, there will be both favorable and unfavorable frequency combinations in relation to the frequencies used on the antennas—on the nearest two chain nodes—pointing towards the train. The results additionally showed that despite that using a lower number of radios in the least favorable frequency combinations did not yield promising results, no increase in the packet loss was seen either.

Note that the simulation study was carried out using IEEE 802.11a as the technology officially approved by Siemens for the hardware for its CBTC project, and, to be able to relate to the results from the field experiment. Nonetheless, in the following scenarios, the use of more advanced IEEE 802.11 technologies with more robust modulation and coding schemes was investigated. The results showed that dramatic decrease in the interference can be achieved, both for the interference caused by the train's transmissions and the interference inside the chain. Specifically, the results showed that when the most robust modulation and coding scheme available was used, the packet loss dropped to approximately one-half of the original.

In the subsequent phase of the study, additional solutions to minimize these shortcomings were investigated. In particular, two extensions to the design were proposed.

First, to address the second shortcoming, additional frequencies were employed in order to optimize the frequency separation distance. Specifically, the number of total frequencies used was increased from the default three to four, five and six. The results showed a substantial improvement as the packet loss dropped as a result of the extended frequency separation distance. The results emphasized that the interference is a function of distance between nodes transmitting on the same frequency—or in other words, their signal ranges—and demonstrated the effectiveness of the design as it allows to extend this distance by employing additional frequencies. At the same time it was noted that it is normal to employ multiple frequencies and radios per train in the conventional CBTC systems in order to enable high availability. Thus, these additional frequencies do not necessarily increase the system's cost. In addition, it is noted that a vast majority of the CBTC systems worldwide operate in the ISM frequency band which is license-free.

In the second extension, to address the first shortcoming, a design that used a separate, dedicated frequency for the train-to-trackside communication was introduced. The results

showed that the interference previously seen on the nodes near the train was completely eliminated as a result. It was noted that while this extension is primarily to enable a separate radio *frequency* for the train-to-track communication, this solution can additionally be used to enable a separate radio *technology* as well, e.g. a LTE or IEEE 802.11p.

In the last phase of the study, scenarios to investigate the impact of parameters such as the number of trains, train speed, headway distance, train's location on the track, train direction, and track layouts, were carried out.

Note that when a packet from the train is received on the top radio of a chain node, being unaware of the end of the chain where the destination TCC is located, the node must forward the packet in both directions, including in the backward direction. The results for the scenarios involving two trains located close to each other highlighted a shortcoming in this backward forwarding mechanism. Specifically, the packets received on the top radio of a chain node turned out erroneous because of the interference between the trains, and as a result, the packets were not forwarded in the backward direction in which the TCC was located. To address this shortcoming, the mechanism was extended so that a side radio also forwards in the backward direction. The results showed that this modification improved the performance significantly.

A number of different headway distances—ranging from 100 meters to 3000 meters—were used in the scenarios in which multiple trains ran in the same direction. The results indicated that trains' transmissions interfere with each other if the headway distance is small. In the scenarios involving three trains, the middle train experienced a particularly large amount of interference. Likewise were the results for the scenarios involving trains running parallel on different tracks, unless they ran at different speeds and the distance between them increased rapidly. The results indicated that in general, the train speed played a minor role in the performance of the network. Rather, the results showed that the packet loss is a function of the number of nodes the packet have to flow through to reach the TCC, i.e. the chain length. In the scenarios in which the trains running at different speeds traveled the same distance, i.e. they met the same number of nodes, the resulting packet loss was identical. Likewise, when a train moved closer to the TCC, or when the TCC was moved to the chain end closer to the train, the packet loss dropped.

The results for the scenario involving two train and bi-directional traffic showed a particularly high packet loss in the range of 29-38%. However, it was noted that four data flows in this case resulted in a high total data rate of 4.4 Mbps $\times\ 4 = 17.6$ Mbps. When the data rate per node was cut to half i.e. 500 packets per second (2.2 Mbps), the packet loss dropped in the range of 9-18%. Likewise, lowering the data rate further to 250 packets per second (1.1 Mbps) reduced the packet loss further, in the range of 5-6%.

The results showed that while the proposed design performs successfully in these scenarios in the last phase of the study, to keep the packet loss within the limits, the data rate per node must be lowered when the number of data traffic flows involved is increased. Accordingly, the results showed that while enabling particularly high data rate per node (i.e. 4.4 Mbps) in these cases is a challenge, the design still successfully supports a significantly high data rate (i.e. 1.1 Mbps) than that required by the CBTC traffic.

Bibliography

[1] Michael Renner and Gary Gardner. *Global Competitiveness in the Rail and Transit Industry*. Tech. rep. Worldwatch Institute, 2010 (cit. on p. 1).

[2] European Commission. *Sector Overview and Competitiveness Survey of the Railway Supply Industry*. Tech. rep. European Commission, 2012. URL: http://ec.europa.eu/DocsRoom/documents/3950/attachments/1/translations/en/renditions/native (cit. on p. 1).

[3] UNIFE. *The Unife World Rail Market Study - Forecast 2014 to 2019*. Tech. rep. UNIFE, 2014 (cit. on p. 1).

[4] Frost & Sullivan. *Strategic Analysis of Communication Based Train Control Systems in the Western European Urban Rail Market*. July 2013. URL: http://www.frost.com/sublib/display-report.do?id=M92D-01-00-00-00 (cit. on p. 1).

[5] S. Morar. "Evolution of Communication Based Train Control worldwide". In: *Proc. IET Professional Development Course on Railway Signalling and Control Systems (RSCS '10)*. June 2010, pp. 281–289 (cit. on pp. 1, 17, 18, 20, 38).

[6] UNIFE. *The Global Rail Market Now to 2016: UNIFE Study Key Findings & Future Outlook*. 2008. URL: http://www.rolandberger.at/media/pdf/rb_press/Roland_Berger_Studie_UNIFE_20080924.pdf (cit. on p. 1).

[7] UNIFE. *Worldwide Rail Market Study - status quo and outlook 2016*. Tech. rep. UNIFE, 2008 (cit. on p. 1).

[8] Wikipedia. *Communications-based train control — Wikipedia, The Free Encyclopedia*. URL: https://en.wikipedia.org/w/index.php?title=Communications-based_train_control&oldid=740770099 (cit. on pp. 1, 16, 18, 41).

[9] R. Alvarez and J. Roman. "ETCS L2 and CBTC over LTE - Convergence of the radio layer in advanced Train Control Systems". In: *IRSE (Institution of Railway Signal Engineers) technical meeting* (2013) (cit. on pp. 1, 11, 21, 22, 38).

[10] B. M. Martínez, Invensys. *ERTMS & CBTC Technology convergence*. presented at MetroRail 2013 (cit. on p. 1).

[11] Parsons. *Benefits and Barriers to CBTC and ETCS convergence*. presented at MetroRail 2012 (cit. on p. 1).

[12] *Wireless LAN Medium Access Control (MAC) and Physical Layer (PHY) Specifications*. 3 Park Avenue, New York, NY 10016-5997, USA: IEEE, 2012 (cit. on pp. 1, 31).

[13] Siemens. *Press Release: Copenhagen's S-Bane network to get signaling from Siemens worth 252 million euros*. Aug. 2011. URL: https://www.siemens.com/press/pool/de/pressemitteilungen/2011/mobility/IMO201108029e.pdf (cit. on p. 2).

[14] Banedanmark. *The Signalling Programme - A Total Renewal of the Danish Signalling Infrastructure*. Tech. rep. Banedanmark, 2010 (cit. on p. 2).

[15] P. Nielsen. *Siemens Internal Report*. Ballerup, Denmark: Siemens A/S, Mar. 2017 (cit. on p. 3).

[16] *Wireless LAN Medium Access Control (MAC) and Physical Layer (PHY) Specifications Amendment 2: Fast Basic Service Set (BSS) Transition*. 3 Park Avenue, New York, NY 10016-5997, USA: IEEE, 2008 (cit. on p. 4).

[17] R. T. Karstensen. "Reliable wireless infrastructure for bridging stationary and moving nodes". MA thesis. Department of Photonics Engineering, Technical University of Denmark, 2015 (cit. on pp. 6, 51).

[18] Siemens AG, L. Bro, M. Voss, and C. Bode. "Ad-hoc kommunikationsnetzwerk, English translation: Ad-hoc communication network". Patent application 10 2017 203 040.2 (German Trademark and Patent Office). Feb. 2017 (cit. on p. 7).

[19] S. Xu and T. Saadawi. "Does the IEEE 802.11 MAC protocol work well in multihop wireless ad hoc networks?" In: *IEEE Communications Magazine* 39.6 (June 2001), pp. 130–137 (cit. on p. 8).

[20] J. Li, C. Blake, D. S. De Couto, H. I. Lee, and R. Morris. "Capacity of Ad Hoc Wireless Networks". In: *Proc. 7th Annual International Conference on Mobile Computing and Networking (MobiCom '01)*. Rome, Italy: ACM, 2001, pp. 61–69. ISBN: 1-58113-422-3 (cit. on p. 8).

[21] Q. Dong, S. Banerjee, and B. Liu. "Throughput Optimization and Fair Bandwidth Allocation in Multi-Hop Wireless LANs". In: *Proc. IEEE International Conference on Computer Communications (INFOCOM '06)*. Apr. 2006 (cit. on p. 8).

[22] T. Tainaka, H. Masuyama, S. Kasahara, and Y. Takahashi. "Performance Analysis of Burst Transmission Mechanism for IEEE 802.11-Based Multi-Hop Wireless LANs". In: *IEEE Transactions on Wireless Communications* 10.9 (2011), pp. 2908–2917 (cit. on p. 8).

[23] K. Xu, M. Gerla, and S. Bae. "How effective is the IEEE 802.11 RTS/CTS handshake in ad hoc networks". In: *Proc. IEEE Global Telecommunications Conference (GLOBECOM '02)*. Nov. 2002 (cit. on p. 8).

[24] F. Ye, S. Yi, and B. Sikdar. “Improving spatial reuse of IEEE 802.11 based ad hoc networks”. In: *Proc. IEEE Global Telecommunications Conference (GLOBECOM ’03)*. Dec. 2003 (cit. on p. 8).

[25] G. Anastasi, E. Borgia, M. Conti, and E. Gregori. “IEEE 802.11 ad hoc networks: performance measurements”. In: *Proc. 23rd International Conference on Distributed Computing Systems Workshops*. May 2003 (cit. on p. 8).

[26] J. Deng and B. L. nad P.K. Varshney. “Tuning the carrier sensing range of IEEE 802.11 MAC”. In: *Proc. IEEE International Conference on Computer Communications (INFOCOM ’04)*. Nov. 2004 (cit. on p. 8).

[27] Z. Zeng, Y. Yang, and J. C. Hou. “How Physical Carrier Sense Affects System Throughput in IEEE 802.11 Wireless Networks”. In: *Proc. IEEE International Conference on Computer Communications (INFOCOM ’08)*. Apr. 2008 (cit. on p. 8).

[28] *Wireless LAN Medium Access Control (MAC) and Physical Layer (PHY) Specifications Amendment 6: Wireless Access in Vehicular Environments*. 3 Park Avenue, New York, NY 10016-5997, USA: IEEE, 2010 (cit. on p. 8).

[29] L. Zhao, X. Hong, J. Zhang, Y. Zhang, and Q. Hao. “Feasibility analysis of multi-radio in DSRC vehicular networks”. In: *Proc. 16th International Symposium on Wireless Personal Multimedia Communications (WPMC)*. June 2013 (cit. on p. 8).

[30] G. V. Rossi, K. K. Leung, and A. Gkelias. “Density-based optimal transmission for throughput enhancement in vehicular ad-hoc networks”. In: *Proc. IEEE International Conference on Communications (ICC)*. June 2015 (cit. on p. 8).

[31] J.-H. Chu, K.-T. Feng, C.-N. Chuah, and C.-F. Liu. “Cognitive Radio Enabled Multi-Channel Access for Vehicular Communications”. In: *Proc. IEEE 72nd Vehicular Technology Conference Fall (VTC 2010-Fall)*. Sept. 2010 (cit. on p. 8).

[32] M. Hadded, P. Muhlethaler, A. Laouiti, and L. A. Saidane. “TDMA-Aware Routing Protocol for Multi-Hop Communications in Vehicular Ad Hoc Networks”. In: *Proc. IEEE Wireless Communications and Networking Conference (WCNC)*. Mar. 2017 (cit. on p. 8).

[33] M. F. Feteiha and M. H. Ahmed. “Best-Relay Selection for Multi-Hop Vehicular Communication in Highways”. In: *Proc. IEEE Global Communications Conference (GLOBECOM)*. Dec. 2015 (cit. on p. 8).

[34] M. J. Farooq, H. ElSawy, and M.-S. Alouini. “A Stochastic Geometry Model for Multi-Hop Highway Vehicular Communication”. In: *IEEE Transactions on Wireless Communications* 15.3 (2016), pp. 2276–2291 (cit. on p. 8).

[35] V. Shivaldova, T. Paulin, A. Paier, and C. F. Mecklenbräuker. “Performance measurements of multi-hop communications in vehicular ad hoc networks”. In: *Proc. IEEE International Conference on Communications (ICC)*. June 2012 (cit. on p. 8).

[36] H. Rhee. “ATO Data of train control system based on Wi-Fi mesh telecommunication”. In: *Proc. The 21st International Conference on Magnetically Levitated Systems and Linear Drives*. 2013 (cit. on pp. 8, 31, 33).

[37] A. Srivatsa and J. Xie. “A Performance Study of Mobile Handoff Delay in IEEE 802.11-Based Wireless Mesh Networks”. In: *Proc. IEEE International Conference on Communications (ICC ’08)*. May 2008, pp. 2485–2489 (cit. on p. 8).

[38] *Communications-Based Train Control (CBTC) Performance and Functional Requirements*. 3 Park Avenue, New York, NY 10016-5997, USA: IEEE, 2004 (cit. on pp. 11, 12, 14–16, 18, 25, 38).

[39] *User Interface Requirements in Communications-Based Train Control (CBTC) Systems*. 3 Park Avenue, New York, NY 10016-5997, USA: IEEE, 2003 (cit. on pp. 11, 38).

[40] G. Theeg and S. Vlasenko. *Railway Signalling and Interlocking*. Eurailpress, 2009. ISBN: 978-3-7771-0394-5 (cit. on pp. 12, 13, 17, 18).

[41] R. Pascoe and T. Eichorn. “What is communication-based train control?” In: *IEEE Vehicular Technology Magazine* 4.4 (Dec. 2009), pp. 16–21 (cit. on pp. 13, 14, 17, 18).

[42] C. Cortes Alcala, S. Lin, R. He, and C. Briso-Rodriguez. “Design and Test of a High QoS Radio Network for CBTC Systems in Subway Tunnels”. In: *Proc. IEEE 73rd Vehicular Technology Conference (VTC 2011-Spring)*. May 2011, pp. 1–5 (cit. on pp. 13, 14, 19, 33).

[43] B. Bu, F. Yu, and T. Tang. “Performance Improved Methods for Communication-Based Train Control Systems With Random Packet Drops”. In: *IEEE Transactions on Intelligent Transportation Systems* 15.3 (June 2014), pp. 1179–1192 (cit. on pp. 13, 14, 17, 18, 22, 25, 28, 31, 33).

[44] T. Tazaki. “Development of CBTC for Global Markets”. In: *Hitachi Review* 61.7 (2012), pp. 347–351 (cit. on pp. 14, 18, 41).

[45] L. Zhu, F. R. Yu, B. Ning, T. Tang, and H. Wang. “Cross-Layer Handoff Design in Communication-Based Train Control (CBTC) Systems Using WLANs”. In: *Proc. IEEE 76th Vehicular Technology Conference (VTC 2012-Fall)*. Sept. 2012, pp. 1–5 (cit. on p. 14).

[46] L. Zhu, F. R. Yu, B. Ning, and T. Tang. “Handoff Performance Improvements in MIMO-Enabled Communication-Based Train Control Systems”. In: *IEEE Transactions on Intelligent Transportation Systems* 13.2 (June 2012), pp. 582–593 (cit. on p. 14).

[47] K. T. P. Nguyen, J. Beugin, M. Berbineau, and M. Kassab. “A New Analytical Approach to Evaluate the Critical-Event Probability Due to Wireless Communication Errors in Train Control Systems”. In: *IEEE Transactions on Intelligent Transportation Systems* (accepted for publication) (cit. on p. 14).

[48] H. Wang, F. R. Yu, L. Zhu, T. Tang, and B. Ning. “A Cognitive Control Approach to Communication-Based Train Control Systems”. In: *IEEE Transactions on Intelligent Transportation Systems* 16.4 (Aug. 2015), pp. 1676–1689 (cit. on p. 14).

[49] L. Zhu, Y. Zhang, B. Ning, and H. Jiang. “Train-Ground Communication in CBTC Based on 802.11b: Design and Performance Research”. In: *Proc. WRI International Conference on Communications and Mobile Computing (CMC ’09)*. Vol. 2. Jan. 2009, pp. 368–372 (cit. on pp. 14, 27, 31, 33).

[50] H. Jiang, H. Zhao, and B. Zhao. “A novel handover scheme in wireless LAN in CBTC system”. In: *Proc. IEEE International Conference on Service Operations, Logistics, and Informatics (SOLI)*. July 2011, pp. 473–477 (cit. on pp. 14, 22, 25, 28, 29, 31).

[51] M. Kassab, M. Wahl, M. Casanova, M. Berbineau, and M. Aguado. “IEEE 802.11a performance for infrastructure-to-train communications in an underground tunnel”. In: *Proc. 9th International Conference on Intelligent Transport Systems Telecommunications (ITST)*. Oct. 2009, pp. 447–452 (cit. on pp. 14, 26, 31).

[52] H.-S. Yun and K.-S. Lee. “A Study on the Development of the Train Control System Data Transmision Technology Using a Wireless Mesh”. In: *Proc. Third International Conference on Multimedia Information Networking and Security (MINES)*. Nov. 2011, pp. 196–200 (cit. on pp. 14, 33).

[53] M. Fitzmaurice. “Use of Wireless Local Area Networks in Rail and Urban Transit Environments”. In: *Transportation Research Record* 1916 (2005), pp. 42–46 (cit. on pp. 14, 29).

[54] T. Changqing, Z. Xin, and Z. Guoxin. “A method to improve the reliability of CBTC wireless link”. In: *Proc. IET International Communication Conference on Wireless Mobile and Computing (CCWMC ’09)*. Dec. 2009, pp. 9–12 (cit. on p. 14).

[55] L. Zhu, F. R. Yu, B. Ning, and T. Tang. “Design and Performance Enhancements in Communication-Based Train Control Systems With Coordinated Multipoint Transmission and Reception”. In: *IEEE Transactions on Intelligent Transportation Systems* 15.3 (June 2014), pp. 1258–1272 (cit. on p. 14).

[56] Y. Zhang, L. Zhu, L. Chen, T. Tang, and S. Liu. “A Method for Simulation and Analysis of Trackside Data Communication System in CBTC”. In: *Proc. WRI International Conference on Communications and Mobile Computing (CMC ’09)*. Vol. 3. Jan. 2009, pp. 529–533 (cit. on pp. 14, 16, 31).

[57] HUBER+SUHNER. *CBTC Connectivity Solutions*. 2011. URL: http://literature.hubersuhner.com/Marketsegments/Transportation/RailCBTCEN/ (cit. on pp. 14, 27).

[58] L. Xiaojuan and Z. Yanpeng. “A fast handoff algorithm with high reliability and efficiency for CBTC systems”. In: *Proc. International Conference on Transportation, Mechanical, and Electrical Engineering (TMEE)*. Dec. 2011, pp. 1461–1464 (cit. on p. 16).

[59] Y. Cao, R. Niu, T. Xu, T. Tang, and J. Mu. “Wireless test platform of Communication Based Train Control (CBTC) system in urban mass transit”. In: *Proc. IEEE International Conference on Vehicular Electronics and Safety (ICVES)*. Dec. 2007, pp. 1–4 (cit. on pp. 16, 31).

[60] B. Bu, F. R. Yu, T. Tang, and C. Gao. “A delay tolerant control scheme for communication-based train control (CBTC) systems with unreliable wireless networks”. In: *Proc. IEEE International Conference on Communications (ICC)*. June 2013, pp. 5173–5177 (cit. on p. 16).

[61] K. K. Yoo and R. Y. Kim. “HiNet: Radio Frequency Communication Based Train Control (RF-CBTC) System Jointly Using Hierarchical Modulation and Network Coding”. In: vol. 7425. Lecture Notes in Computer Science. Springer, 2012. Chap. Convergence and Hybrid Information Technology: 6th International Conference, ICHIT 2012, Proceedings, pp. 130–137 (cit. on pp. 16, 20, 31, 33).

[62] T. Xu and T. Tang. “The modeling and Analysis of Data Communication System (DCS) in Communication Based Train Control (CBTC) with Colored Petri Nets”. In: *Proc. Eighth International Symposium on Autonomous Decentralized Systems (ISADS ’07)*. Mar. 2007, pp. 83–92 (cit. on pp. 16, 22).

[63] X. TianHua, T. Tao, G. ChunHai, and C. BaiGen. “Dependability analysis of the data communication system in train control system”. In: *IEEE Transactions on Intelligent Transportation Systems* 52.9 (2009), pp. 2605–2618 (cit. on pp. 16, 22, 25, 37).

[64] Siemens. *Trainguard MT: Optimal performance with the world’s leading automatic train control system for mass transit*. 2014. URL: http://www.siemens.com/press/pool/de/feature/2013/infrastructure-cities/mobility-logistics/2013-02-trainguardmt/broschuere-trainguard-mt-e.pdf (cit. on pp. 16, 19, 38, 41).

[65] I. Silajev. *Thales CBTC - Communication Based Train Control Rail Signalling Solutions*. URL: http://www.rpknis.rs/ictforum2010/PPTprezentacije/English/CBTC-Communication%20Based%20Train%20Control%20-%20Igor%20Silajev.pdf (cit. on pp. 16, 38, 41).

[66] Siemens. *Redundant networks for industry*. 2012. URL: http://w3app.siemens.com/mcms/infocenter/dokumentencenter/sc/ic/Documentsu20Brochures/BR_Redundante_Netzwerke_112012_en.pdf (cit. on p. 17).

[67] L. Wisniewski, M. Hameed, S. Schriegel, and J. Jasperneite. “A Survey of Ethernet Redundancy Methods for Real-Time Ethernet Networks and its Possible Improvements”. In: *IFAC Proceedings Volumes: 8th IFAC Conference on Fieldbuses and Networks in Industrial and Embedded Systems* 42.3 (2009), pp. 163–170 (cit. on p. 17).

[68] Wikipedia. *Cab signalling — Wikipedia, The Free Encyclopedia*. URL: https://en.wikipedia.org/w/index.php?title=Cab_signalling&oldid=689260800 (cit. on p. 17).

[69] R. Lardennois, Siemens. *Wireless Communication for Signaling in Mass Transit*. Sept. 2003. URL: http://www.tsd.org/papers/SiemensWirelessCommsInMassTransit.pdf (cit. on pp. 18–20, 34).

[70] APTA (American Public Transportation Association). *First application of Communications Based Train Control (CBTC)*. 2014. URL: http://www.apta.com/resources/safetyandsecurity/Lists/Safety%20Innovations/DispForm.aspx?ID=82&RootFolder=/resources/safetyandsecurity/Lists/Safety%20Innovations&Source=http://www.apta.com/resources/safetyandsecurity/Pages/Safety-Inn (cit. on p. 18).

[71] B. T. Sullivan. “CBTC Radios - What to Do? Which Way to Go?” In: *Railway Age* (2005). URL: http://www.tsd.org/papers/CBTCRadios.pdf (cit. on pp. 18–20).

[72] E. Kuun. “Open standards for CBTC and CCTV radio-based communication”. In: *Proc. APTA Rail Transit Conference*. 2004 (cit. on pp. 18, 20, 27, 32–34).

[73] Siemens. *Cityval and Airval - Automated transportation systems*. 2013. URL: http://www.mobility.siemens.com/mobility/global/SiteCollectionDocuments/en/rail-solutions/automated-people-mover/airval-cityval-en.pdf (cit. on p. 18).

[74] Siemens. *Trainguard MT CBTC: The Moving Block Communications-Based Train Control Solution* (cit. on pp. 18, 38, 41).

[75] *Transportation Systems Design, Inc - Communications Based Train Control*. URL: http://www.tsd.org/cbtc/ (cit. on pp. 18, 19).

[76] *Driver’s Reference Guide*. URL: http://www.railsimroutes.net/driversguide/signalling.php (cit. on p. 18).

[77] *ATP Beacons and Moving Block*. URL: http://www.railway-technical.com/sigtxt3.shtml (cit. on p. 18).

[78] *Original Docklands Light Railway Signalling*. URL: http://www.railway-technical.com/Sigdock.shtml (cit. on p. 18).

[79] M. Aguado, E. Jacob, P. Saiz, J. Unzilla, M. Higuero, and J. Matias. “Railway signaling systems and new trends in wireless data communication”. In: *Proc. IEEE 62nd Vehicular Technology Conference (VTC 2005-Fall)*. Vol. 2. Sept. 2005, pp. 1333–1336 (cit. on p. 18).

[80] T. Sullivan. “NYCT gets resignaled”. In: *Mass Transit* 25.1 (1998), pp. 34–40 (cit. on p. 19).

[81] *Advanced Public Transportation Systems: The State of the Art Update 2000*. Tech. rep. U.S. Department of Transportation - Federal Transit Administration, 2000 (cit. on p. 19).

[82] RailwayAge. *Siemens, Thales land NYCT QBL West Phase 1 CBTC contracts*. Aug. 2015. URL: http://www.railwayage.com/index.php/communications/siemens-lands-nyct-qbl-phase-1-cbtc-contract.html (cit. on p. 19).

[83] M. Fitzmaurice. “Wayside Communications: CBTC Data Communications Subsystems”. In: *IEEE Vehicular Technology Magazine* 8.3 (Sept. 2013), pp. 73–80 (cit. on pp. 19, 22–24, 30, 41).

[84] M. Heddebaut. “Leaky Waveguide for Train-to-Wayside Communication-Based Train Control”. In: *IEEE Transactions on Vehicular Technology* 58.3 (Mar. 2009), pp. 1068–1076. ISSN: 0018-9545 (cit. on p. 19).

[85] B. Bing, W. Hongwei, Z. Hongli, and J. Hailin. “A research on the hybrid train-to-ground communication method in CBTC”. In: *Proc. IEEE International Conference on Service Operations, Logistics, and Informatics (SOLI)*. July 2011, pp. 512–516 (cit. on pp. 19, 31, 33).

[86] S. Shirlaw. “Radio and communications-based train control: Migration, interoperation and system engineering issues”. In: *Proc. International Conference on Railway Engineering - Challenges for Railway Transportation in Information Age (ICRE ’08)*. Mar. 2008, pp. 1–5 (cit. on pp. 19, 33).

[87] P. Hsu. *Moxa White Paper: The Future of Railway Wireless Networks: What You Need to Know*. Apr. 2010. URL: http://www.moxa.com/support/request_catalog_detail.aspx?id=137 (cit. on p. 20).

[88] Wikipedia. *ISM band — Wikipedia, The Free Encyclopedia*. URL: https://en.wikipedia.org/w/index.php?title=ISM_band&oldid=700868788 (cit. on p. 22).

[89] ITU-R. *Radio Regulations, Edition of 2012*. 2012. URL: https://www.itu.int/dms_pub/itu-s/oth/02/02/S02020000244501PDFE.PDF (cit. on p. 22).

[90] *Is 5GHz Wireless better than 2.4GHz?* URL: http://www.speedguide.net/faq/is-5ghz-wireless-better-than-24ghz-340 (cit. on pp. 22, 24).

[91] *Here’s why you should use 5GHz WiFi instead of 2.4GHz*. URL: http://pocketnow.com/2014/01/23/5ghz-wifi (cit. on p. 22).

[92] Wikipedia. *List of 2.4 GHz radio use — Wikipedia, The Free Encyclopedia*. URL: https://en.wikipedia.org/w/index.php?title=List_of_2.4_GHz_radio_use&oldid=699126813 (cit. on p. 22).

[93] PC Magazine. *ISM band*. URL: http://www.pcmag.com/encyclopedia/term/45467/ism-band (cit. on p. 22).

[94] M. Fitzmaurice. “Use of 2.4 GHz frequency band for Communications Based Train Control data communications systems”. In: *Proc. IEEE/ASME Joint Rail Conference*. Apr. 2006, pp. 263–267 (cit. on p. 23).

[95] M. Voss. *Siemens Internal Report*. Braunschweig, Germany: Siemens AG, Nov. 2015 (cit. on p. 23).

[96] China Daily USA. *Shenzhen Metro disruption leads to call to ban Wi-Fi devices on subways*. 2012. URL: http://usa.chinadaily.com.cn/epaper/2012-11/06/content_15880678.htm (cit. on p. 23).

[97] South China Morning Post. *Public Wi-Fi signal may have caused Shenzhen subway train stoppage*. Nov. 2012. URL: http://www.scmp.com/news/china/article/1076596/public-wi-fi-signal-may-have-caused-shenzhen-subway-train-stoppage (cit. on p. 23).

[98] Wikipedia. *IEEE 802.11 — Wikipedia, The Free Encyclopedia*. URL: https://en.wikipedia.org/w/index.php?title=IEEE_802.11&oldid=702229246 (cit. on p. 24).

[99] Y. Wei, H. Lu, and Z. He. “Research of the Digital Communication System for CBTC Based on 802.11”. In: *Proc. Third International Conference on Multimedia Information Networking and Security (MINES)*. Nov. 2011, pp. 95–99 (cit. on pp. 24, 25).

[100] L. Zhu, F. Yu, and B. Ning. “Availability Improvement for WLAN-Based Train-Ground Communication Systems in Communication-Based Train Control (CBTC)”. In: *Proc. IEEE 72nd Vehicular Technology Conference Fall (VTC 2010-Fall)*. Sept. 2010, pp. 1–5 (cit. on pp. 25, 37, 38).

[101] Y.-B. Lin, S.-N. Yang, and C.-T. Wu. “Improving Handover and Drop-off Performance on High-Speed Trains With Multi-RAT”. In: *IEEE Transactions on Intelligent Transportation Systems* 15.6 (Dec. 2014), pp. 2720–2725. ISSN: 1524-9050 (cit. on p. 25).

[102] A. Böhm and M. Jonsson. *Handover in IEEE 802.11p-based Delay-Sensitive Vehicle-to-Infrastructure Communication*. Tech. rep. School of Information Science, Computer and Electrical Engineering (IDE), Halmstad University, Sweden, 2007 (cit. on p. 26).

[103] P. Roshan and J. Leary. *IEEE 802.11 Wireless LAN Fundamentals*. Cisco Press, 2003. ISBN: 978-1-58705-077-0 (cit. on pp. 27, 31, 32).

[104] A. Mishra, M. Shin, and W. Arbaugh. “An Empirical Analysis of the IEEE 802.11 MAC Layer Handoff Process”. In: *SIGCOMM Computer Communication Review* 33.2 (Apr. 2003), pp. 93–102. ISSN: 0146-4833 (cit. on p. 28).

[105] J. Montavont, N. Montavont, and T. Noel. “Enhanced schemes for L2 handover in IEEE 802.11 networks and their evaluations”. In: *Proc. IEEE 16th International Symposium on Personal, Indoor and Mobile Radio Communications (PIMRC ’05)*. Vol. 3. Sept. 2005, pp. 1429–1434 (cit. on p. 28).

[106] *Local and Metropolitan Area Networks–Port-Based Network Access Control*. 3 Park Avenue, New York, NY 10016-5997, USA: IEEE, 2010 (cit. on p. 29).

[107] *WLAN Roaming - the basics*. Mar. 2010. URL: http://www.techworld.com/mobile/wlan-roaming--the-basics-435/ (cit. on p. 29).

[108] *Trial-Use Recommended Practice for Multi-Vendor Access Point Interoperability Via an Inter-Access Point Protocol Across Distribution Systems Supporting IEEE 802.11 Operation*. 3 Park Avenue, New York, NY 10016-5997, USA: IEEE, 2003 (cit. on p. 29).

[109] EETimes. *The Range vs. Rate Dilemma of WLANs*. 2004. URL: http://www.eetimes.com/document.asp?doc_id=1271995 (cit. on p. 30).

[110] A. F. Molisch. *Wireless Communications*. 2nd ed. Wiley, 2011. ISBN: 978-0-470-74186-3 (cit. on pp. 30, 34).

[111] L. Bro. *Siemens Internal Report*. Ballerup, Denmark: Siemens A/S, July 2014 (cit. on p. 31).

[112] J. S. Reigadas, A. Martinez-Fernandez, J. Ramos-Lopez, and J. Seoane-Pascual. "Modeling and Optimizing IEEE 802.11 DCF for Long-Distance Links". In: *IEEE Transactions on Mobile Computing* 9.6 (June 2010), pp. 881–896 (cit. on p. 31).

[113] K. K. Leung, M. V. Clark, B. McNair, Z. Kostic, L. J. Cimini, and J. H. Winters. "Outdoor IEEE 802.11 Cellular Networks: Radio and MAC Design and Their Performance". In: *IEEE Transactions on Vehicular Technology* 56.5 (Sept. 2007), pp. 2673–2684 (cit. on p. 31).

[114] A. Hrovat, G. Kandus, and T. Javornik. "A Survey of Radio Propagation Modeling for Tunnels". In: *IEEE Communications Surveys & Tutorials* 16.2 (second quarter 2014), pp. 658–669 (cit. on p. 32).

[115] T. Changqing, Z. Guoxin, W. Hui, K. Kai, and R. Yanrong. "Propagation in tunnel in case of WLAN applied to Communications-Based Train Control system". In: *Proc. IET International Communication Conference on Wireless Mobile and Computing (CCWMC '09)*. Dec. 2009, pp. 393–396 (cit. on p. 33).

[116] Thales. *SelTrac CBTC worldwide references*. Aug. 2014. URL: https://www.thalesgroup.com/sites/default/files/asset/document/seltrac_cbtc_references.pdf (cit. on pp. 33, 38, 41).

[117] Alstom. *ATM (Azienda Trasporti Milanesi) Boosting capacity on Milan Metro Line 1 with Alstom's URBALIS CBTC solution*. 2012. URL: http://www.alstom.com/Global/Transport/Resources/Documents/brochure2014/Milan%20metro%20L1%20CBTC%20-%20Case%20Study%20-%20EN.pdf?epslanguage=en-GB (cit. on p. 33).

[118] *Recommended Practice for Communications-Based Train Control (CBTC) System Design and Functional Allocations*. 3 Park Avenue, New York, NY 10016-5997, USA: IEEE, 2008 (cit. on p. 38).

[119] Alstom. *URBALIS. Communication Based Train Control (CBTC). Delivery Performance and Flexibility*. Mar. 2009. URL: https://signallingsolutions.com/wp-content/uploads/files/urbalis.pdf (cit. on pp. 38, 41).

[120] Alstom. *URBALIS CBTC solution - Performance you can rely on*. 2012. URL: http://www.alstom.com/Global/Transport/Resources/Documents/Brochure%20-%20Signalling%20-%20Urbalis%20-%20English%20.pdf (cit. on pp. 38, 41).

[121] Alstom. *Signaling Product Solutions: URBALIS 400*. 2012. URL: http://www.alstom.com/Global/Transport/Resources/Documents/brochure2014/URBALIS%20400%20-%20Product%20Sheet%20-%20EN.pdf?epslanguage=en-GB (cit. on pp. 38, 41).

[122] Alstom. *Signaling Product Solutions: URBALIS Fluence*. 2013. URL: http://www.alstom.com/Global/Transport/Resources/Documents/brochure2014/URBALIS%20Fluence%20-%20Product%20Sheet%20-%20EN.pdf?epslanguage=en-GB (cit. on pp. 38, 41).

[123] Alstom. *URBALIS Solutions: Beyond CBTC Basics*. 2013. URL: http://www.alstom.com/Global/Transport/Resources/Documents/brochure2014/Urbalis%20range%20-%20Brochure%20-%20EN.pdf?epslanguage=en-GB (cit. on pp. 38, 41).

[124] Thales. *Ground Transportation: SelTrac CBTC communications-based train control for urban rail*. URL: https://www.thalesgroup.com/sites/default/files/asset/document/cbtc_brochure_0.pdf (cit. on pp. 38, 41).

[125] Thales. *Rail Signalling Solutions: SelTrac CBTC Communications-Based Train Control For Urban Rail*. URL: https://www.thalesgroup.com/sites/default/files/asset/document/SelTracBrochure_CBTCSolutions_eng.pdf (cit. on pp. 38, 41).

[126] Ansaldo STS. *CBTC - Communication Based Train Control*. URL: http://www.ansaldo-sts.com/sites/ansaldosts.message-asp.com/files/imce/asts_hitachi_cbtc_ingl_lr.pdf (cit. on pp. 38, 41).

[127] Ansaldo STS. *CBTC - Communication Based Train Control*. URL: http://www.ansaldo-sts.com/sites/ansaldosts.message-asp.com/files/imce/ASTS_CBTC%20d_%20eng_0.pdf (cit. on pp. 38, 41).

[128] Bombardier. *Rail Control Solutions: CITYFLO: Signalling for mass transit*. 2012 (cit. on pp. 38, 41).

[129] Bombardier. *CITYFLO 650 - Metro Madrid: Solving the capacity challenge*. 2011. URL: http://www.infrasig.net/media/86165/metro_madrid_march_2011_10922_en_low_res.pdf (cit. on pp. 38, 41).

[130] Bombardier. *CITYFLO 650 - A new generation for driverless automated transit systems*. URL: http://www.bombardier.com/en/transportation/products-services/rail-control-solutions/mass-transit-solutions/cityflo-650.html (cit. on pp. 38, 41).

[131] GE Transportation. *GE Transportation's CBTC Solution: Enabling intelligent commuting* (cit. on pp. 38, 41).

[132] GE Transportation. *Tempo* CBTC Solution Smart signaling for smart urban transit services*. 2012. URL: http://www.getransportation.com/sites/default/files/Tempo%20CBTC%20Brochure%20FINAL.pdf (cit. on pp. 38, 41).

[133] Siemens. *Trainguard MT: The scalable automatic train control system for maximum flexibility in modern mass transit*. 2010. URL: http://w1.siemens.ch/mobility/ch/SiteCollectionDocuments/en/rail-solutions/rail-automation/train-control-systems/trainguard-mt-en.pdf (cit. on pp. 38, 41).

[134] CENELEC. *Global Partners IEC*. URL: http://www.cenelec.eu/aboutcenelec/whoweare/globalpartners/iec.html (cit. on p. 38).

[135] IEC. "IEC 62290-1 Ed.2: Railway applications - Urban guided transport management and command/control systems - Part 1: System principles and fundamental concepts". In: (2014) (cit. on p. 38).

[136] IEC. "IEC 62290-2 Ed.2: Railway applications - Urban guided transport management and command/control systems - Part 2: Functional requirements specification". In: (2014) (cit. on p. 38).

[137] IEC. "IEC 62290-3: Railway applications - Urban guided transport management and command/control systems - Part 3: System requirements specifications (proposed future IEC 62290-3)". In: (2015) (cit. on p. 38).

[138] IEC. "IEC 62278:2002: Railway applications - Specification and demonstration of reliability, availability, maintainability and safety (RAMS)". In: (2002) (cit. on p. 38).

[139] CENELEC. "EN 50126-1:1999: Railway applications - The specification and demonstration of Reliability, Availability, Maintainability and Safety (RAMS) - Part 1: Basic requirements and generic process". In: (1999) (cit. on p. 38).

[140] CENELEC. "CLC/TR 50126-2:2007: Railway applications - The specification and demonstration of Reliability, Availability, Maintainability and Safety (RAMS) - Part 2: Guide to the application of EN 50126-1 for safety". In: (2007) (cit. on p. 38).

[141] CENELEC. "EN 50128:2011: Railway applications - Communication, signalling and processing systems - Software for railway control and protection systems". In: (2011) (cit. on p. 38).

[142] CENELEC. "EN 50159:2010: Railway applications - Communication, signalling and processing systems - Safety-related communication in transmission systems". In: (2010) (cit. on p. 38).

[143] J.-L. Boulanger. *CENELEC 50128 and IEC 62279 Standards*. Wiley, 2015. ISBN: 978-1-84821-634-1 (cit. on p. 38).

[144] J. B. Balliet. *Bridging the European and US Rail Safety. The Feasibility of Cross Acceptance*. Tech. rep. AREMA, 2011 (cit. on p. 38).

[145] AREMA. *Communications and Signals Manual of Recommended Practices*. URL: https://www.arema.org/publications/cs/index.aspx (cit. on p. 38).

[146] European Commission. *MODURBAN - next generation urban rail systems*. URL: http://ec.europa.eu/research/transport/projects/items/modurban___next_generation_urban_rail_systems_en.htm (cit. on p. 38).

[147] Ansaldo STS. *Mass Transit Solutions*. URL: http://www.ansaldo-sts.com/en/activities-and-services/references-and-technologies/mass-transit-solutions (cit. on p. 41).

[148] Bombardier. *Bombardier's Rail Control Division Further Expands North American Presence*. Oct. 2015. URL: http://www.bombardier.com/en/media/newsList/details.bt-20151008-bombardiers-rail-control-division-further-expands-no.bombardiercom.html (cit. on p. 41).

[149] Bombardier. *Bombardier Transportation: Projects*. URL: http://www.bombardier.com/en/transportation/projects.html (cit. on p. 41).

[150] Siemens. *Press Release: Siemens provides trains and automatic train control system for new metro line in Sofia*. Mar. 2016. URL: http://www.siemens.com/press/en/pressrelease/?press=/en/pressrelease/2016/mobility/pr2016030218moen.htm&content[]=MO (cit. on p. 41).

[151] Siemens. *Worldwide references for Trainguard MT*. Tech. rep. Feb. 2013. URL: http://www.siemens.com/press/pool/de/feature/2013/infrastructure-cities/mobility-logistics/2013-02-trainguardmt/references-trainguardmt-worldwide-e.pdf (cit. on p. 41).

[152] Hitachi. *Communication Based Train Control (CBTC)*. URL: http://www.hitachi-rail.com/products/signalling/cbtc/ (cit. on p. 41).

[153] Alstom. *GE - Alstom transaction*. URL: http://www.alstom.com/ge-alstom-transaction/ (cit. on p. 41).

[154] Railway Gazette. *Hitachi completes Ansaldo deal*. Nov. 2015. URL: http://www.railwaygazette.com/news/business/single-view/view/hitachi-completes-ansaldo-deal.html (cit. on p. 41).

[155] E. Kohler, R. Morris, B. Chen, J. Jannotti, and M. F. Kaashoek. "The Click Modular Router". In: *ACM Transactions on Computer Systems* 18.3 (2000), pp. 263–297 (cit. on p. 51).

[156] J. Banks, J. S. Carson, B. L. Nelson, and D. M. Nicol. *Discrete-Event System Simulation*. 3rd ed. Prentice Hall, 2000. ISBN: 978-0-130-88702-3 (cit. on pp. 59, 60).

[157] A. M. Law and W. D. Kelton. *Simulation Modelling and Analysis*. 3rd ed. McGraw-Hill, 2000. ISBN: 978-0-071-16537-2 (cit. on pp. 59, 60).

[158] R. G. Ingalls. "Introduction to simulation". In: *Proc. 40th Winter Simulation Conference (WSC)*. Miami, Florida, Dec. 2008. ISBN: 978-1-4244-2708-6 (cit. on pp. 59, 60).

[159] *OPNET Modeler*. https://www.riverbed.com/dk/products/steelcentral/opnet.html. Riverbed Technology (cit. on p. 60).

[160] *Siemens Internal Document: BST TGMT Safe braking model specification*. Ballerup, Denmark: Siemens A/S, Sept. 2017 (cit. on p. 106).

Jahanzeb Farooq received his B.Sc. and M.Sc. degrees in computer science from Hamdard University, Pakistan, and Umeå University, Sweden, in 2004 and 2006, respectively. Jahanzeb has previously worked at the French Institute for Research in Computer Science and Automation (INRIA), France, where he was involved in the modeling and simulation of WiMAX networks. Since 2010, Jahanzeb has been working for Siemens A/S, Denmark, where he has been involved in the research and development of Siemens' Communications-Based Train Control (CBTC) system. Recently, he has been involved in the implementation of the Copenhagen S-train CBTC project. In 2014, Jahanzeb started his PhD at the Technical University of Denmark (DTU). His PhD which was sponsored by Siemens A/S and partly by the Ministry of Higher Education and Science, Denmark (InnovationsFonden).

DTU Fotonik
Networks Technology & Service Platforms
Technical University of Denmark

Ørsteds Plads 343
2800 Kgs. Lyngby
Denmark
Tlf. +45 4525 6352
Fax +45 4593 6581

www.fotonik.dtu.dk